Supplementary Information

Activation and Characterization of a Cryptic Gene Cluster Reveal a Cyclization Cascade for Polycyclic Tetramate Macrolactams

Subhasish Saha,‡[a] Wenjun Zhang,‡[a] Guangtao Zhang,‡[a] Yiguang Zhu,[a] Yuchan Chen,[b] Wei Liu,[a,c] Chengshan Yuan,[a] Qingbo Zhang,[a] Haibo Zhang,[a] Liping Zhang,[a] Weimin Zhang,[b] and Changsheng Zhang[a,c, *]

[a] CAS Key Laboratory of Tropical Marine Bio-resources and Ecology, Guangdong Key Laboratory of Marine Materia Medica, RNAM Center for Marine Microbiology; South China Sea Institute of Oceanology, Chinese Academy of Sciences, 164 West Xingang Road, Guangzhou 510301, China;

[b] State Key Laboratory of Applied Microbiology Southern China, Guangdong Institute of Microbiology, 100 Central Xianlie Road, Guangzhou 510070, China.

[c] South China Sea Resource Exploitation and Protection Collaborative Innovation Center (SCS-REPIC).

‡These authors contributed equally to this work.

* Correspondence and requests for materials should be addressed to C.Z. (email: czhang2006@gmail.com; czhang@scsio.ac.cn)

Content

Author contributions ... S3
Supplementary methods ... S3
Materials and reagents ... S3
Promoter engineering ... S3
In-frame deletion of the *ptm* genes ... S3
Cultivation, fermentation of *Streptomyces pactum* strains and isolation of pactamides ... S4
Heterologous expression, fermentation, and PTM isolation in *S. lividans* TK64 ... S5
Structure elucidation ... S5
Expression and purification of recombinant PtmC ... S9
PtmC enzyme assays ... S9
Enzymatic preparation and isolation of compound **18** ... S9
S. lividans-mediated biotransformation of compound **15** ... S9
Cytotoxic activity assay ... S10
Table S1. The genetic organization of *ptm*- and *xia*-gene cluster in pCSG2404 and the predicted functions of individual Orfs ... S11
Table S2. Strains and plasmids used and constructed in this study ... S12
Table S3. Primers used in this study ... S13
Table S4. ^{1}H (500 MHz) NMR Data for pactamides A-C (**11**-**13**) ... S14
Table S5. ^{13}C (125 MHz) NMR Data for pactamides A-C (**11**-**13**) ... S15
Table S6. ^{1}H NMR data for pactamides D-F **(14-16)** ... S16
Table S7. ^{13}CNMR data for pactamides D-F **(14-16)** ... S17
Table S8. ^{1}H (500 MHz) and ^{13}C (125 MHz) NMR data for **18** ... S18
Fig. S1. Scheme for inserting *ermE**p promoter in front of *ptmA* ... S19
Fig. S2. Scheme for inserting *ermE**p promoter in front of *ptmD* ... S20
Fig. S3. In-frame deletion of *ptmC* with *ermE**p promoter inserted in front of *ptmA* ... S21
Fig. S4. In-frame deletion of *ptmB1* with *ermE**p promoter inserted in front of *ptmA* ... S22
Fig. S5. In-frame deletion of *ptmB2* with *ermE**p promoter inserted in front of *ptmA* ... S23
Fig. S6. Characterization of compound **10** produced by *S. lividans* TK64/pCSG2814 ... S24
Fig. S7. Spectral data for pactamide A (**11**) ... S25
Fig. S8. Comparison of ECD spectra of pactamides, lysobacteramide B (**4**) and HSAF. ... S33
Fig. S9. Spectral data for pactamide B (**12**) ... S34
Fig. S10. Spectral data for pactamide C (**13**) ... S41
Fig. S11. Spectral data for pactamide D (**14**) ... S49
Fig. S12. Spectral data for pactamide E (**15**) ... S56
Fig. S13. Spectral data for pactamide F (**16**) ... S63
Fig. S14. Chemical structures of other PTMs ... S70
Fig. S15. SDS-PAGE analysis of purified proteins ... S71
Fig. S16. LC-MS analysis of PtmC reactions with deuterium labelling ... S72
Fig. S17. Spectral data for isoikarugamycin (**18**) ... S73
Fig. S18. *Streptomyces*-mediated Biotranformation of compound **15.** ... S76
Fig. S19. phylogenetic analysis of PtmD and its analogues ... S77
Fig. S20. Comparison of highly similar PTM gene clusters and their distinct products ... S78
Supplementary References ... S79

Author Contributions

S.S., W.Z., G.Z., and C.Z. designed the research and wrote the manuscript; S.S., G.Z., Y.Z., and L.Z. performed the *in vivo* and *in vitro* genetic and biochemical experiments; W.Z., W.L., C.Y., Q.Z., and H.Z. isolated compounds and determined their structures. Y.C. and W.Z. performed the bioactivity assays.

Supplementary methods

Materials and reagents. Bacterial strains, plasmids and primers are listed in Tables S2 and S3. Chemicals and reagents for biochemical and molecular biology are purchased from standard commercial sources.

Promoter engineering. The 300 bp *ermE**p promoter from pPWW50[1] and 1.4 kb *aadA* marker gene (for positive selection against spectinomycin) from pIJ778 were respectively PCR amplified and were linked by the "bridge PCR" strategy. The resulting 1.7 kb fragment was inserted in front of *ptmA* in pCSG2404 by homologous recombination via PCR targeting strategy to afford pCSG2802, which was subsequently modified to be pCSG2804 by replacing the *neo* gene with a DNA fragment containing *oriT*, *aac(3)IV* and *Int ϕC31* from pSET152A'B[2] to facilitate the conjugation into *Streptomyces lividans* TK64 (Fig. S1). Similarly, the cosmids pCSG2803 and pCSG2805 were constructed to insert the *erm*E promoter and *aadA* marker in front of *ptmD* (Fig. S2). *In situ* activation of PTM gene cluster was carried out by inserting the *ermE**p promoter in front of *ptmA* of *S. pactum* SCSIO 2999XM47i (Table S2) by using pCSG2802 (Fig. S2) via homologous recombination to afford 2999PTMp1 (Table S2).

In-frame deletion of the *ptm* genes. The cosmid pCSG2801 was constructed by inserting a DNA fragment containing *oriT*, *aac(3)IV* and *Int ϕC31* from pSET152A'B into the *neo* gene of pCSG2404.[3] Next, the *ptmC* gene in pCSG2801 was partially replaced by *aadA* and *oriT* from pIJ778 through PCR-targeting to afford pCSG2806 (Fig. S3). In-frame deletion of *ptmC* in pCSG2806 was performed by heating-induced FLP-recombinase to remove the inserted *aadA*/*oriT* cassette, to yield pCSG2808. Finally, the 1.7 kb *ermE**p promoter and *aadA* marker gene were inserted in front of *ptmA* in pCSG2808 via the above-mentioned promoter engineering strategy to afford

pCSG2809 (Fig. S3). Similarly, the cosmids pCSG2811 (carrying the in-frame deleted *ptmB1* and the *ermE**p promoter inserted in front of *ptmA*, Table S2, Fig. S4) and pCSG2814 (carrying the in-frame deleted *ptmB2* and the *ermE**p promoter inserted in front of *ptmA*, Table S2, Fig. S5) were constructed.

Cultivation, fermentation of *Streptomyces pactum* strains and isolation of pactamides. *Streptomyces pactum* SCSIO 02999 was a marine actinobacteria isolated from the marine sediment sample obtained from South China Sea (E109°53.171', N16°3.576') at the depth of 880 m.[4] The strains SCSIO 02999, 2999XM47i, and 2999PTMp1 were cultivated on the medium 38# agar plate supplemented with 3% sea salts. Three independent single colonies of each strain were inoculated into 50 mL of the R5 media (sucrose 103 g/L, K_2SO_4 0.25 g/L, $MgCl_2{\cdot}6H_2O$ 10.12 g/L, glucose 10 g/L, casamino acid 0.1 g/L, yeast extract 5.0 g/L, K_2HPO_4 0.5 g/L, trace elements 0.1 mL/L, pH 7.2-7.4) and incubated at 28 °C for 5–7 days. The production of PTM-like compounds was monitored via HPLC analysis on Agilent. HPLC was carried out using a reversed phase column Luna C18, 5 μm, 150 × 4.6 mm (Phenomenex), with UV detection at 300 nm under the following program: solvent system (solvent A, 10% acetonitrile in water supplementing with 0.1% formic acid; solvent B, 90% acetonitrile in water); 5% B to 100% B (linear gradient, 0−18 min), 100% B (18−23 min), 100% B to 5% B (23−27 min), 5% B (27−32min); flow rate at 1 mL/min.

A fresh single colony of the strain 2999PTMp1 from the Medium 38# plate was inoculated into 50 mL seed R5 medium with 3% sea salt in a 250 mL Erlenmeyer flask and incubated at 28 ºC on a rotary shaker (200 r.p.m.) for 5−7 days. Then 30 mL of the seed culture were inoculated into to 200 mL of the production R5 medium with 3% sea salt into a 1000 mL Erlenmeyer flask, and were cultured on a rotary shaker (200 r.p.m) at 28 ºC for 7 days. The broths of a total of 20 L fermentation of 2999PTMp1 were extracted three times with 5 L Butanone, respectively, to afford the crude extracts (7.0 g) after evaporation. The residue (7.0 g) was dissolved in a 1:1 mixture of $CHCl_3$-MeOH and mixed with an appropriate amount of silica gel for normal phase silica gel column chromatography (Silica Flash Column 14.5 × 2.5 cm, 40 g), eluted with a gradient elution of $CHCl_3$/MeOH mixture from 100/0, 95/5, 90/10, and 80/20 to yield four fractions (Fr1-Fr4). Fr2 (500 mg) was purified by Sephadex LH-20 (120 × 3.5 cm i.d.), eluting with $CHCl_3$/MeOH (5:5 v/v) to give Fr2B-Fr2D, Fr2B (100 mg) was further purified by prepare HPLC with C-18 reverse phased column (250 × 10.0 mm

i.d., 5μm) to afford pactamide B (**11**, 26 mg) and pactamide E (**15**, 2.5 mg). Fr2C (200 mg) was further purified by semi-preparative HPLC with C-18 reverse phased column (250 × 10.0 mm i.d., 5μm) to afford pactamide A (**12**, 30 mg), pactamide D (**14**, 3.2 mg). Pactamide E (**16**, 4.7 mg) was obtained from Fr2D by semi-preparative HPLC.

Heterologous expression, fermentation, and PTM isolation in *S. lividans* TK64. The cosmids pCSG2801, pCSG2804, pCSG2805, pCSG2809, pCSG2811 and pCSG2814 (Table S2 and Fig. S1-S5), together with the vector control pSET152, were introduced into the heterologous strain *Streptomyces lividans* TK64 by conventional conjugation.[5] Three independent transconjugants for each cosmid were inoculated into 50 mL R5 production medium and incubated at 28 °C for 5–7 days. The production of PTM-like compounds was monitored by HPLC using the same conditions as described for monitoring *Streptomyces pactum* strains. The crude extracts (4.7 g) of butanone extraction from 10 L fermentation of *S. lividans* TK64/pCSG2809 were subjected to column chromatography (CC) over a Silica Flash Column (14.5 × 2.5 cm, 40 g), eluting with a gradient of $CHCl_3$/MeOH (100:0 → 0:100) to give four fractions (Fr.1-Fr.4). Fr 2 (165 mg) was further purified sequentially by Sephadex LH-20 (120 × 3.5 cm i.d.) and C-18 reverse phase column (250 × 10.0 mm ID, 5 μm) to get compound **13** (25 mg).

Structure elucidation.

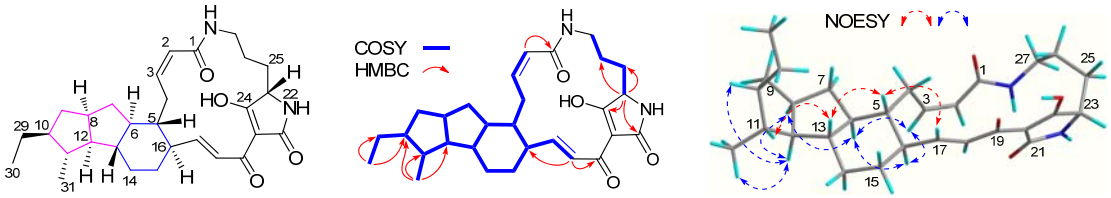

pactamide A (**11**) **11** **11**

The molecular formula of pactamide A (**11**) was established as $C_{29}H_{40}N_2O_4$ by HRESIMS (*m/z* 481.3098 $[M + H]^+$, calcd 481.3066). The NMR spectroscopic data of **11** (Tables S4-S5 and Fig. S7) were very similar to those of lysobacteramide B (**4**, Scheme 1),[6] except that signals for the C-14 hydroxy group and the N-22 methyl group in **4** were absent in **11**. The relative configuration of **11** was deduced by proton coupling constants ($Z\Delta^{2,3}$ $J_{2,3}$ 11.5 Hz; $E\Delta^{17,18}$ $J_{17,18}$ 15.0 Hz, Table S4) and NOESY correlations (Fig. S7). The assignment of H-5/H-11/H-13 on the same side of the 5/5/6-tricyclic ring system in **11**, while H-6/H-8/H-10/H-12/H-16/H_3-31 on another side,

was supported by the observed NOESY correlations (Fig. S7). On the basis of the biosynthetic origin of L-orinithine of PTMs,[6, 7] the *S*-configuration was assignable to C-23. Although the relative configuration of C-10 in **11** and **4** appeared to be opposite, both **11** and **4** exhibited almost identical ECD spectra (Fig. S8).[6] Thus, the absolute configuration of **11** was deduced as 5*R*, 6*S*, 8*S*, 10*S*, 11*R*, 12*R*, 13*S*, 16*R* and 23*S*.

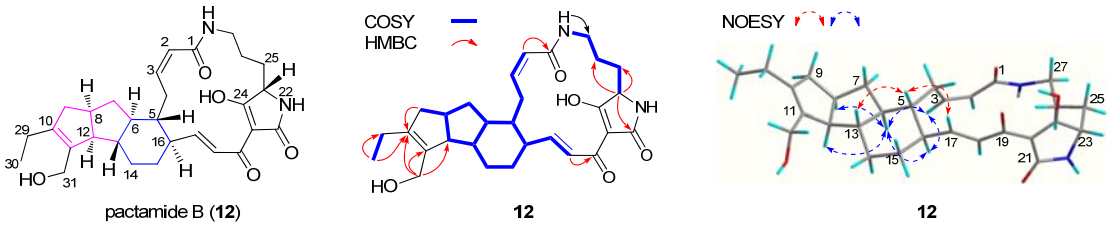

pactamide B (**12**) **12** **12**

Pactamide B (**12**) was isolated as a white powder. Its molecular formula was established as $C_{29}H_{38}N_2O_5$ by HRESIMS (*m/z* 493.2707 $[M - H]^-$, calcd 493.2708). Comparison of highly similar NMR spectroscopic data of **11** and **12** (Tables S4-S5 and Fig. S9) suggested the absence of the methyl at the C-31 position in **12**, while two mutually coupled methylene doublets appeared at δ_H 3.05, 4.05. Compound **12** had two additional sp^2 quaternary carbons (δ_C: 136.6, and 137.4) compared with **11**. HMBC from H-30 to C-10 (δ_C: 136.6) indicated that C-C single bond in **11** was transformed into C=C double bond in **12**. HMBC correlations from H-31a/H31b (δ_H 3.05, 4.05) to C-10/C-11/C-12 confirmed that a hydroxymethyl group was located at C-11 in **12**, different from the methyl group in **11.** These assignments were further supported by detailed 2D NMR analysis (Fig. S9), thus establishing the planar structure of **12**. The relative configuration of double bonds in **12** was established by proton coupling constants ($Z\Delta^{2,3}$ $J_{2,3}$ 11.5 Hz; $E\Delta^{17,18}$ $J_{17,18}$ 15.5 Hz, Table S4). The assignment of H-5/H-13 on the same side of the 5/5/6-tricyclic ring system in **12**, while H-6/H-8/H-12/H-16 on another side, was supported by the observed NOESY correlations (Fig. S9). By comparing ECD spectra (Fig. S8) of **12** and lysobacteramide B (**4**),[6] the absolute configuration of **12** was deduced to be 5*R*, 6*S*, 8*R*, 12*S*, 13*S*, 16*R* and 23*S*.

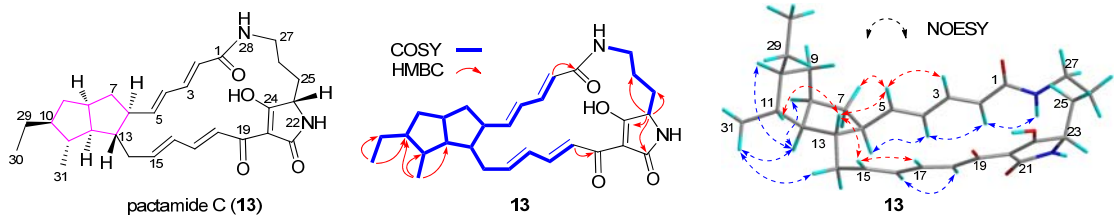

pactamide C (**13**) **13** **13**

The molecular formula of pactamide C (**13**) was determined as $C_{29}H_{38}N_2O_4$ by HRESIMS (*m/z* 479.2901 $[M + H]^+$, calcd 479.2904). Detailed analyses and

comparison of NMR spectra of **13** and **11**, confirmed that **13** differed from **11** by the absence of the six-membered ring (Tables S4-S5 and Fig. S10). The relative configuration of **13** was established by proton coupling constants ($E\Delta^{2,3}$ $J_{2,3}$ 15.0 Hz; $E\Delta^{4,5}$ $J_{4,5}$ 14.5 Hz; $E\Delta^{15,16}$ $J_{15,16}$ 14.5 Hz; $E\Delta^{17,18}$ $J_{17,18}$ 15.0 Hz, Table S4) and NOESY correlations (Fig. S10). The assignment of H-11/H-13 on the same side of the 5/5-bicyclic ring system in **13**, while H-6/H-8/H-10/H-12/H_3-31 on another side, was supported by the observed NOESY correlations (Fig. S10). The absolute configuration of **13** was tentatively assigned as 6*S*, 8*S*, 10*S*, 11*R*, 12*R*, 13*S*, and 23*S* upon considering it as a biosynthetic precursor of **11**.

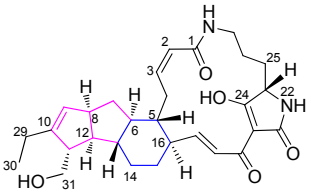

pactamide D (**14**)

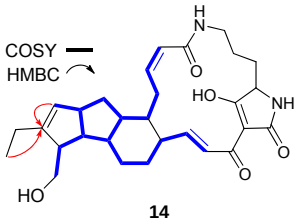

14

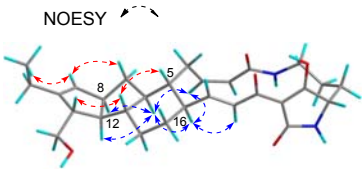

14

The molecular formula of pactamide D (**14**) was established as $C_{29}H_{38}N_2O_5$ by HRESIMS (*m/z* 517.2665 $[M + Na]^+$, calcd 517.2678). The NMR spectroscopic data of **14** and **12** were very similar. The carbon C-11 in **12** was a sp^2 quaternary carbon, however, the carbon C-11 in **14** was a sp^3 methine (δ_H 2.72 br s, δ_C 46.8, C-11) (Tables S4-S7, Fig. S11). HMBC correlation from H_3-30 to a sp^2 quaternary carbon (C-10) in **14** suggested a $\Delta^{9,10}$ double bond. This assignment was further supported by the HMBC correlation from H-9 to C-10, the COSY correlation between H-8/H-9, and NOSEY correlations of H-9/H-30, H-9/H-7 (Fig. S11). The relative configuration of double bonds in **14** was established to be the same as that of **12**, by proton coupling constants ($Z\Delta^{2,3}$ $J_{2,3}$ 11.0 Hz; $E\Delta^{17,18}$ $J_{17,18}$ 14.5 Hz, Table S6). The assignment of H-5/H-11/H-13 on the same side of the 5/5/6-tricyclic ring system in **14**, while H-6/H-8/H-12/H-16 on another side, was supported by the observed NOESY correlations (Fig. S11). The absolute configuration of **14** was assigned as 5*R*, 6*S*, 8*S*, 11*S*, 12*R*, 13*S*, 16*R* and 23*S* by comparing ECD spectra of **14** and **4** (Fig. S8).[6]

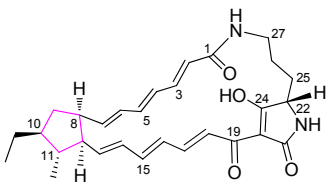

pactamide E (**15**)

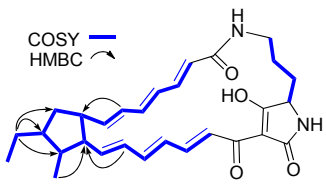

15

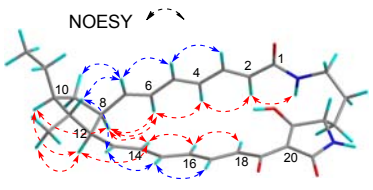

15

Pactamide E (**15**) was isolated as a pale-yellow powder. Its molecular formula

was determined as $C_{29}H_{36}N_2O_4$ by HRESIMS (*m/z* 499.2581 [M + Na]$^+$, calcd 499.2567). The NMR data (Table S6-S7, Fig. S12) of **15** were similar to those of compound **13**, the difference was that **15** had twelve olefins, which suggested that **15** had only one five-membered ring compared with **13**. The structure **15** was further supported by detailed 2D NMR analysis. The relative configuration of double bonds in **15** was established by proton coupling constants ($E\Delta^{2,3}$ $J_{2,3}$ 15.0 Hz; $E\Delta^{4,5}$ $J_{4,5}$ 14.5 Hz; $E\Delta^{6,7}$ $J_{6,7}$ 15.0 Hz; $E\Delta^{13,14}$ $J_{13,14}$ 15.5 Hz; $E\Delta^{15,16}$ $J_{15,16}$ 15.0 Hz; $E\Delta^{17,18}$ $J_{17,18}$ 14.5 Hz, Table S6). The assignment of H-8/H-10/H-12/H_3-31 on the same side of the outer 5-membered ring system in **15**, was supported by the observed NOESY correlations (Fig. S12). The absolute configuration of **15** was tentatively assigned as 8*S*, 10*S*, 11*R*, 12*S*, upon considering it as a biosynthetic precursor of **13**.

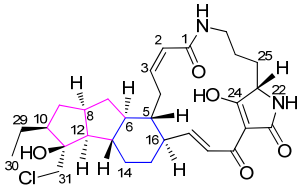

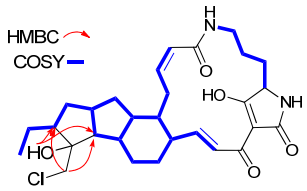

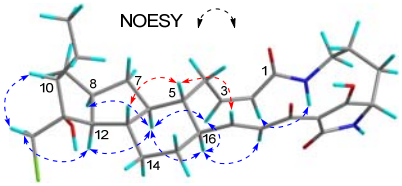

The molecular formula of pactamide F (**16**) was established as $C_{29}H_{39}ClN_2O_5$ by HRESIMS (*m/z* 531.2606 [M + H]$^+$, calcd 531.2626), which exhibited a typical chlorine isotope pattern (Fig. S13). The NMR spectroscopic data of **16** and **11** were very similar (Tables S4-S7). The methyl doublets typical for H_3-31 in **11** were absent in **16**, while signals for a methylene (H_2-31) were found in **16** (Fig. S13), suggesting the chlorine /or –OH substitution should be assigned at C-31. HMBC correlations from OH-11 to C-10 and C-12 located the OH group at C-11. The planar structure of **16** was further supported by detailed NMR analyses (Tables S6-S7 and Fig. S13). The relative configuration of **16** was deduced by proton coupling constants ($Z\Delta^{2,3}$ $J_{2,3}$ 10.5 Hz; $E\Delta^{17,18}$ $J_{17,18}$ 15.0 Hz, Table S6) and NOESY correlations (Fig. S13). The assignment of H-5/H-13 on the same side of the 5/5/6-tricyclic ring system, while H-6/H-8/H-10/H-12/H-16 on another side in **16**, was supported by the observed NOESY correlations (Fig. S13). The absolute configuration of **16** was assigned as 5*R*, 6*S*, 8*R,* 10*S*, 11*S*, 12*S*, 13*S*, 16*R*, 23*S*, given almost identical ECD spectra of **16** and **4** (Fig. S8).[6]

Expression and purification of recombinant PtmC. The *ptmC* gene was PCR-amplified from genomic DNA of *S. pactum* SCSIO 02999 using the primer pairs EptmCF/EptmCR (Table S3) with high fidelity DNA polymerase FastPfu (TransGen

Biotech). PCR products were digested with *Nde*I/*Bam*HI and inserted into the vector pET28a to give the expression plasmid pCSG3621 (Table S2) after sequence confirmation. The expression and purification of *N*-$(His)_6$-tagged PtmC was performed from *E. coli* BL21(DE3) carrying pCSG3621 according to the same procedure as described for IkaC.[8] *C*-$(His)_6$-tagged TaGDH and *N*-$(His)_6$-tagged BmGDH proteins were purified via Ni^{2+}-NTA agarose (Invitrogen) from *E. coli* BL21(DE3)/pCSG3622 and *E. coli* BL21(DE3)/pRSF-BmGDH (Table S3) as previously described.[8]

PtmC enzyme assays. A standard PtmC assay contained 200 μM **13** (or **17**), 2 mM NADPH, and 10 μg of purified recombinant PtmC in 200 mM sodium phosphate buffer (pH 8.0) in a total volume of 100 μL. The reaction was performed at 28 °C for 10 h. The enzyme reactions were terminated by addition of equal volume of cold methanol. After removal of the precipitated protein by centrifugation at 14,000 r.p.m. for 30 min, the reaction mixtures were concentrated on a rotating vacuum evaporator at 30 °C to a final volume of 100 μL before injection into HPLC. The PtmC/GDH coupling assays were performed as previously reported.[8] The reaction was stopped by the addition of 200 μL methanol. The enzyme assays were analyzed by HPLC on an Agilent series 1260 by using a using a reversed phase column Luna C18, 5 μm, 150 × 4.6 mm (Phenomenex) with UV detection at 300 nm under the following program: solvent system (solvent A, 10% acetonitrile in water supplementing with 0.1% formic acid; solvent B, 90% acetonitrile in water); 5% B to 100% B (linear gradient, 0−15 min), 100% B (15−22min), 100% B to 5%B (22−24 min), 5% B (24−30 min); flow rate at 1 mL/min.

Enzymatic preparation and isolation of compound 18. The PtmC reaction was carried out in a total volume of 100 mL containing 20 mg compound **18**, 10 mg purified recombinant PtmC, and 1 mM NADPH. The reaction was incubated at 28 °C for 12 h. The reaction product was freeze-dried and dissolved in a 1:1 mixture of $CHCl_3$-MeOH. $CHCl_3$-MeOH extract was evaporated to dryness. The residue (8 mg) were subjected to semi-preparative HPLC with C-18 reverse phased column (250 × 10.0 mm i.d., 5 μm) to yield isoikarugamycin (**18**, 1.7 mg).

***S. lividans*-mediated biotransformation of compound 15**. The biotransformation of compound **15** was carried out with the strain *S. lividans* TK64 harboring pCSG2814. The strain was inoculated into 30 mL of AM6 medium containing 50 μg/mL apramycin and 50 μM compound **15**, and was grown at 28 °C for 5 days. The products were extracted by butanone and were analyzed by HPLC. HPLC analysis (Agilent system)

was carried out using a reversed phase column Luna C18, 5 μm, 150 × 4.6 mm (Phenomenex), with UV detection at 300 nm under the following program: solvent system (solvent A, 10% acetonitrile in water supplementing with 0.1% formic acid; solvent B, 90% acetonitrile in water); 5% B to 100% B (linear gradient, 0−18 min), 100% B (18−23 min), 100% B to 5% B (23−27 min), 5% B (27−32min); flow rate at 1 mL/min]. *S. lividans* TK64 harboring pCSG2814 without adding compound **15** was treated in the same manner to serve as a negative control.

Cytotoxic activity assay. Pactamides A-F (**11**-**16**) were evaluated for their cytotoxic activities against SF-268 (human glioma cell line), MCF-7 (human breast adenocarcinoma cell line), NCI-H460 (human non-small cell lung cancer cell line), and HepG2 (human liver hepatocellular cell line) with the SRB method.[9] Cells (180 μL) with a density of 3 × 10^4 cells/mL of media were seeded onto 96-well plates and incubated for 24 h at 37 °C, 5% CO_2. Then 20 μL of various concentrations of compounds were added to plate wells. The plates were further incubated for 72 h. After incubation, cell monolayers were fixed with 50% (wt/v) trichloroacetic acid (50 μL) and stained for 30 min with 0.4% (wt/v) SRB dissolved in 1% acetic acid. Unbound dye was removed by washing repeatedly with 1% acetic acid. The protein-bound dye was dissolved in 10 mM Tris base solution (200 μL) for OD determination at 570 nm using a microplate reader. Cisplatin was used as a positive control possessing potent cytotoxic activity. All data were obtained in triplicate and are presented as means ±S.D. IC_{50} values were calculated with the SigmaPlot 10.0 software using a non-linear curve-fitting method.

Table S1. The genetic organization of *ptm*- and *xia*-gene cluster in pCSG2404 and the predicted functions of individual Orfs.

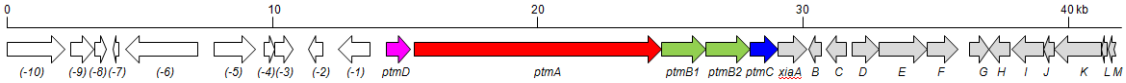

Name	AA	Proposed function	Closest homologue, Acc. No., Source	I/S%
orf(-10)	722	alpha-mannosidase	SMCF_5217, EHN75294, *Streptomyces coelicoflavus* ZG0656	91/95
orf(-9)	286	transcriptional regulator	SCO6003, NP_630118, *Streptomyces coelicolor* A3(2)	84/90
orf(-8)	143	hypothetical protein	NP_630117, NP_630115, *Streptomyces coelicolor* A3(2)	57/71
orf(-7)	65	hypothetical protein	SCO6000, *Streptomyces coelicolor* A3(2),	67/73
orf(-6)	913	aconitate hydratase	SMCF_5190, EHN75342, *Streptomyces coelicoflavus* ZG0656	97/98
orf(-5)	509	UDP-N-acetylglucosamine 1-carboxyvinyltransferase	WP_031042816, *Streptomyces*	100/100
orf(-4)	130	hypothetical protein	WP_030580287, *Streptomyces sclerotialus*	92/96
orf(-3)	225	hypothetical protein STRIP9103_07747	EKX63740, *Streptomyces ipomoeae* 91-03	95/97
orf(-2)	172	hypothetical protein	WP_037762956, *Streptomyces* sp. FXJ7.023	98/98
orf(-1)	396	hypothetical protein	WP_031042807, *Streptomyces olivaceus*	97/98
ptmD	301	hydroxylase	WP_037762956, *Streptomyces* sp. FXJ7.023	98/98
ptmA	3114	PKS/NRPS	WP_031042761, *Streptomyces olivaceus*	98/98
ptmB1	561	FAD-dependent oxidoreductase	WP_031042758, *Streptomyces olivaceus*	99/99
ptmB2	552	phytoene dehydrogenase	WP_033302652, *Streptomyces atroolivaceus*	99/99
ptmC	351	alcohol dehydrogenase	WP_043224439, *Streptomyces* sp. NRRL F-5193	98/98
xiaA	363	Rieske 2Fe-2S domain-containing aromatic ring-hydroxylating dioxygenases	Strvi_4991, AEM84537, *Streptomyces violaceusniger* Tu 4113	42/56
xiaB	164	flavin reductase domain protein FMN-binding	Strvi_6224, AEM85702, *Streptomyces violaceusniger* Tu 4113	76/84
xiaC	258	IclR family transcriptional regulator,	IclR, WP_014985470, *Nocardia brasiliensis*,	33/51

Table S2. Strains and plasmids used and constructed in this study.

Strains/Plasmids	Description	Reference
E. coli		
DH5α	Host strain for cloning	Invitrogen
BW25113/pIJ790	Host strain for PCR targeting	[10]
ET12567/pUZ8002	Donor strain for conjugation	[11]
BL21(DE3)	Host strain for protein expression	Transgen
Streptomyces		
Streptomyces pactum SCSIO 02999	Wild-type strain	[4]
Streptomyces lividans TK64	Host strain for heterologous expression	[5]
2999XM47i	*Streptomyces pactum* SCSIO 02999 derivative where *xiaP* gene was in-frame deleted	This study
2999PTMp1	*Streptomyces pactum* SCSIO 02999XM47i derived where *ermE**p promoter was inserted in front of *ptmA*	This study
Plasmids		
BT340	Cm^r, express FLP-recombinase to form in-frame deletion genes	[10]
pET28a	expression vector, Km^r	Novagen
pPWW50A	Ap^r, vector for *Streptoymes* heterologous expression	[12]
pIJ778	the template for amplifying the *aadA* cassette	[13]
pSET152	*Streptomyces* integrative vector; Ap^r	
pCSG2404	genomic library cosmid of *S. pactum* SCSIO 02999	[3]
pCSG2801	pCSG2404 derivative where the *neo* gene was replaced with *aac(3)IV-oriT-Int* ϕC31 fragment	This study (Fig. S3)
pCSG2802	pCSG2404 derivative with *aadA* and *ermE**p promoter inserted in front of *ptmA*	This study (Fig. S1)
pCSG2803	pCSG2404 derivative with *aadA* and *ermE**p promoter inserted in front of *ptmD*	This study (Fig. S2)
pCSG2804	pCSG2802 derivative where the *neo* gene was replaced with *aac(3)IV-oriT-Int ϕC31* fragment	This study (Fig. S1)
pCSG2805	pCSG2803 derivative where the *neo* gene was replaced with *aac(3)IV-oriT-Int ϕC31*	This study (Fig. S2)
pCSG2806	pCSG2801 derivative where the *ptmC* gene was disrupted by insertional mutation with *aadA*	This study (Fig. S3)
pCSG2807	pCSG2801 derivative where the *ptmB1* gene was disrupted by insertional mutation with *aadA*	This study (Fig. S4)
pCSG2808	pCSG2806 derivative where *ptmC* gene was in-frame deleted	This study (Fig. S3)
pCSG2809	pCSG2808 derivative where *aadA* and *ermE**p promoter inserted in front of *ptmA*	This study (Fig. S3)
pCSG2810	pCSG2807 derivative where *ptmB1* gene was in-frame deleted	This study (Fig. S4)
pCSG2811	pCSG2810 derivative where *aadA* and *ermE**p promoter inserted in front of *ptmA*	This study (Fig. S4)
pCSG2812	pCSG2801 derivative where the *ptmB2* gene was disrupted by insertional mutation with *aadA*	This study (Fig. S5)
pCSG2813	pCSG2812 derivative where *ptmB2* gene was in-frame deleted	This study (Fig. S5)
pCSG2814	pCSG2813 derivative where *aadA* and *ermE**p promoter inserted in front of *ptmA*	This study (Fig. S5)
pCSG3641	pET-28a derivative containing a 1.1 kb *Nde*I/*Bam*HI *ptmC* PCR fragment from genomic DNA of *S. pactum* SCSIO 02999	This study

Table S3. Primers used in this study.

Primers	Gene Target	Sequence
For insertion of the *ermEp promoter**		
ermEp-F		GAAGCAGCTCCAGCCTACACAGGCGGTACCAGCCCGACC
ermE-p1-R		GACCTTGTCGCGGTGGGCGGCGCTGGGTGAGTCCGTCATGGTTCGCCCGCTCTCCTCT
p1-aadA-F		CTGCTCCACCCCGTGCGCCGCCCGACCCACACCGCGTAGattccggggatccgtcgacc
p-aadA-R		GGTCGGGCTGGTACCGCCTGtgtaggctggagctgcttc
ermE-p2-R		ATTCGCCGGCAGCGACCCCGTATCGGGTCGATCTTCCATGGTTCGCCCGCTCTCCTCT
p2-aadA-F		TGGCTCACGCCCCGACTCTAAGAGCTGGAGATCAAGTAAattccggggatccgtcgacc
For detection of promoter insertion		
ermE-P1-det		CAGCGTCTCGAAGCCGAGGT
ermE-P1-det		CGGATTCTCCGCCGACTGC
ermE-P2-det		CCGCTCCAGCGCCGCGAGAT
ermE-P2-det		GTCGCCGTCCGTCGTCCGT
For construction of gene disruption mutant		
ptmC-dis-F	*ptmC*	CTCCACGGGATCGCCCTGGACACCCCGGCGGGCGACCACattccggggatccgtcgacc
ptmC-dis-R		GAGCATCGTGAAGACGGTGTCGGTCATGACCCCGCCGAGtgtaggctggagctgcttc
ptmB1-dis-F	*ptmB2*	CGAACGCTGCTCGCGATCCTGCCGGCGTTCCGGCTGTACattccggggatccgtcgacc
ptmB1-dis-R		CATCCCGGTCCACTGCCCGGCCATCGAGAAGCCGCTCAGtgtaggctggagctgcttc
ptmB2-dis-F	*ptmB2*	ACGGTGCGCGGCCGGGACGGGCGGGCGGTCCACTTCTACattccggggatccgtcgacc
ptmB2-dis-R		GCGGCGGATCCGGGTGAACTGCTCGGGACCGGTGCTCAGtgtaggctggagctgcttc
For detection of gene disruption mutant/in-frame deletion mutant		
ptmC-det F	*ptmC*	CCCAGTTGTCCTCGGTGAAC
ptmC-det R		AGAAGTGGATCGTCAGCGA
ptmB1-det F	*ptmB1*	GGCCACCGCCGCCTTCCCGG
ptmB1-det R		CCCGGACCGGCTCCAGAAC
ptmB2-det F	*ptmB2*	CTCGCCGCTGTCCACGAACG
ptmB2-det R		AGATCCCGGGCGGCTCCTG
For ptmC protein expression		
EptmCF	*ptmC*	GCGCATATGAAGACCGAGAAGTGGATCGT
EptmCR		GCGGGATCCTCACAGCTCGACCAGCACCTTG

Table S4. ^{1}H (500 MHz) NMR Data for pactamides A-C (**11**-**13**).

No.	**11**[a]	**12**[b]	**13**[b]
	δ_H, mult. (*J* in Hz)	**δ_H, mult. (*J* in Hz)**	**δ_H, mult. (*J* in Hz)**
2	5.73, d (11.5)	5.75, d (11.5)	5.81, d (15.0)
3	5.97, dd (11.5, 10.5)	5.99, dd (11.5, 10.6)	6.73, dd (15.0, 11.0)
4	2.01, m	1.99, m	6.16, dd (14.5, 11.0)
	3.37, m	3.54, t (13.1)	
5	1.24, m	1.29, m	5.65, dd (14.5, 10.0)
6	1.43, m	1.43, m	2.44, m
7	0.77, m	0.80, m	1.13, m
	1.97, m	2.10, m	1.88, m
8	2.29, m	2.52, m	2.36, m
9	0.72, m	2.00, m	0.86, m
	1.98, m	2.52	1.97, m
10	1.27, m		1.33, m
11	1.13, m		1.27, m
12	1.54, m	2.83, t (7.2)	1.63, m
13	1.01, m	1.02, m	1.41, m
14	1.01, m	1.20, m	2.10, m
	1.87, m	2.13, m	2.47, m
15	1.20, m	1.31, m	5.80, overlapping
	1.67, m	1.66, m	
16	1.94, m	2.00, m	6.06, dd (14.5, 11.0)
17	6.52, dd (15.0, 9.0)	6.60, dd (15.5, 10.8)	6.93, dd (15.0, 11.0)
18	7.38, d (15.0)	6.98, d (15.5)	7.40, d (15.0)
22		NH 8.66, br s	
23	3.61, br s	3.81, br s	3.54, br s
25	1.77, m	1.75, m	1.76, m
	1.86, m	1.86, m	1.85, m
26	1.30, m	1.16, m	0.87, m
	1.44, m	1.32, m	1.31, m
27	2.57, m	2.42, t (11.7)	2.35, m
	3.31, m	3.24, d (11.7)	3.54, m
28		NH 7.58	
29	0.97, m,	2.03, m	1.07, m
	1.49, m		1.54, m
30	0.81, t (7.0)	0.92, t(7.4)	0.86, t (7.0)
31	0.92, d (6.5)	3.90, d (11.5)	0.98, d (6.0)
		4.05, d (11.5)	

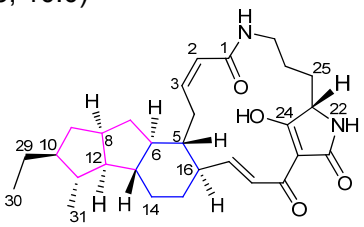

pactuamide A (**11**)

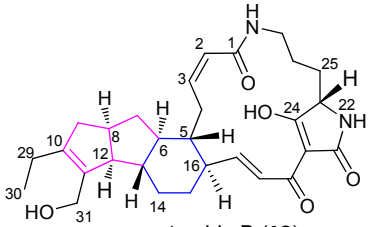

pactamide B (**12**)

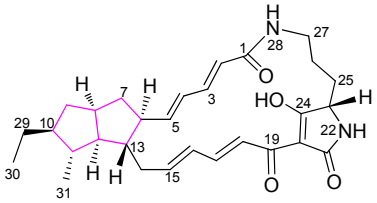

pactamide C (**13**)

[a]measured in 90% $CDCl_3$/methanol-d_4; [b]measured in DMSO-d_6.

Table S5. ^{13}C (125 MHz) NMR Data for pactamides A-C (**11**-**13**).

No.	**11**[a]	**12**[b]	**13**[b]
	δ_C, type	δ_C, type	δ_C, type
1	167.8, C	165.5, C	165.5, C
2	123.3, CH	124.2, CH	123.9, CH
3	141.7, CH	139.1, CH	139.1, CH
4	28.9, CH_2	28.6, CH_2	128.6, CH
5	44.6, CH	43.8, CH	145.4, CH
6	49.6, CH	46.7, CH	56.7, CH
7	37.4, CH_2	38.7, CH_2	42.2, CH_2
8	41.5, CH	37.4, CH	41.0, CH
9	40.7, CH_2	41.6, CH_2	40.1, CH_2
10	53.9, CH	136.6, C	53.6, CH
11	46.7, CH	137.4, C	46.9, CH
12	58.8, CH	57.6, CH	60.1, CH
13	53.4, CH	52.3, CH	51.1, CH
14	30.4, CH_2	30.5, CH_2	39.1, CH_2
15	32.8, CH_2	32.0, CH_2	139.8, CH
16	45.7, CH	46.3, CH	133.7, CH
17	147.8, CH	150.7, CH	138.4, CH
18	128.3, CH	121.4, CH	129.2, CH
19	183.7 C	171.5, C	181.4, C
20	101.5, C	100.6, C	102.4, C
21	178.2, C	175.2, C	177.9, C
23	59.6, CH	61.0, CH	59.7, CH
24	196.8, C	195.8, C	195.4, C
25	25.6, CH_2	26.1, CH_2	27.4, CH_2
26	20.8, CH_2	20.4, CH_2	22.1, CH_2
27	38.4, CH_2	38.0, CH_2	38.4, CH_2
29	26.1, CH_2	20.9, CH_2	26.2, CH_2
30	12.6, CH_3	13.0, CH_3	12.9, CH_3
31	19.2, CH_3	55.9, CH_2	19.4, CH_3

[a]measured in 90% $CDCl_3$/methanol-d_4; [b]measured in DMSO-d_6.

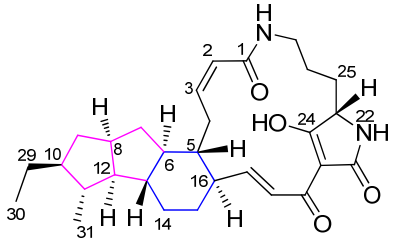

pactamide A (**11**)

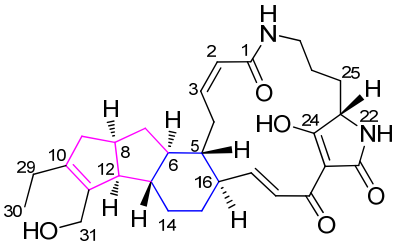

pactamide B (**12**)

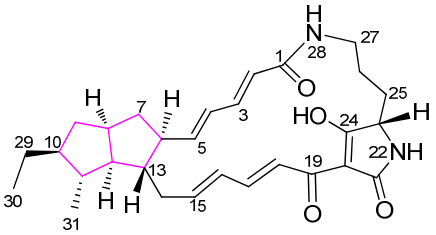

pactamide C (**13**)

Table S6. ^{1}H NMR data for pactamides D-F (**14-16**).

No.	**14**[a]	**15**[b]	**16**[a]
	δ_H, mult. (*J* in Hz)	δ_H, mult. (*J* in Hz)	δ_H, mult. (*J* in Hz)
2	5.77, d (11.0)	5.92, d (15.0)	5.78, d (10.5)
3	5.92, dd (11.0, 10.0)	6.90, dd (15.0, 11.1,)	5.92, t (11.1, 10.5)
4	1.90, m	6.29, dd (14.5, 11.1)	1.92, m
	3.39,m		3.34, m
5	1.16, m	6.38, dd (14.5, 10.5)	1.25, m
6	1.45, m	6.02, dd, (15.0, 10.5)	1.58, m
7	0.76, m	5.44, dd, (15.0, 8.9)	0.83, m
	1.98, m		1.92, m
8	2.96, br s	2.93, m	2.25, m
9	5.24, br s	1.12, m,	1.05, m
		2.07, m,	1.92, m
10		1.36, m	1.76, m
11	2.72, br s	1.39, m,	
12	2.36, m	2.45, m	2.19, m
13	1.25, m	5.55, dd (15.5, 8.2)	1.59, m
14	1.74, m	5.98, dd, (15.5, 10.5)	1.04, m
	2.15, m		1.99, m
15	1.21, m	6.46, dd, (15.0, 10.5)	1.21, m
	1.60, m		1.61, m
16	1.88, m	6.21, dd, (15.0, 11.5)	1.92, m
17	6.22, dd (10.5, 14.5)	7.06, dd (14.5, 11.5)	6.25, dd (15.0, 10.0)
18	7.42, d (14.5)	7.50, d (14.5)	7.41, d (15.0)
22		7.64, s	
23	3.44, m	3.52, m	3.46, m
25	1.72, m	1.77, m,	1.74, m
		1.70. m	
26	1.19, m	0.95, m,	1.21, m
	1.25, m	1.50, m	1.26, m
27	2.33, m	2.56, m	2.32, m
	3.29, m	3.49, m	3.29, m
28	7.74, br s	7.74, br s	7.71, br s
29	1.89, m	1.14, m	1.22, m
	2.22, m	1.61, m	1.40, m
30	0.97, t	0.92, t (7.4)	0.83, t (7.0)
31	3.54, m	0.99, d (7.4)	3.51, s
	3.63, m		
10-OH			4.33, s
31-OH	4.49		

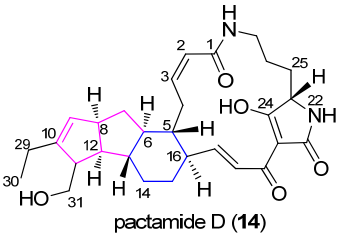
pactamide D (**14**)

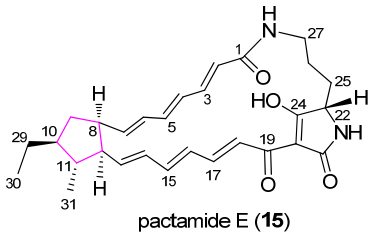
pactamide E (**15**)

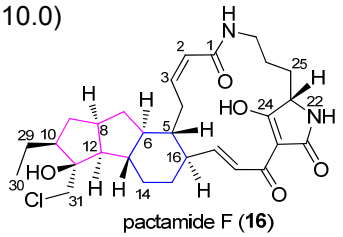
pactamide F (**16**)

[a]measured at 500 MHz in DMSO-d_6; [b]measured at 600 MHz in DMSO-d_6

Table S7. ^{13}C NMR data for pactamides D-F (**14-16**).

No.	**14**[a]	**15**[b]	**16**[a]
	δ_C, type	δ_C, type	δ_C, type
1	165.5, C	165.6, C	165.4, C
2	124.5, CH	124.7, CH	124.5, CH
3	138.3, CH	139.0, CH	138.3, CH
4	28.6, CH_2	128.6, CH	28.4, CH_2
5	45.0, CH	138.7, CH	44.5, CH
6	46.5, CH	131.3, CH	48.7, CH
7	35.6, CH_2	142.1, CH	36.7, CH_2
8	50.6, CH	46.2, CH	40.4, CH
9	127.8, CH	38.4, CH_2	36.4, CH_2
10	144.0, C	49.3, CH	51.1, CH
11	46.8, CH	45.9, CH	79.4, C
12	50.3, CH	52.2, CH	56.1, CH
13	44.5, CH	139.1, CH	48.7, CH
14	30.8, CH_2	134.8, CH	31.4, CH_2
15	32.8, CH_2	138.1, CH	32.9, CH_2
16	44.7, CH	130.6, CH	44.4, CH
17	143.8, CH	138.6, CH	145.5, CH
18	129.1, CH	130.2, CH	128.7, CH
19	181.0, C	181.2, C	180.6, C
20	102.0, C	102.1, C	101.6, C
21	177.1, C	177.6, C	177.5, C
23	59.1, CH	59.7, CH	59.2, CH
24	195.4, C	195.9, C	195.1, C
25	26.5, CH_2	28.2, CH_2	26.5, CH_2
26	20.9, CH_2	23.4, CH_2	20.9, CH_2
27	37.8, CH_2	38.3, CH_2	37.7, CH_2
29	22.2, CH_2	26.6, CH_2	20.3, CH_2
30	12.3, CH_3	12.9, CH_3	12.9, CH_3
31	59.4, CH_2	18.5, CH_3	49.8, CH_2

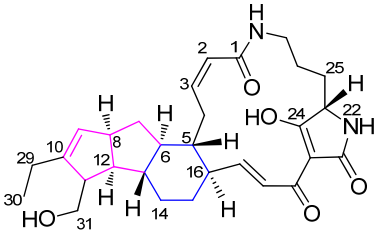

pactamide D (**14**)

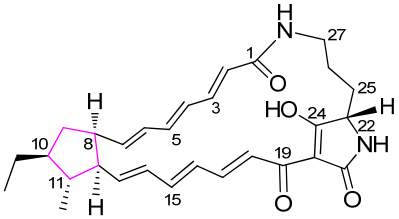

pactamide E (**15**)

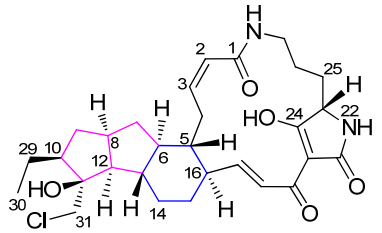

pactamide F (**16**)

[a]measured at 500 MHz in DMSO-d_6; [b]measured at 600 MHz in DMSO-d_6

Table S8. ^{1}H (500 MHz) and ^{13}C (125 MHz) NMR data for **18**.[14]

No.	**18**	
	δ_H, mult. (*J* in Hz)	**δ_C, type**
1		174.5, C
2	2.90, br d (12.0)	42.9, CH_2
	3.34, m[a]	
3	5.41, dd (9.0, 14.5)	130.8, CH
4	5.29, dd (9.0, 14.5)	136.4, CH
5	1.81, m	53.0, CH
6	2.23, m	50.2, CH
7	5.50, d (10.0)	133.2, CH
8	5.82, d (10.0)	135.4, CH
9	1.53, m	49.2, CH
10	1.30, m	49.2, CH
11	2.23, m	35.3, CH
12	0.69, m	40.7, CH_2
	2.06, m	
13	1.09, m	51.0, CH
14	2.06, m	44.6, CH
15	1.37, m	39.4, CH_2
	2.23, m	
16	2.46, m	51.7, CH
17	6.64, br s	157.7, CH
18	7.05, br s	129.4, CH
19		181.3, C
20		99.9, C
21		187.0, C
23	3.80, br s	58.3, CH
24		200.0, C
25	1.81, m	32.0, CH_2
	1.95, m	
26	1.09, m	24.7, CH_2
	1.53, m	
27	2.90, m	40.6, CH_2
	3.34, ovelapping	
29	1.30, m	23.9, CH_2
	1.40, m	
30	0.82, d (7.0)	15.5, CH_3
31	0.88, t (7.0, 7.0)	20.0, CH_3

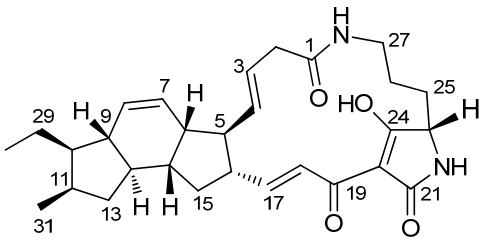

isoikarugamycin (**18**)

[a]Overlapping; measured in 90% $CDCl_3$/methanol-d_4; data were recorded on Bruker DRX-500 MHz.

Fig. S1. Scheme for inserting *ermE**p promoter in front of *ptmA*.

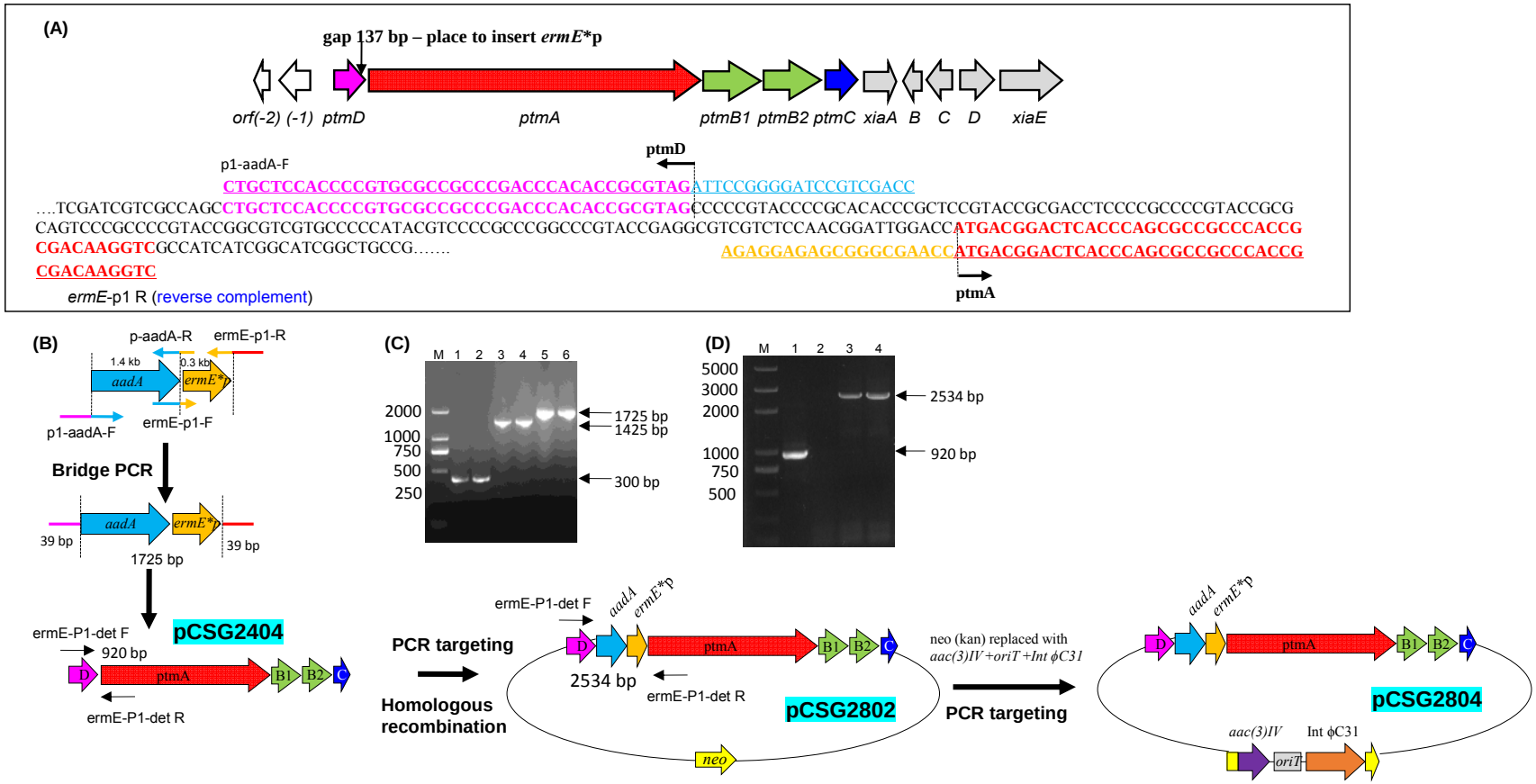

(A) the insertion of the *ermE**p promoter in front of *ptmA* and the design of primers used for the insertion. (B) a schematic depiction for constructing pCSG2804. (C) Gel electrophoresis of for Bridge PCR. Lane M, DNA marker D2000 (GenStar); lanes 1-2, 300 bp *ermE**p promoter from pPWW50A; lanes 3-4, 1425 bp *aadA* from pIJ773; lanes 5-6, 1725 bp fragment containg *ermE**p and *aadA* by bridge PCR. (D) Gel electrophoresis of PCR products for proofing of promoter insertion in front of *ptmA* using detection primers ermE-P1-det F and R. Lane M, DNA marker D2000; lane 1, pCSG2404 as a template; lanes 2-3, pCSG2802 as a template. The cosmid pCSG2804 was selected by the phenotype as Apr^R/Neo^S.

Fig. S2. Scheme for inserting *ermE**p promoter in front of *ptmD*.

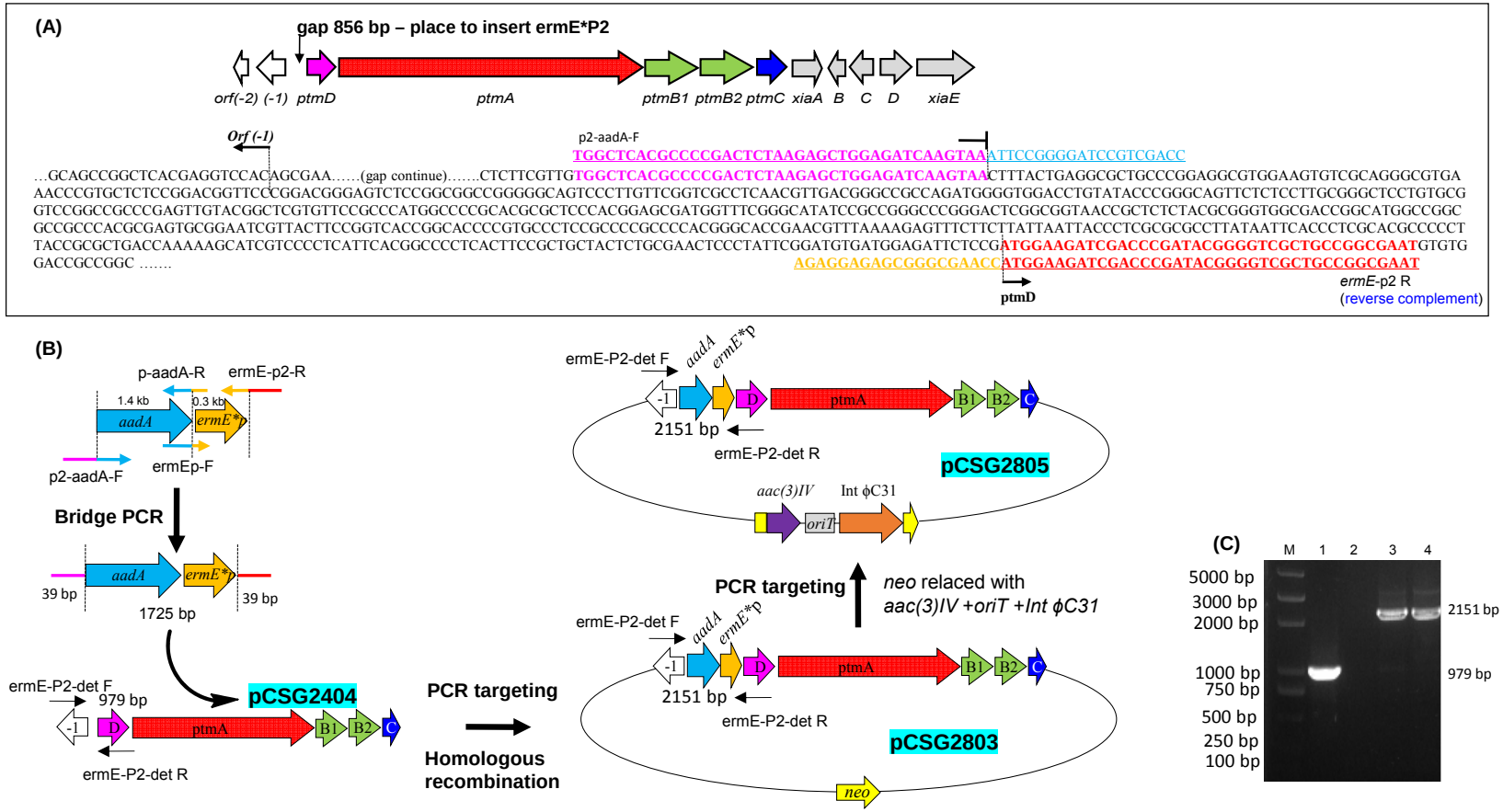

(A) the insertion of the *ermE**p promoter in front of *ptmD* and the design of primers used for the insertion. (B) a schematic depiction for constructing pCSG2805. (D) Gel electrophoresis of PCR products for proofing of promoter insertion in front of *ptmD* using detection primers ermE-P2-det F and R. Lane M, DNA marker D2000; lane 1, pCSG2404 as a template; lanes 2-3, pCSG2803 as a template. The cosmid pCSG2805 was selected by the phenotype as Apr^R/Neo^S.

Fig. S3. In-frame deletion of *ptmC* with *ermE**p promoter inserted in front of *ptmA*.

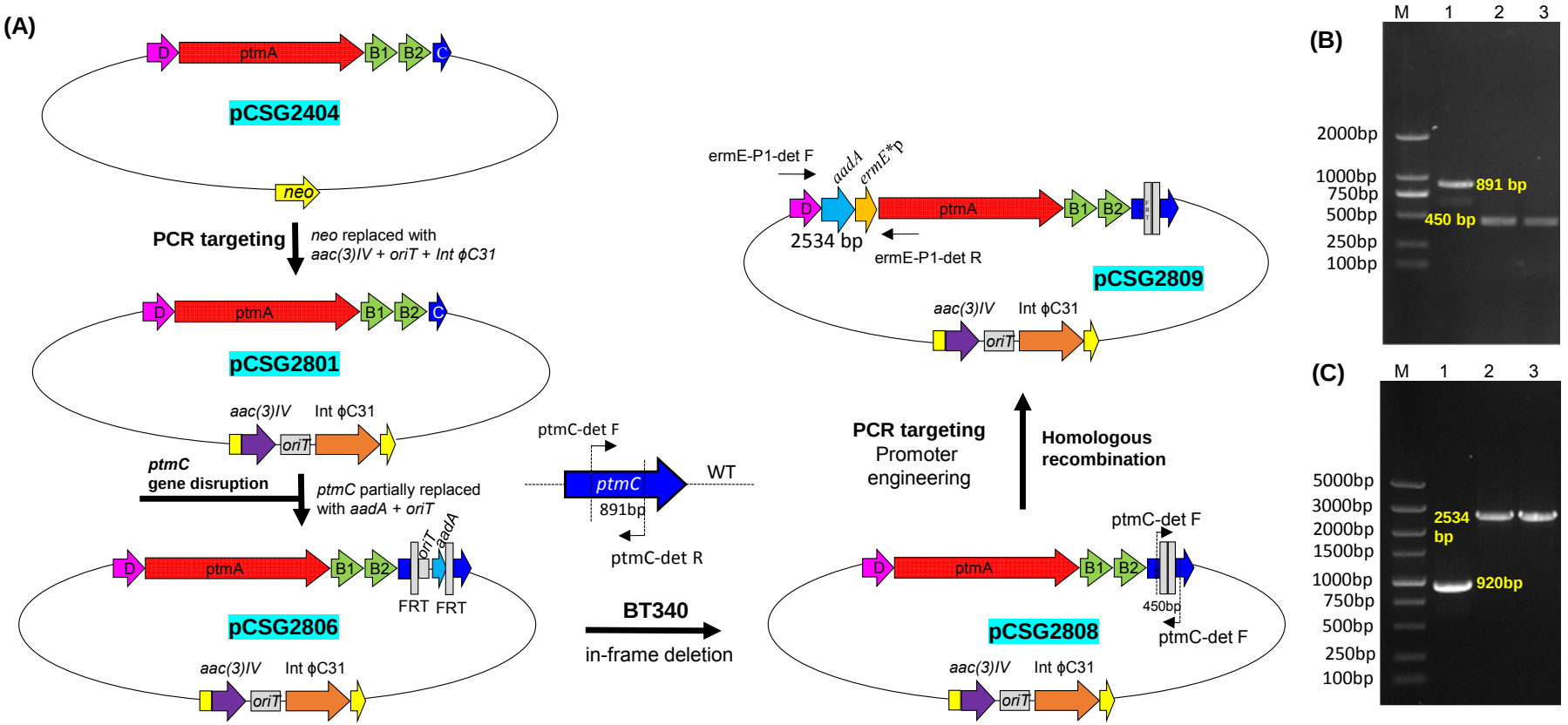

(A) a schematic depiction for constructing pCSG2809 where *ptmC* was disrupted by in-frame deletion and the *ermE**p promoter was inserted in front of *ptmA*. (B) Gel electrophoresis of PCR products for proofing pCSG2808. Lane M, DNA marker D2000; lane 1, pCSG2404 as a template using primers ptmC-det F and R; lanes 2-3, pCSG2808 as a template. (C) Gel electrophoresis of PCR products for proofing promoter insertion in pCSG2809. Lane M, DNA marker D5000; lane 1, pCSG2404 as a template using primers ermE-P1-det F and R; lanes 2-3, pCSG2809 as a template. The cosmid pCSG2809 was selected by the phenotype as Apr^R/Neo^S

Fig. S4. In-frame deletion of *ptmB1* with *ermE**p promoter inserted in front of *ptmA*.

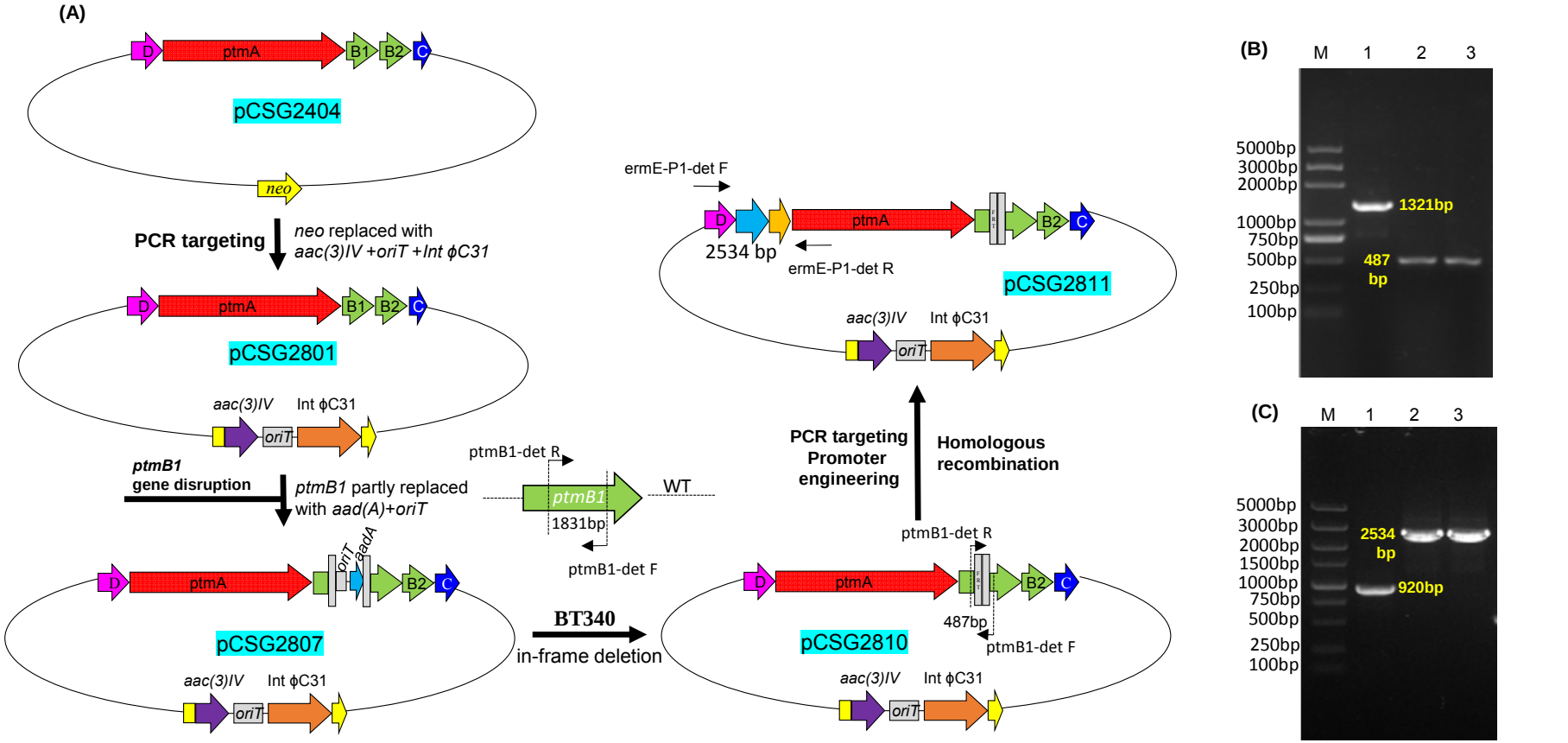

(A) a schematic depiction for constructing pCSG2811where *ptmB1* was disrupted by in-frame deletion and the *ermE**p promoter was inserted in front of *ptmA*. (B) Gel electrophoresis of PCR products for proofing pCSG2810. Lane M, DNA marker D2000 plus; lane 1, pCSG2404 as a template using primers ptmB1-det F and R; lanes 2-3, pCSG2810 as a template. (C) Gel electrophoresis of PCR products for proofing promoter insertion in pCSG2811. Lane M, DNA marker D5000; lane 1, pCSG2404 as a template using primers ermE-P1-det F and R; lanes 2-3, pCSG2811 as a template. The cosmid pCSG2811 was selected by the phenotype as Apr^R/Neo^S

Fig. S5. In-frame deletion of *ptmB2* with *ermE**p promoter inserted in front of *ptmA*.

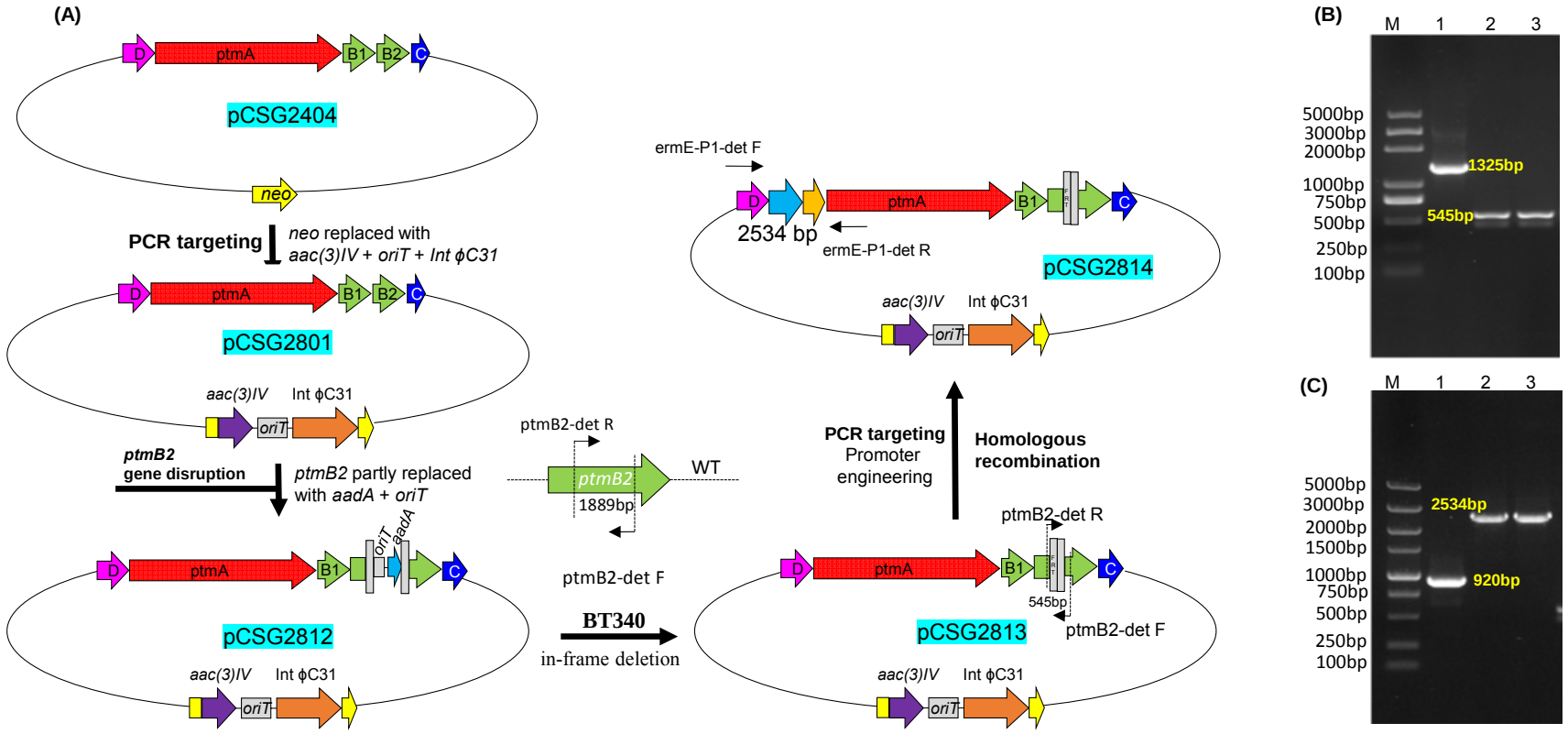

(A) a schematic depiction for constructing pCSG2814where *ptmB2* was disrupted by in-frame deletion and the *ermE**p promoter was inserted in front of *ptmA*. (B) Gel electrophoresis of PCR products for proofing pCSG2813. Lane M, DNA marker D2000 plus; lane 1, pCSG2404 as a template using primers ptmB2-det F and R; lanes 2-3, pCSG2813 as a template. (C) Gel electrophoresis of PCR products for proofing promoter insertion in pCSG2814. Lane M, DNA marker D5000; lane 1, pCSG2404 as a template using primers ermE-P1-det F and R; lanes 2-3, pCSG2814 as a template. The cosmid pCSG2814 was selected by the phenotype as Apr^{R}/Neo^{S}

Fig. S6. Characterization of compound **10** produced by *S. lividans* TK64/pCSG2814.

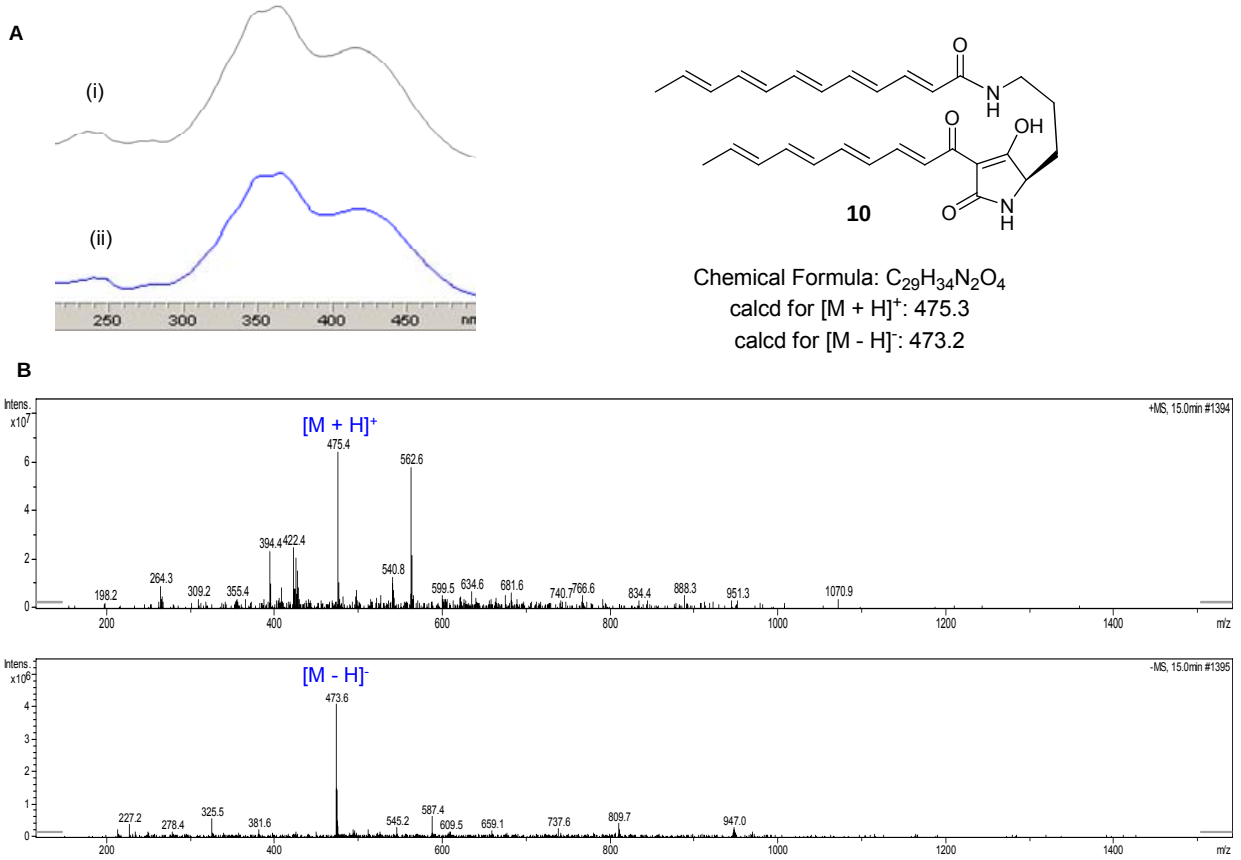

(A) comparison of UV spectra of compound **10** from (i) the Δ*ikaB* mutant of *Streptomyces* sp. ZJ306[8] and (ii) *S. pactum* 2999PTMp1. (B) the LC-MS data of compound **10** from *S. lividans* TK64/pCSG2814.

Fig. S7. Spectral data for pactamide A (**11**).
(**A**) HRESIMS.

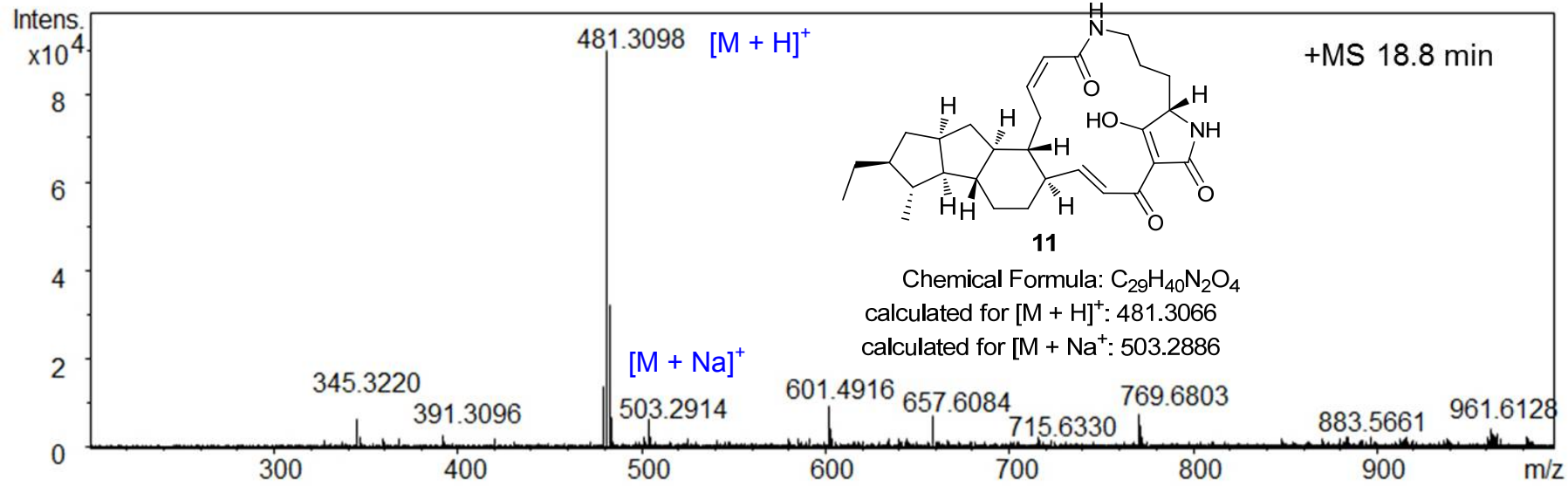

Fig. S7. Spectral data for pactamide A (**11**) (continued).
(**B**) ^{1}H NMR spectrum of pactamide A (**11**) in $CDCl_3/CD_3OD$ (9:1).

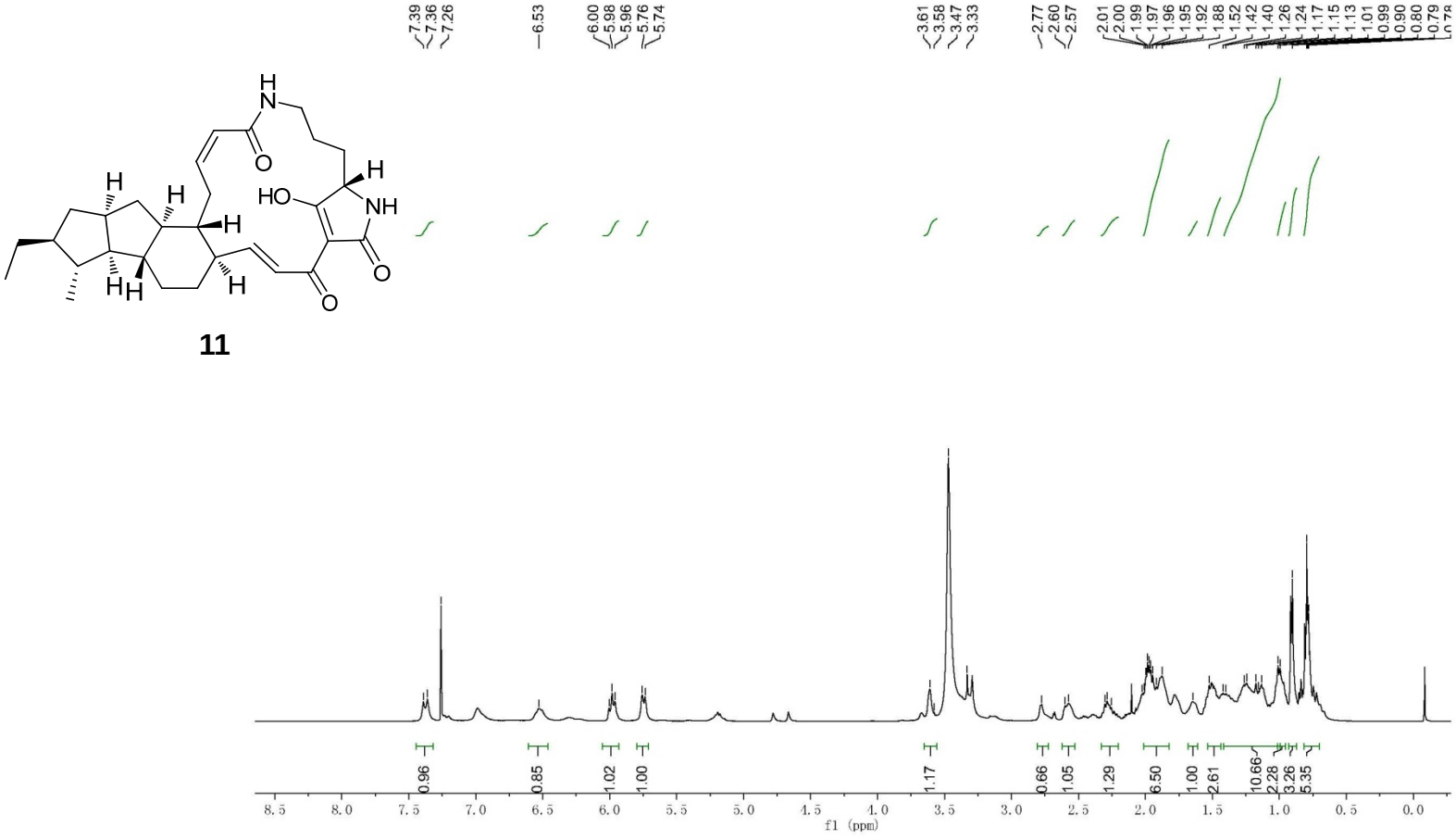

11

Fig. S7. Spectral data for pactamide A (**11**) (continued).

(**C**) The ^{13}C NMR spectrum of pactamide A (**11**) in $CDCl_3/CD_3OD$ (9:1).

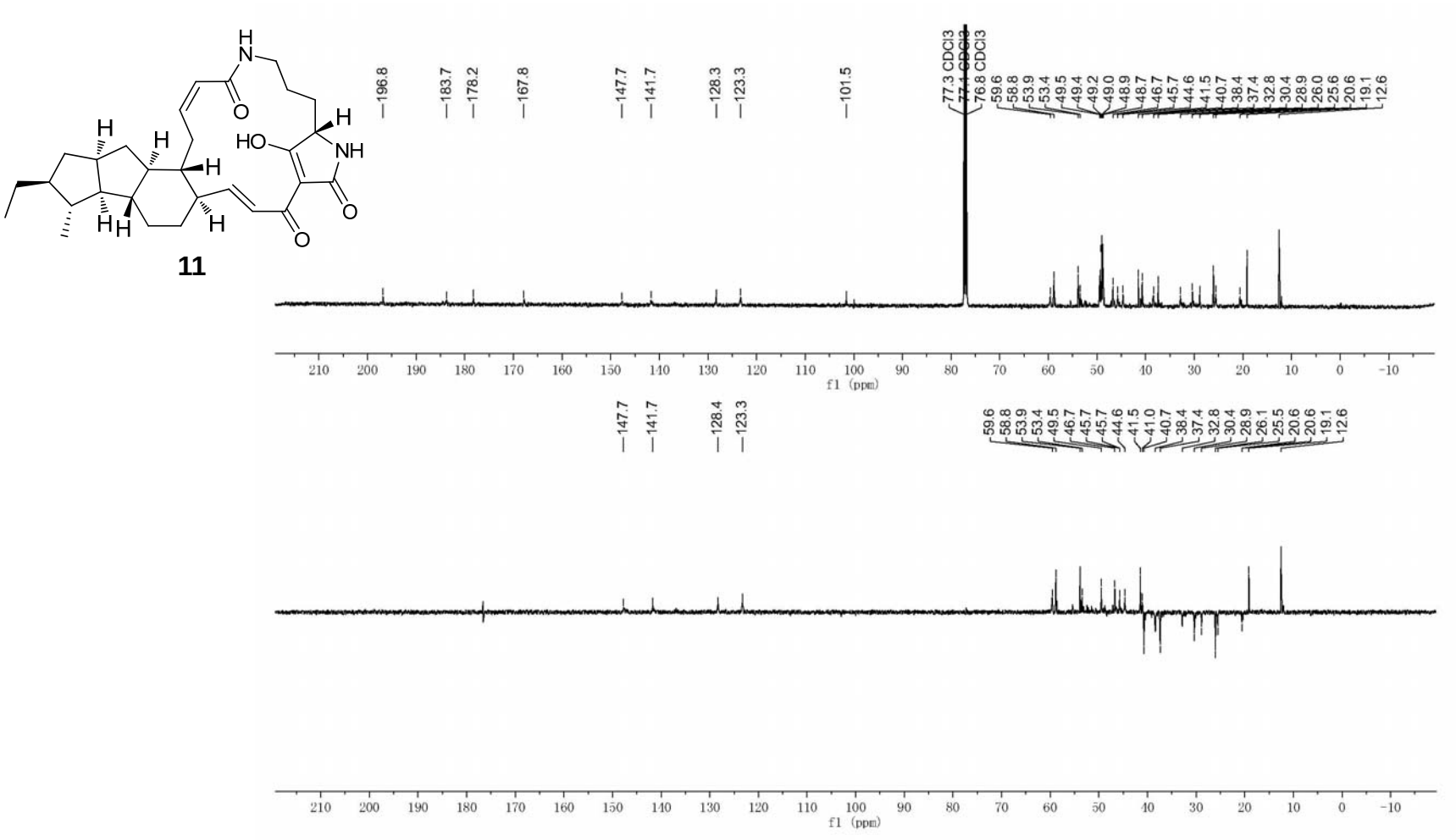

Fig. S7. Spectral data for pactamide A (**11**) (continued).
(**D**) The HSQC spectrum of pactamide A (**11**) in $CDCl_3/CD_3OD$ (9:1).

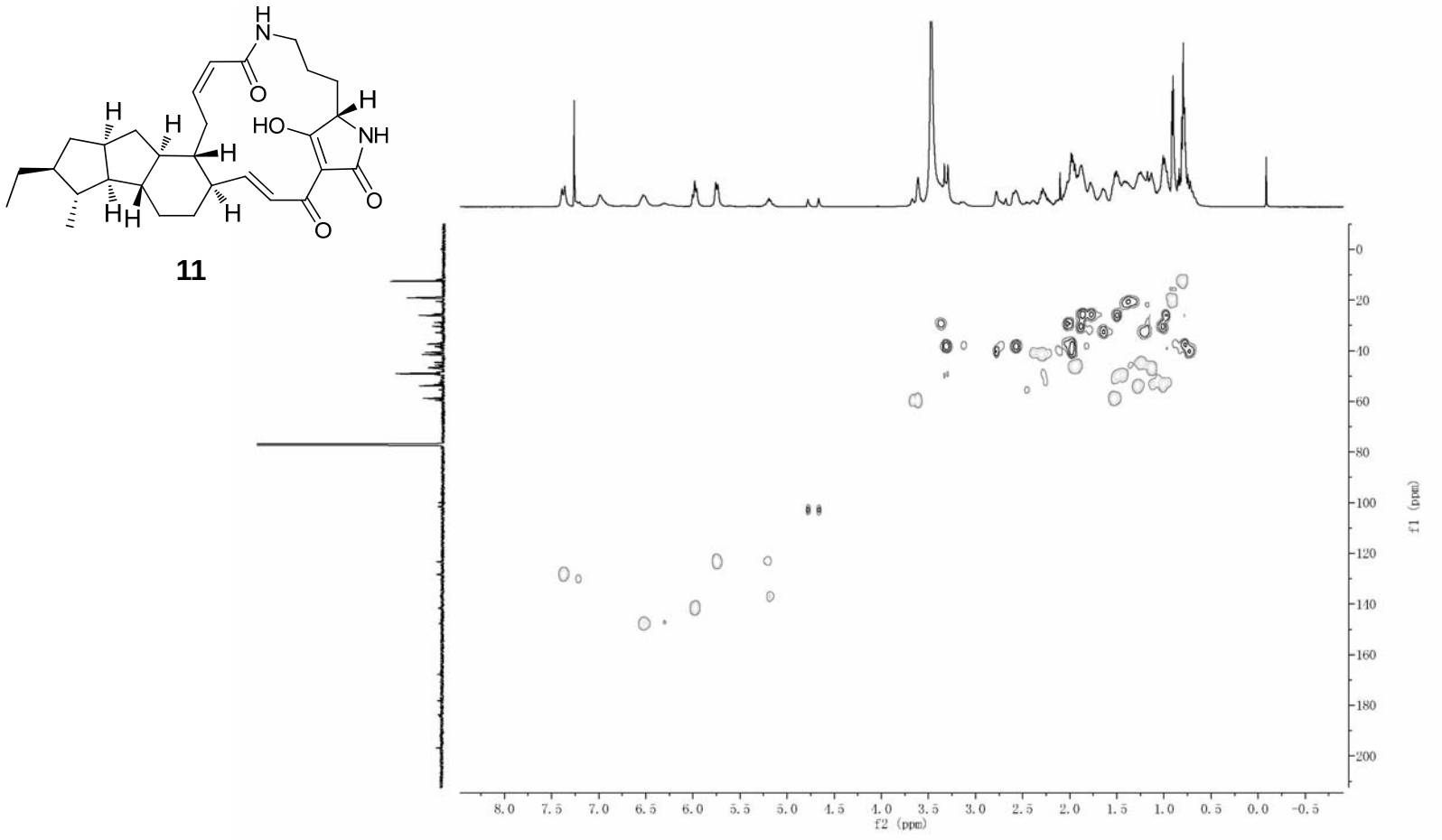

Fig. S7. Spectral data for pactamide A (**11**) (continued).

(**E**) The HMBC spectrum of pactamide A (**11**) in $CDCl_3/CD_3OD$ (9:1).

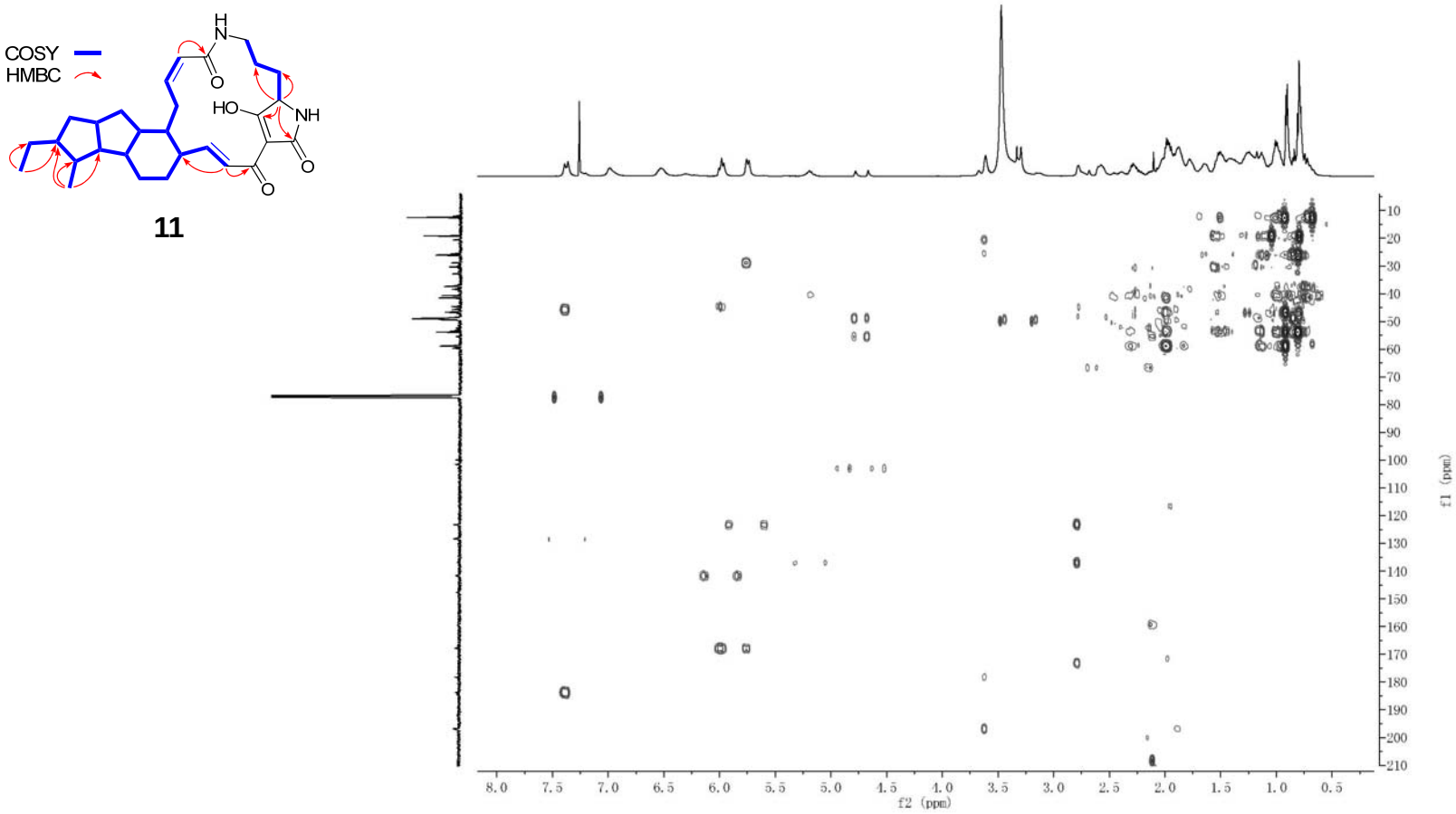

Fig. S7. Spectral data for pactamide A (**11**) (continued).
(**F**) The COSY spectrum of pactamide A (**11**) in $CDCl_3/CD_3OD$ (9:1).

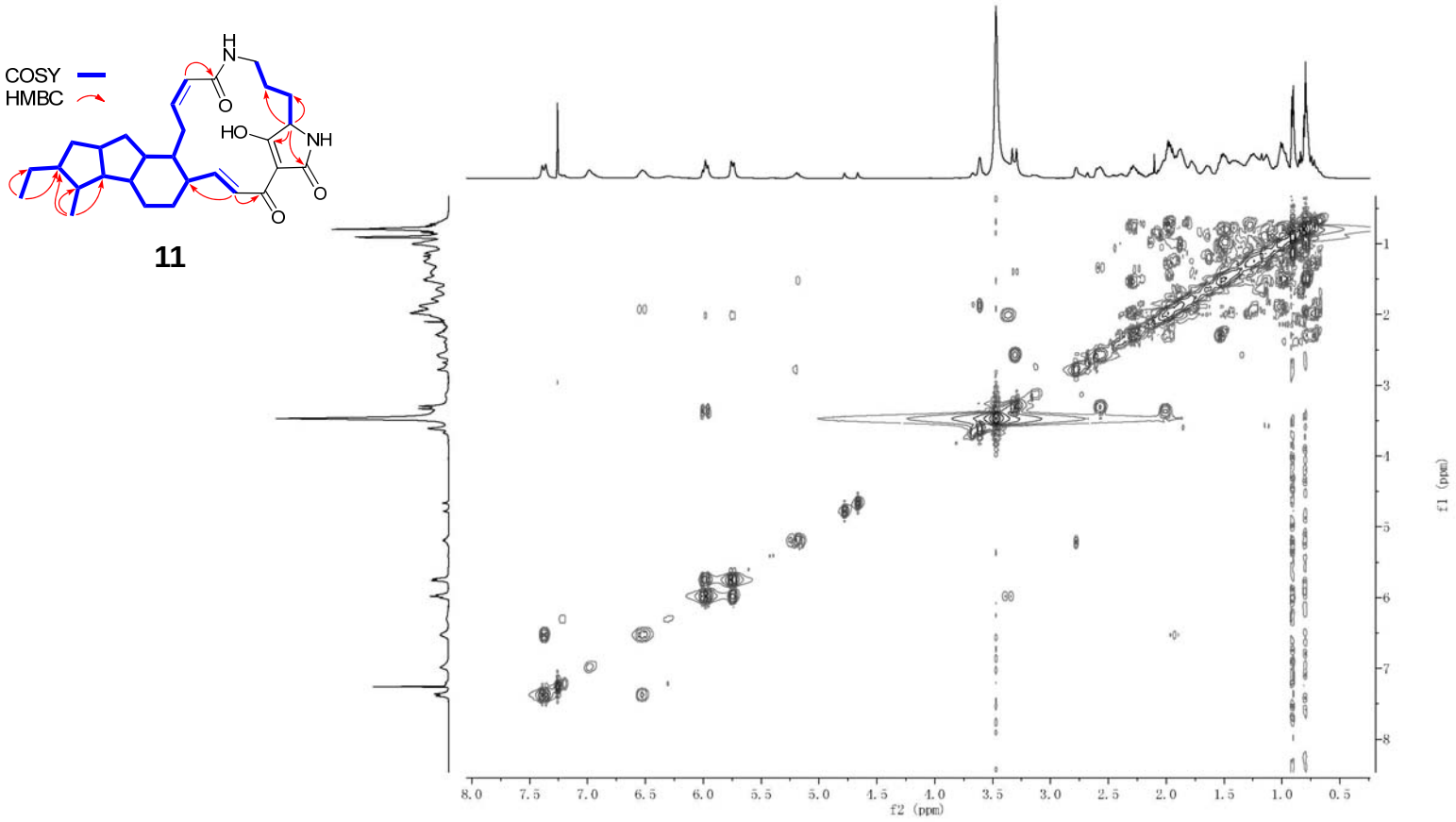

Fig. S7. Spectral data for pactamide A (**11**) (continued).
(**G**) The NOESY spectrum of pactamide A (**11**) in $CDCl_3/CD_3OD$ (9:1).

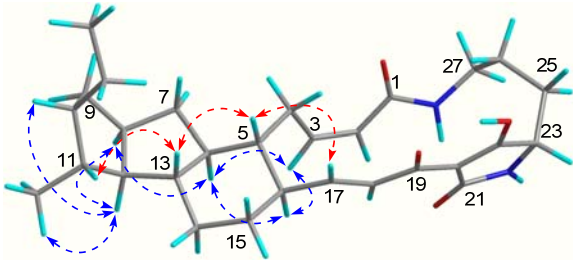

11

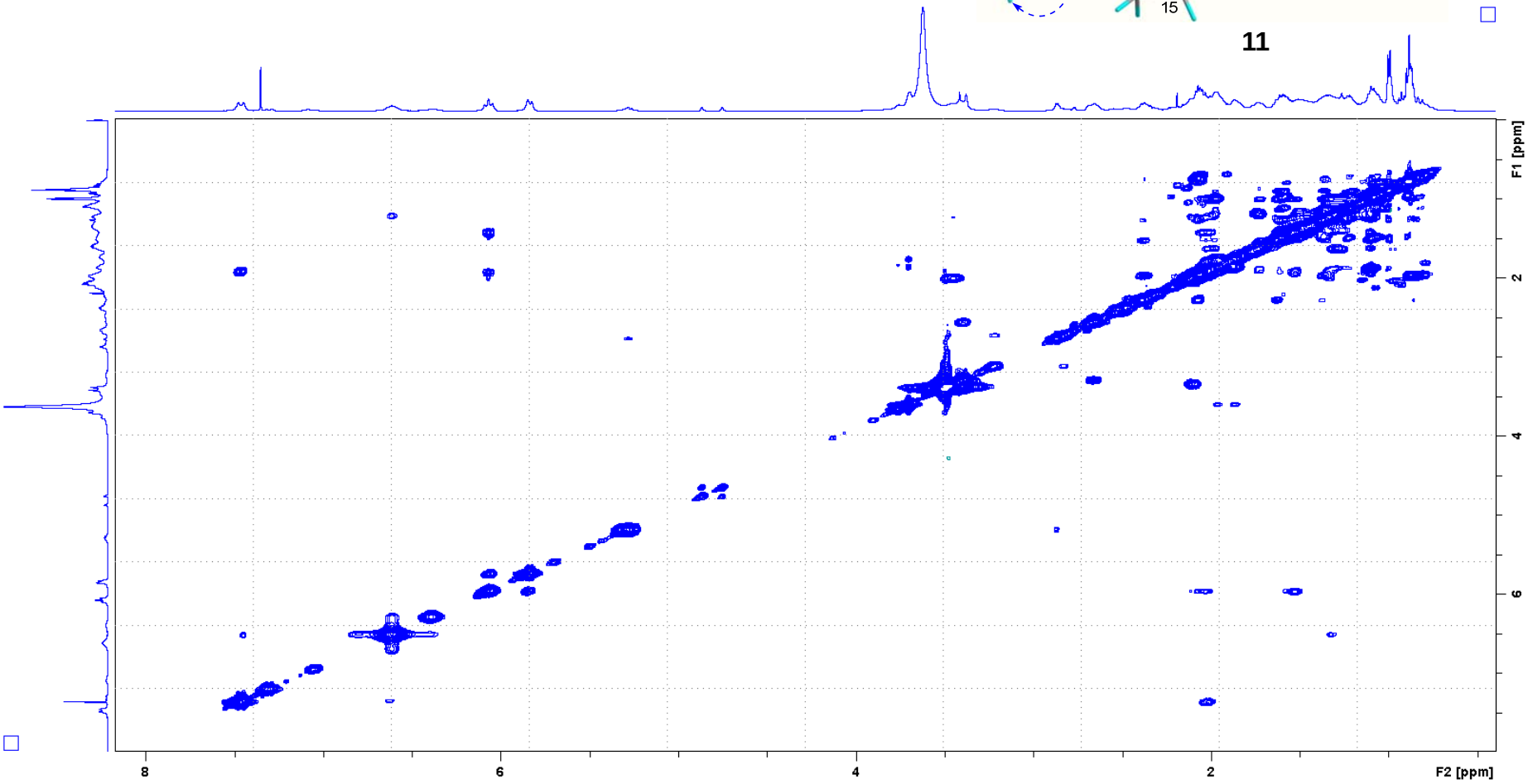

Fig. S7. Spectral data for pactamide A (**11**) (continued).
(**H**) The NOESY spectrum of pactamide A (**11**) in $CDCl_3/CD_3OD$ (9:1).

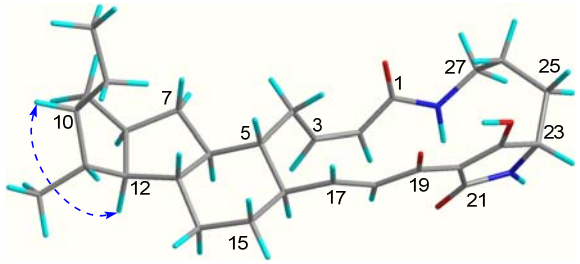

11

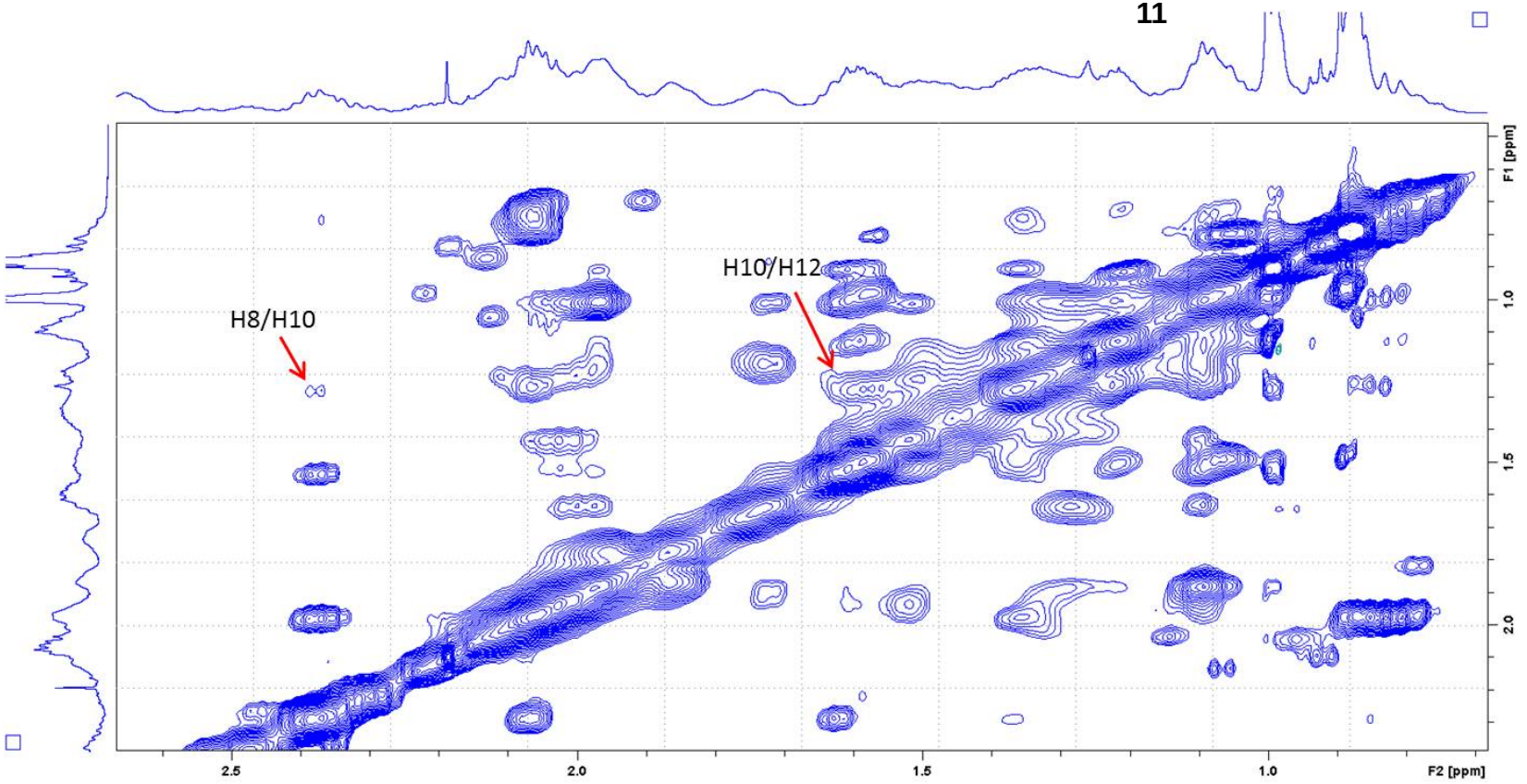

Fig. S8. Comparison of ECD spectra of pactamides, lysobacteramide B (**4**) and HSAF.

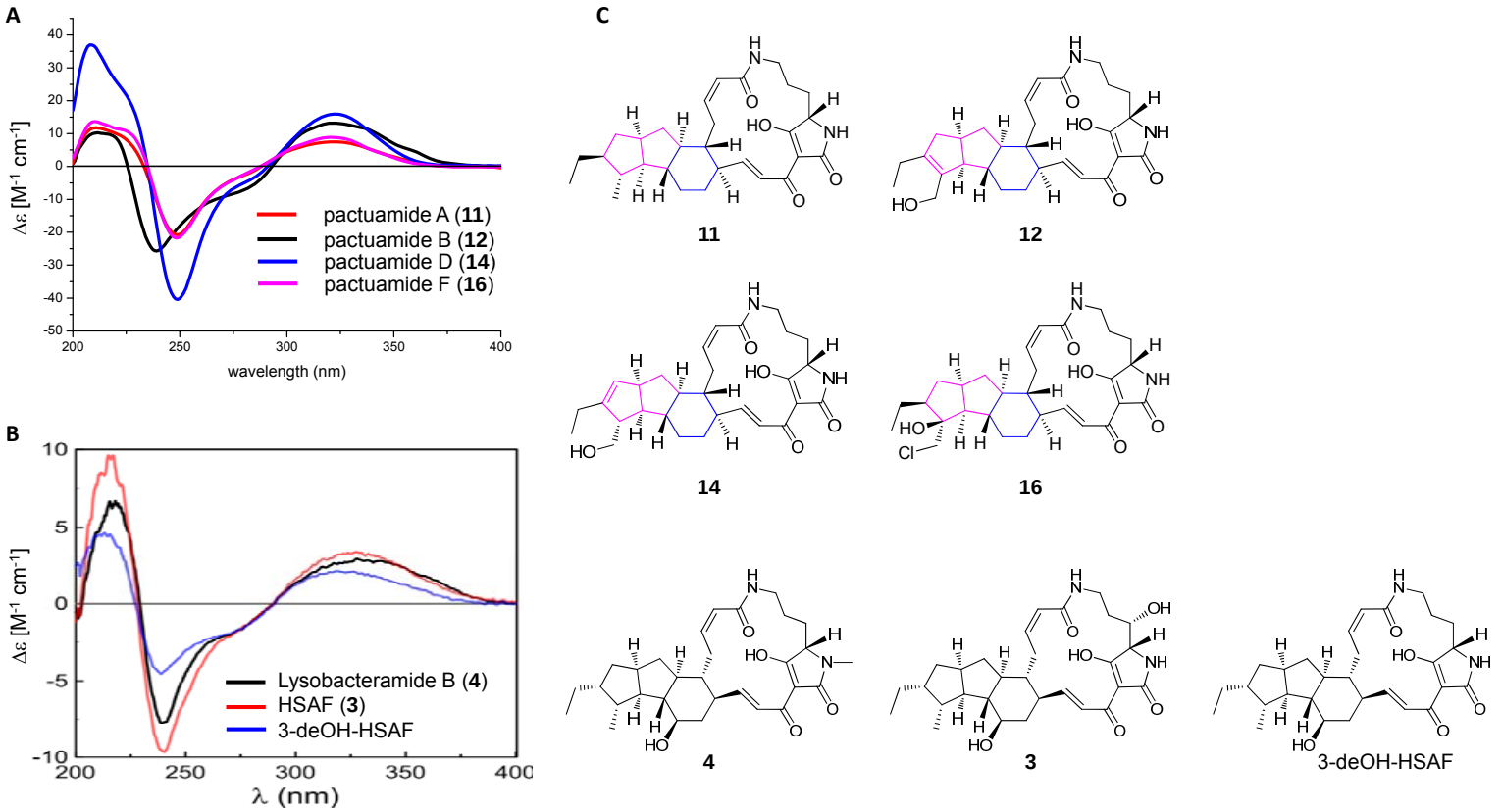

(A) ECD spectra measured for pactamides A (**11**), B (**12**), D (**14**) and F (**16**); (B) ECD spectra of lysobacteramide B (**4**), HSAF (**3**) and 3-deOH-HSAF from reference.[6] (C) Chemical structures.

Fig. S9. Spectral data for pactamide B (**12**).

(**A**) HRESIMS.

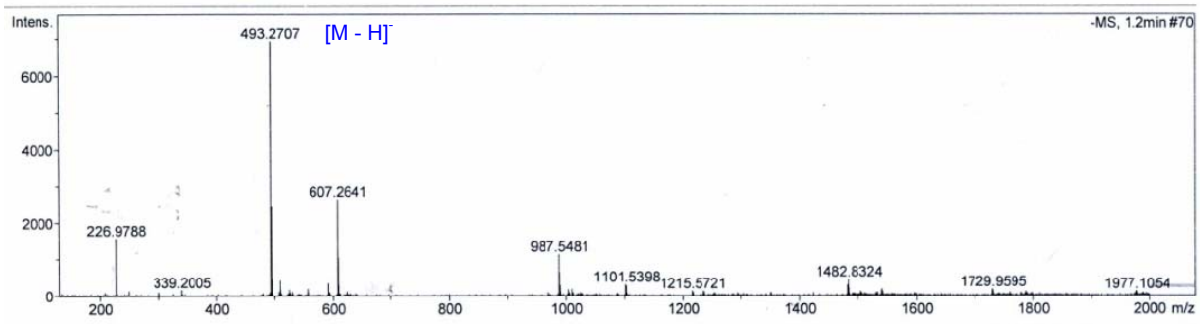

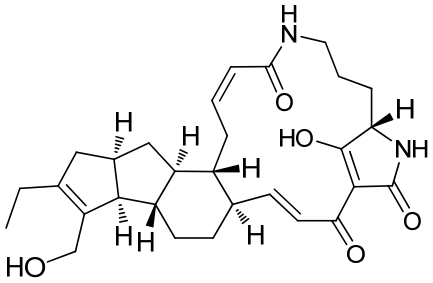

12

Chemical Formula: $C_{29}H_{38}N_2O_5$

calculated for $[M - H]^-$: 493.2702

Fig. S9. Spectral data for pactamide B (**12**) (continued).
(**B**) The ^{1}H NMR spectrum of pactamide B (**12**) in DMSO-d_6.

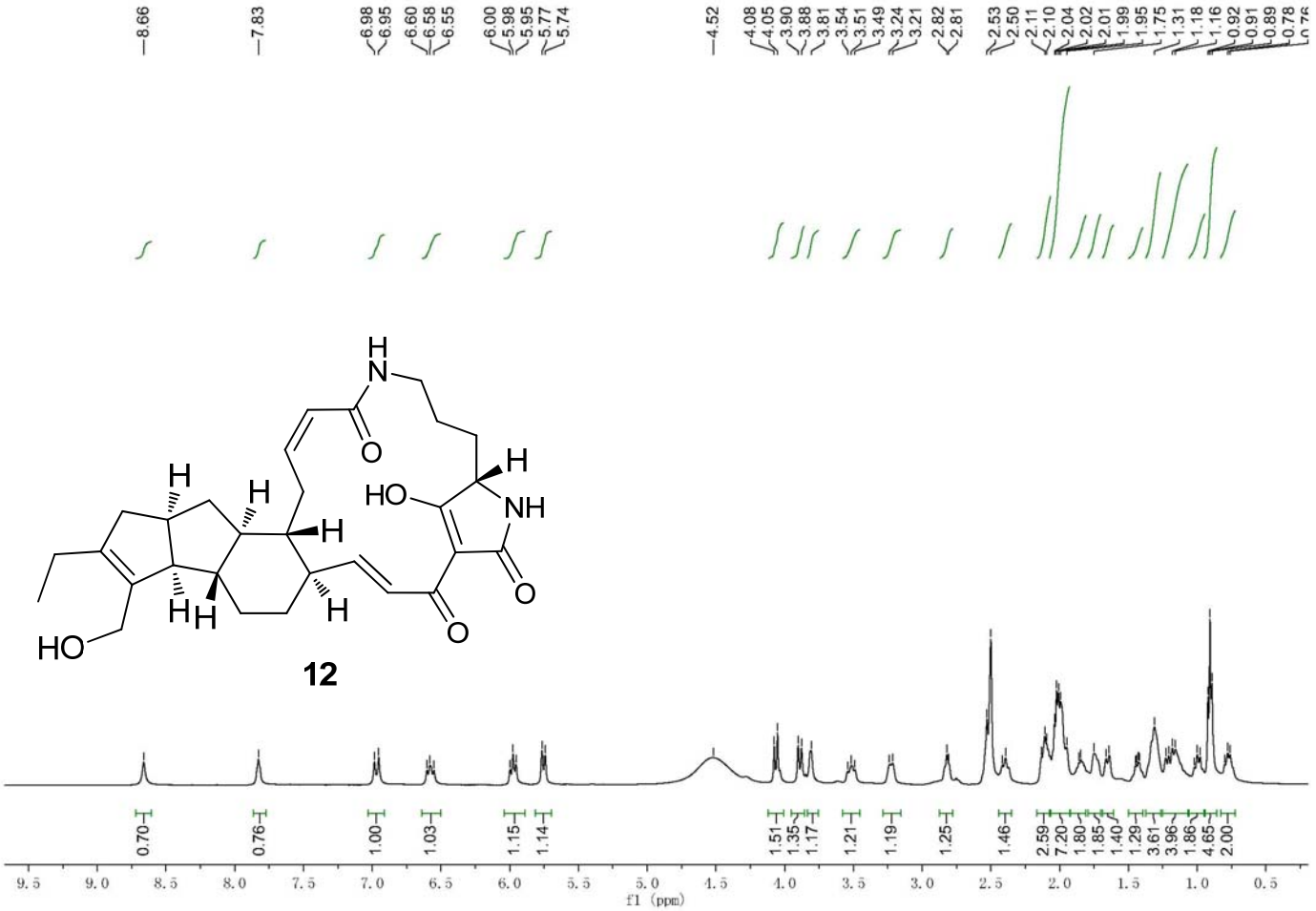

Fig. S9. Spectral data for pactamide B (**12**) (continued).
(**C**)The ^{13}C NMR spectrum of pactamide B (**12**) in DMSO-d_6.

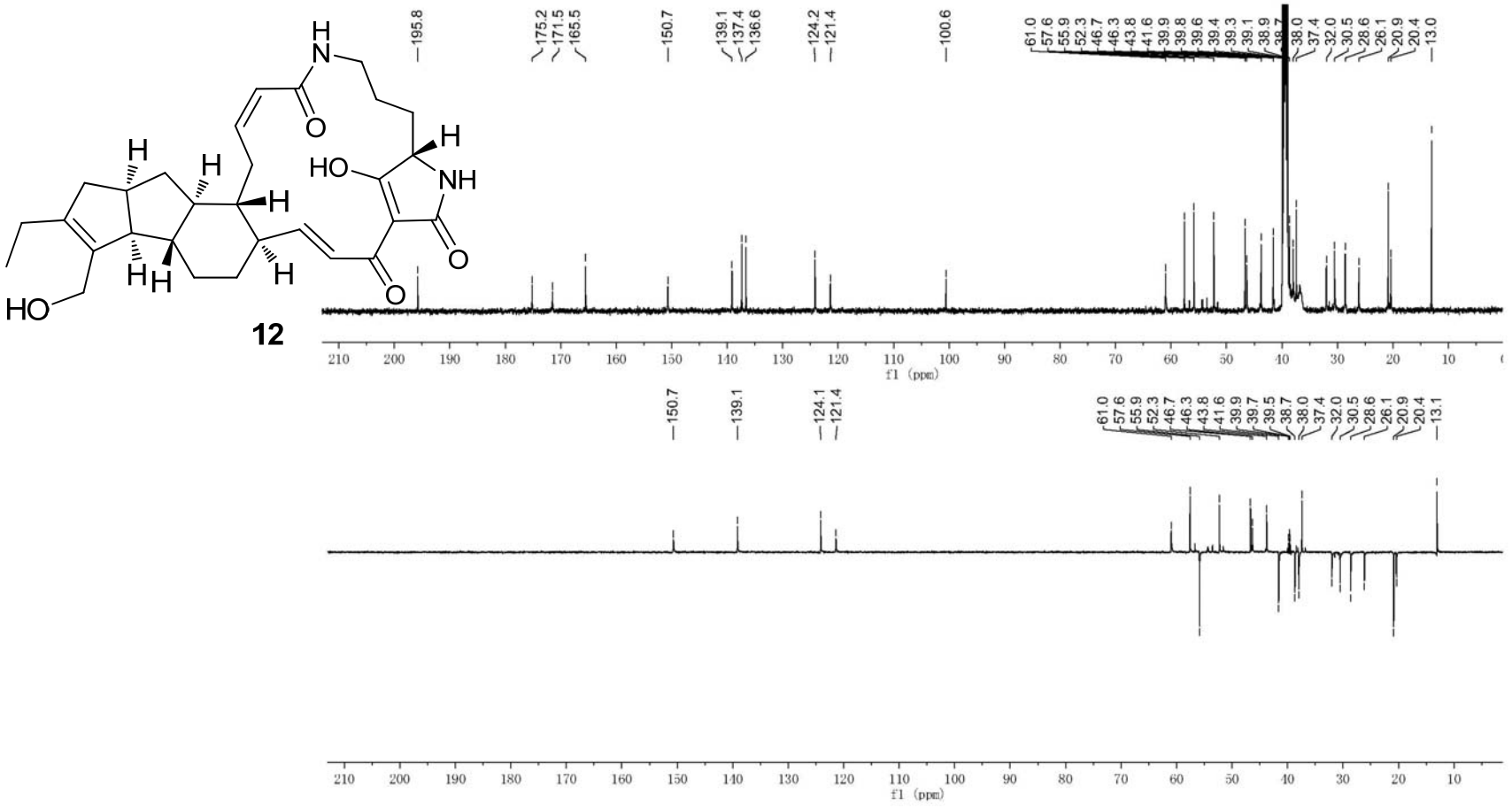

Fig. S9. Spectral data for pactamide B (**12**) (continued).
(**D**) The HSQC spectrum of pactamide B (**12**) in DMSO-d_6.

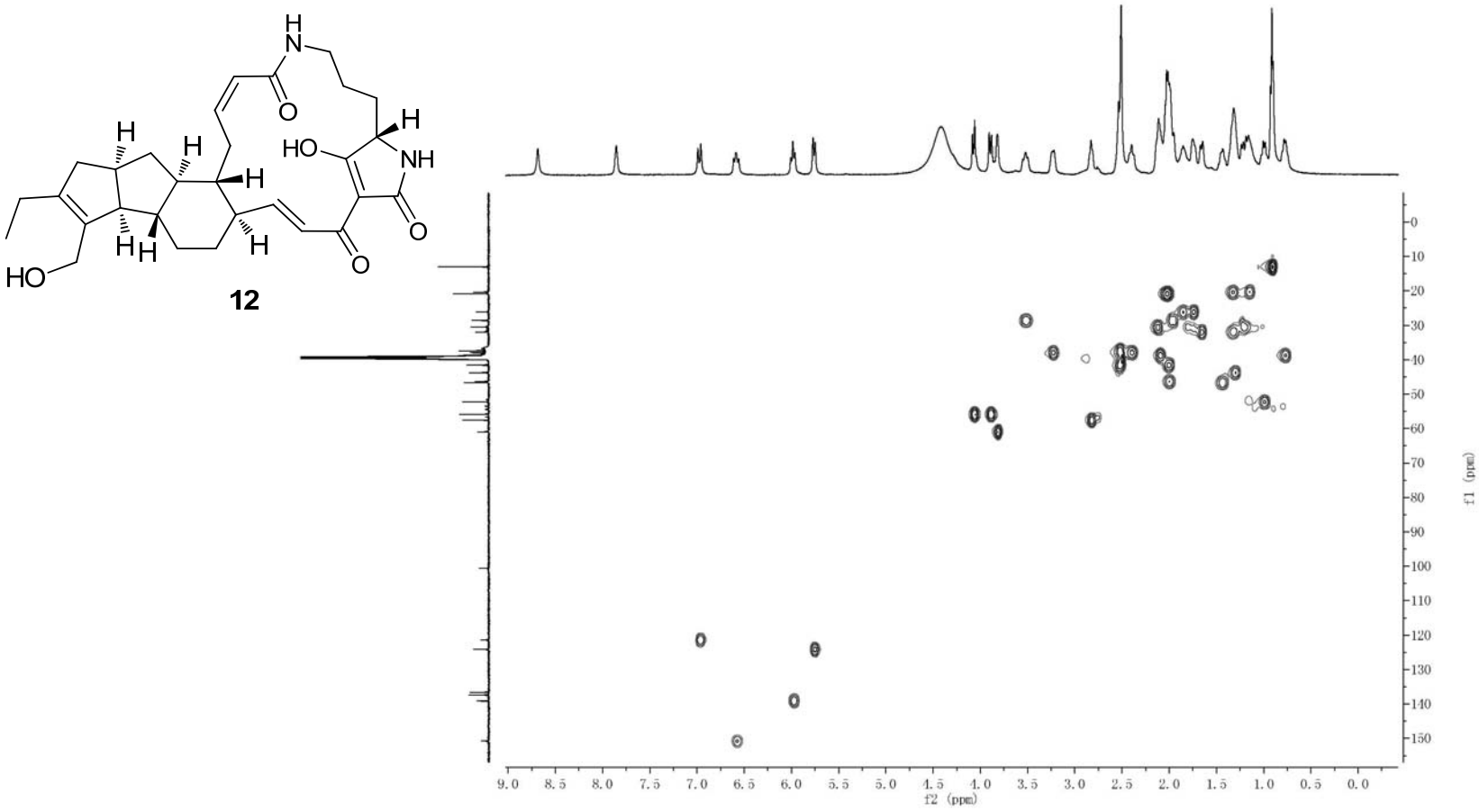

Fig. S9. Spectral data for pactamide B (**12**) (continued).
(**E**) The HMBC spectrum of pactamide B (**12**) in DMSO-d_6.

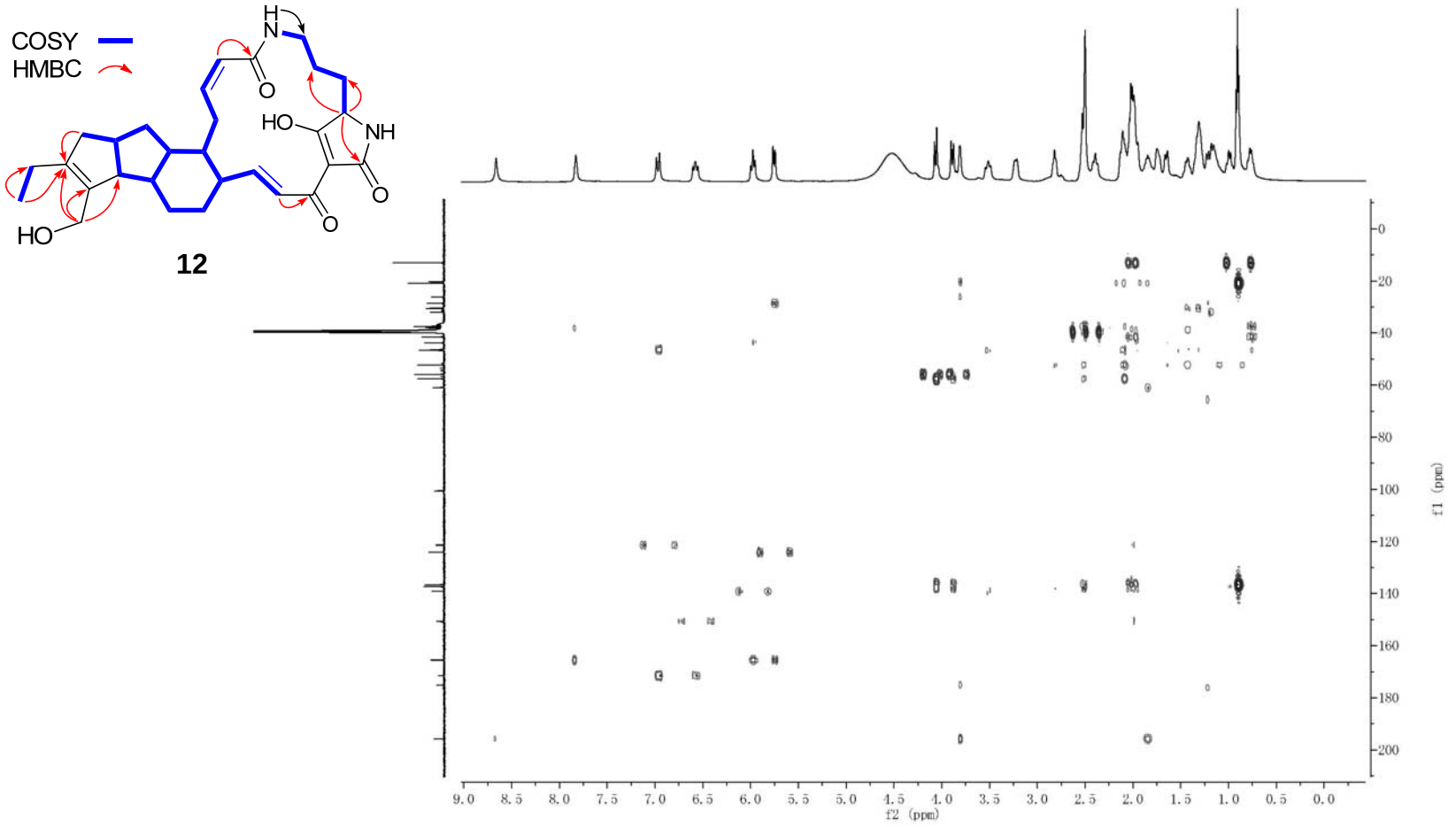

Fig. S9. Spectral data for pactamide B (**12**) (continued).
(**F**) The COSY spectrum of pactamide B (**12**) in DMSO-d_6.

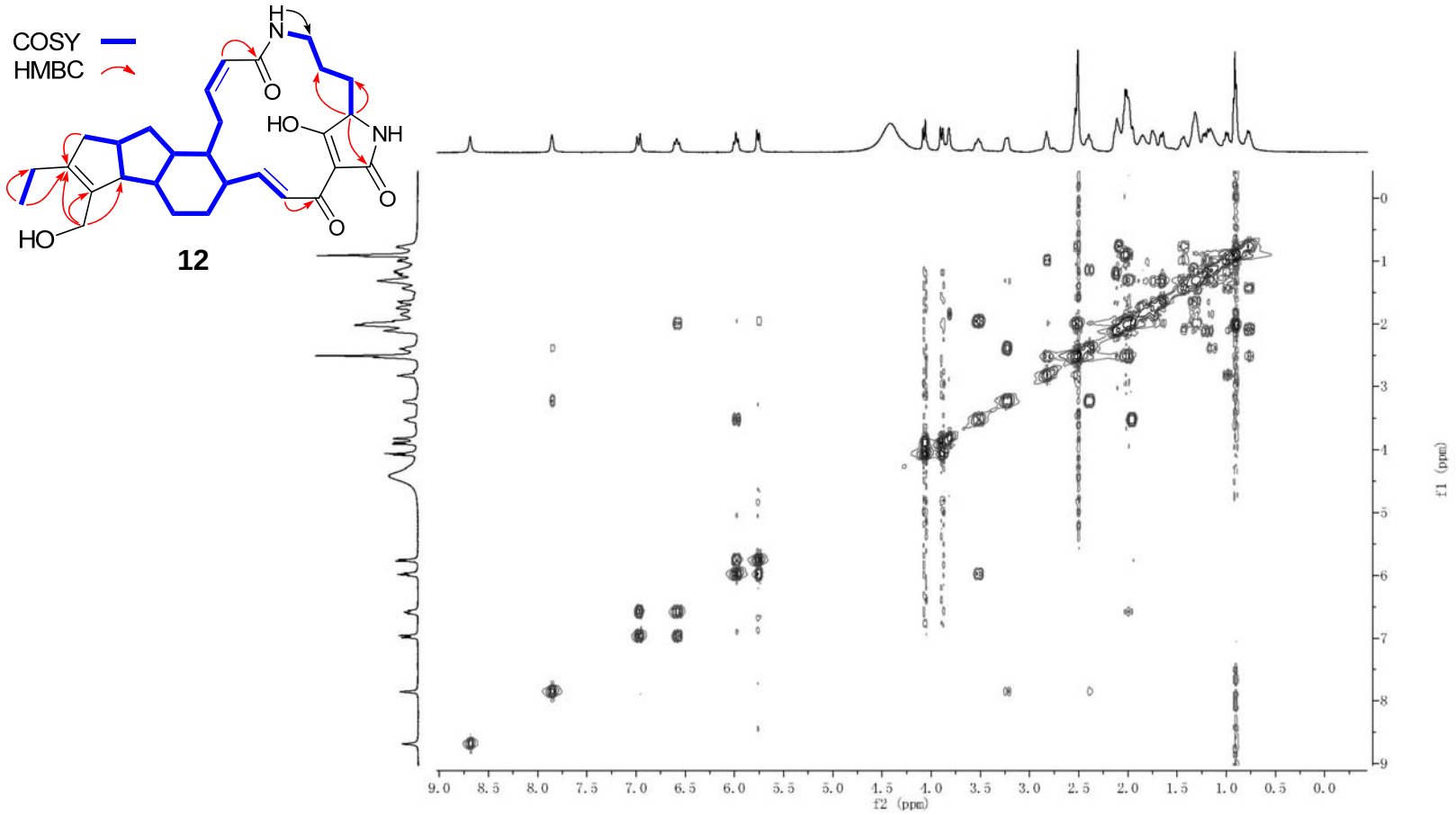

Fig. S9. Spectral data for pactamide B (**12**) (continued).
(**G**) The NOESY spectrum of pactamide B (**12**) in DMSO-d_6.

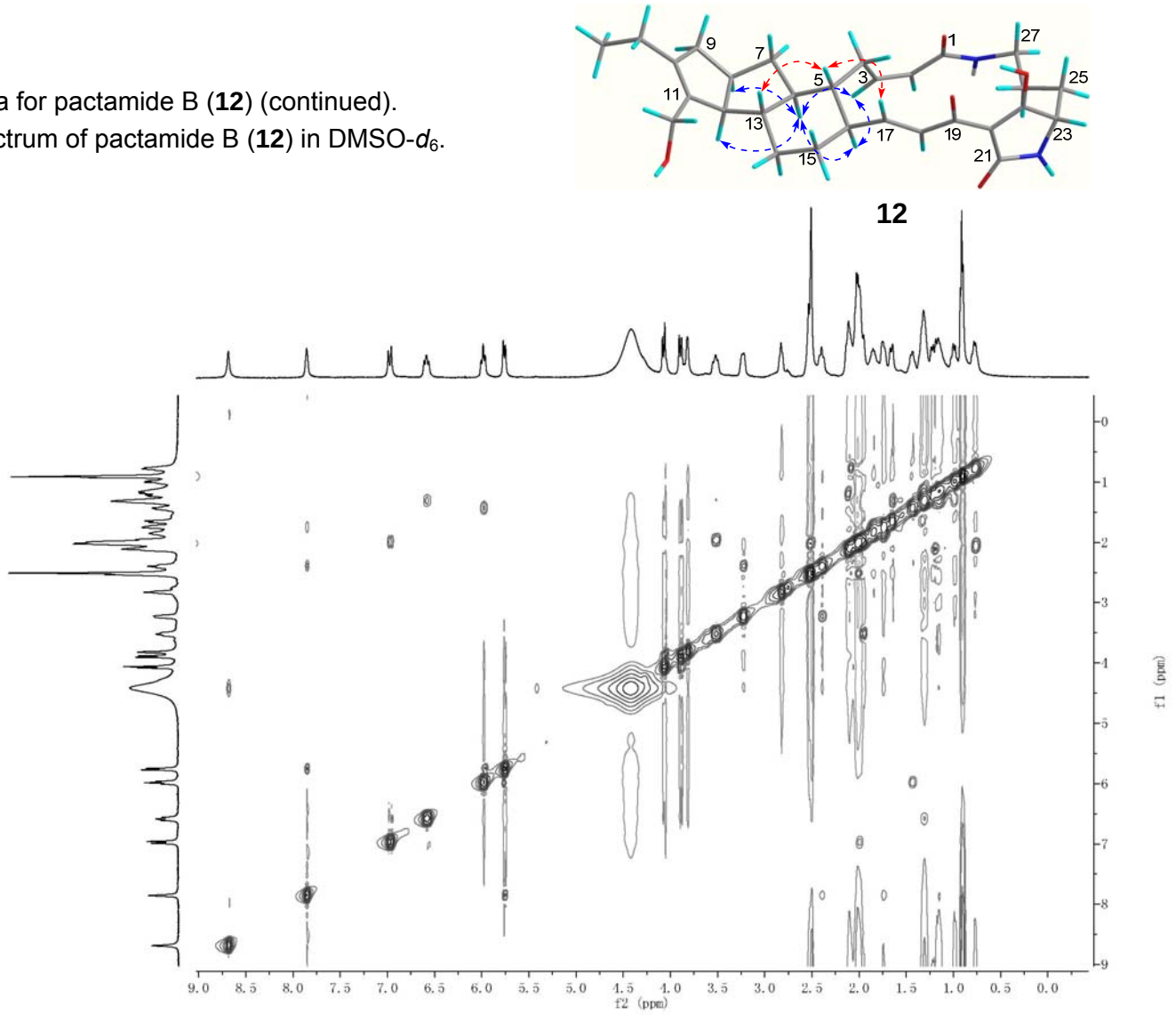

Fig. S10. Spectral data for pactamide C (**13**).

(**A**) HRESIMS (**13**)

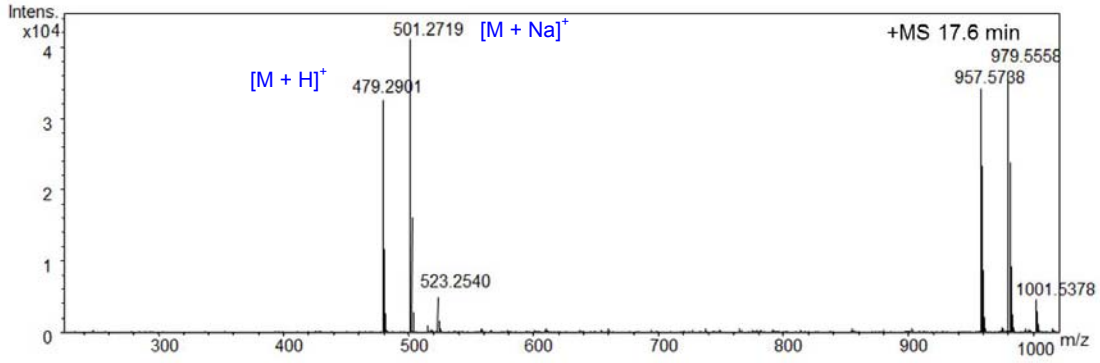

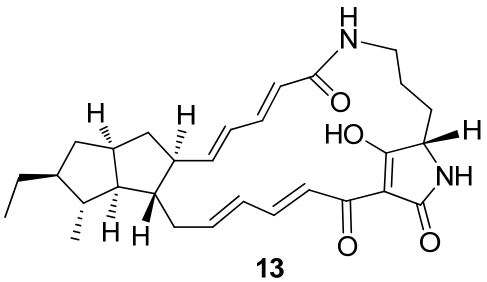

13

Chemical Formula: $C_{29}H_{38}N_2O_4$

calculated for $[M + H]^+$: 479.2910

calculated for $[M + Na]^+$: 501.2729

Fig. S10. Spectral data for pactamide C (**13**) (continued).
(**B**) The ^{1}H NMR spectrum of pactamide C (**13**) in DMSO-d_6.

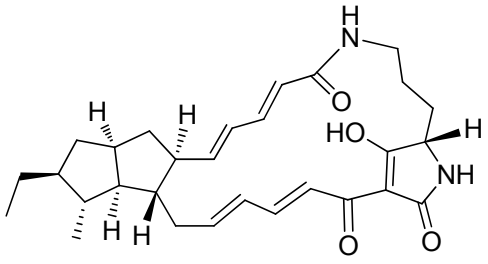

13

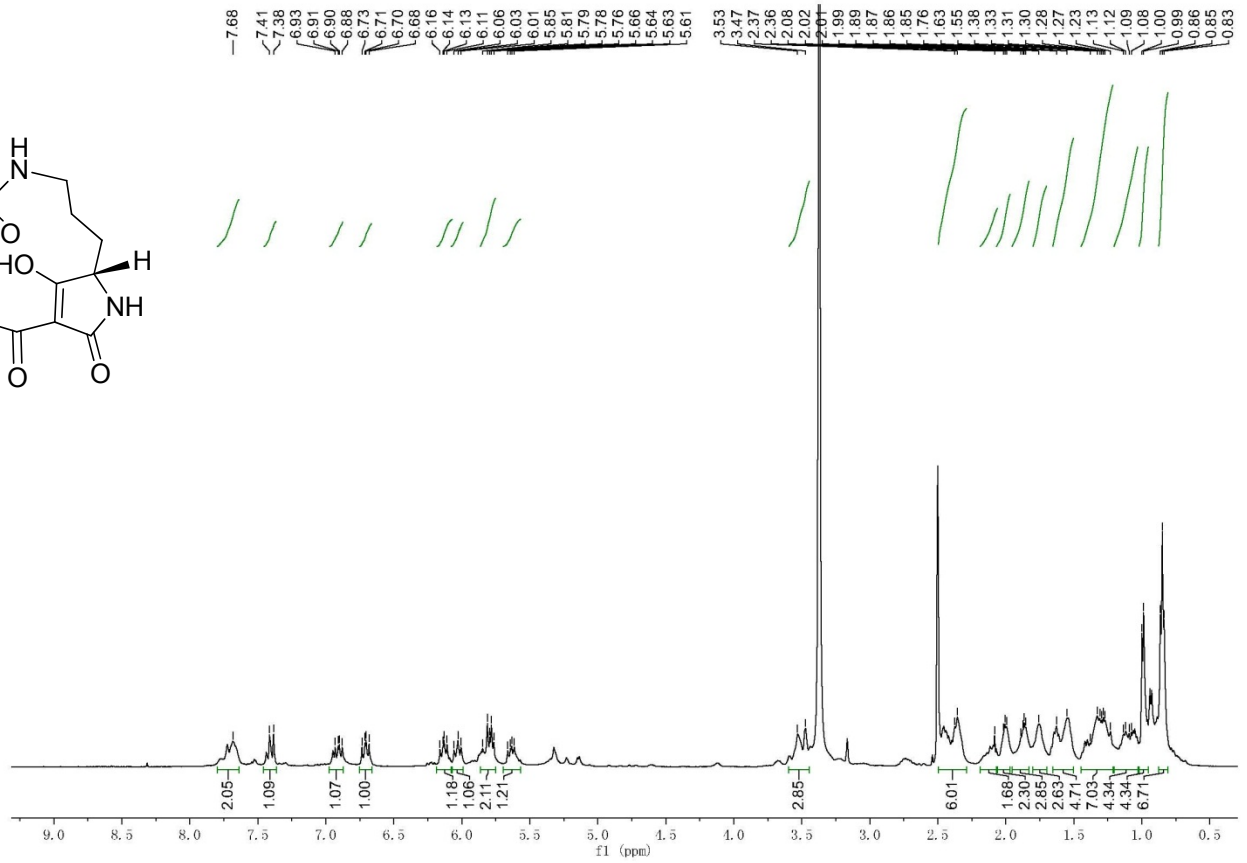

Fig. S10. Spectral data for pactamide C (**13**) (continued).
(**C**)The ^{13}C NMR spectrum of pactamide C (**13**) in DMSO-d_6.

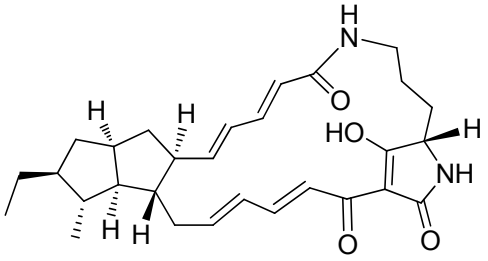

13

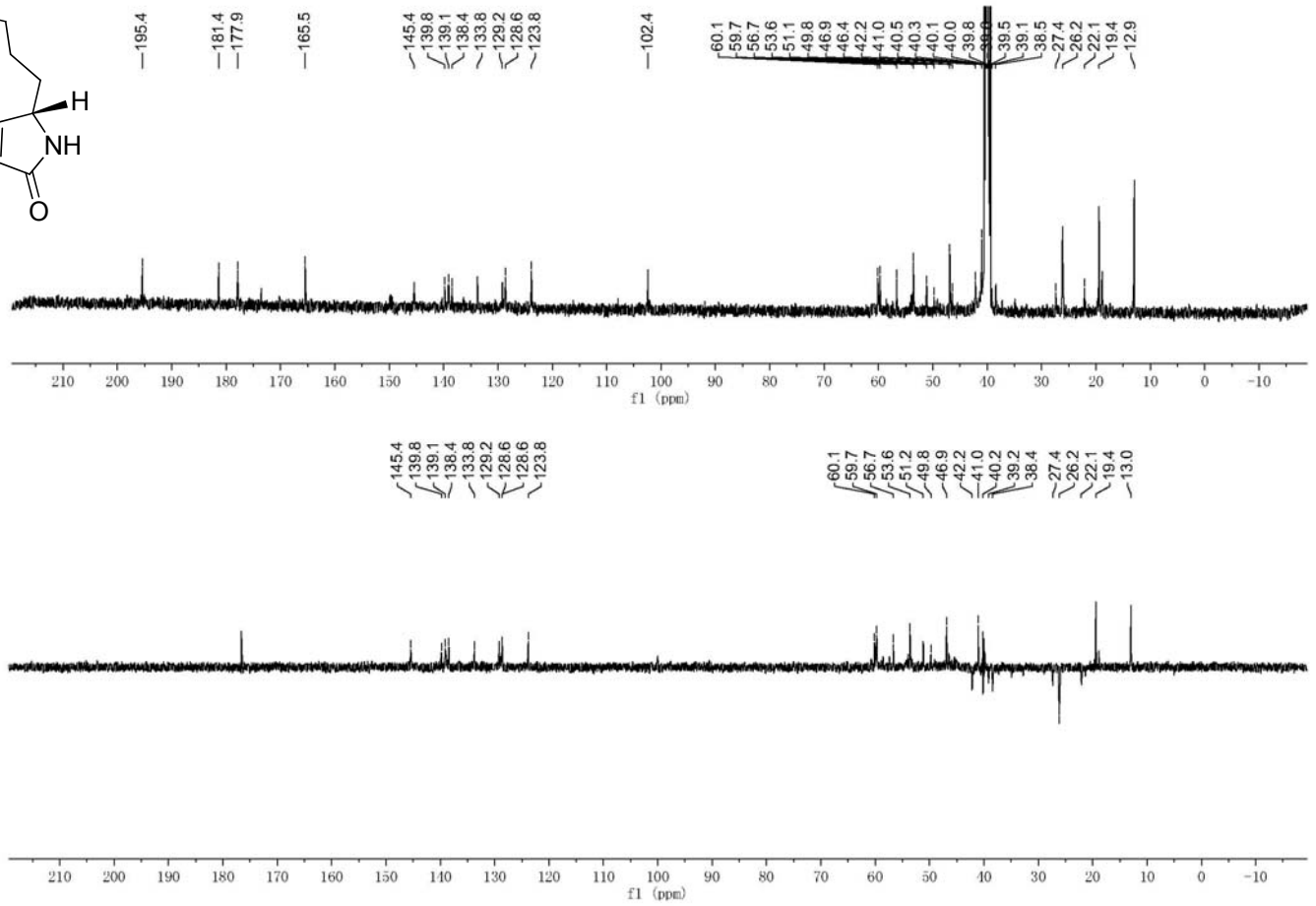

Fig. S10. Spectral data pactamide C (**13**) (continued).
(**D**) The HSQC spectrum of pactamide C (**13**) in DMSO-d_6.

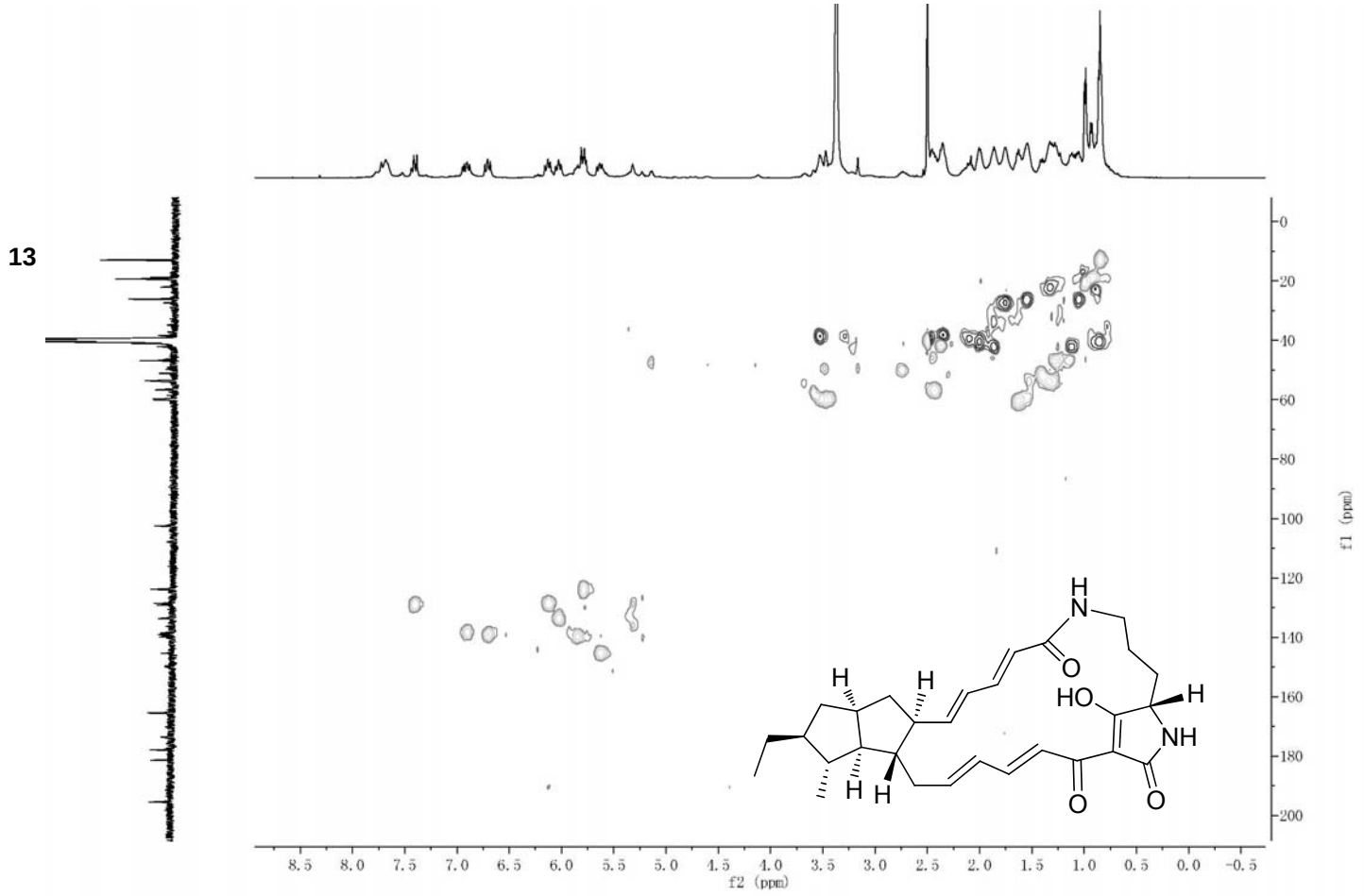

Fig. S10. Spectral data for pactamide C (**13**) (continued).

(**E**) The HMBC spectrum of pactamide C (**13**) in DMSO-d_6.

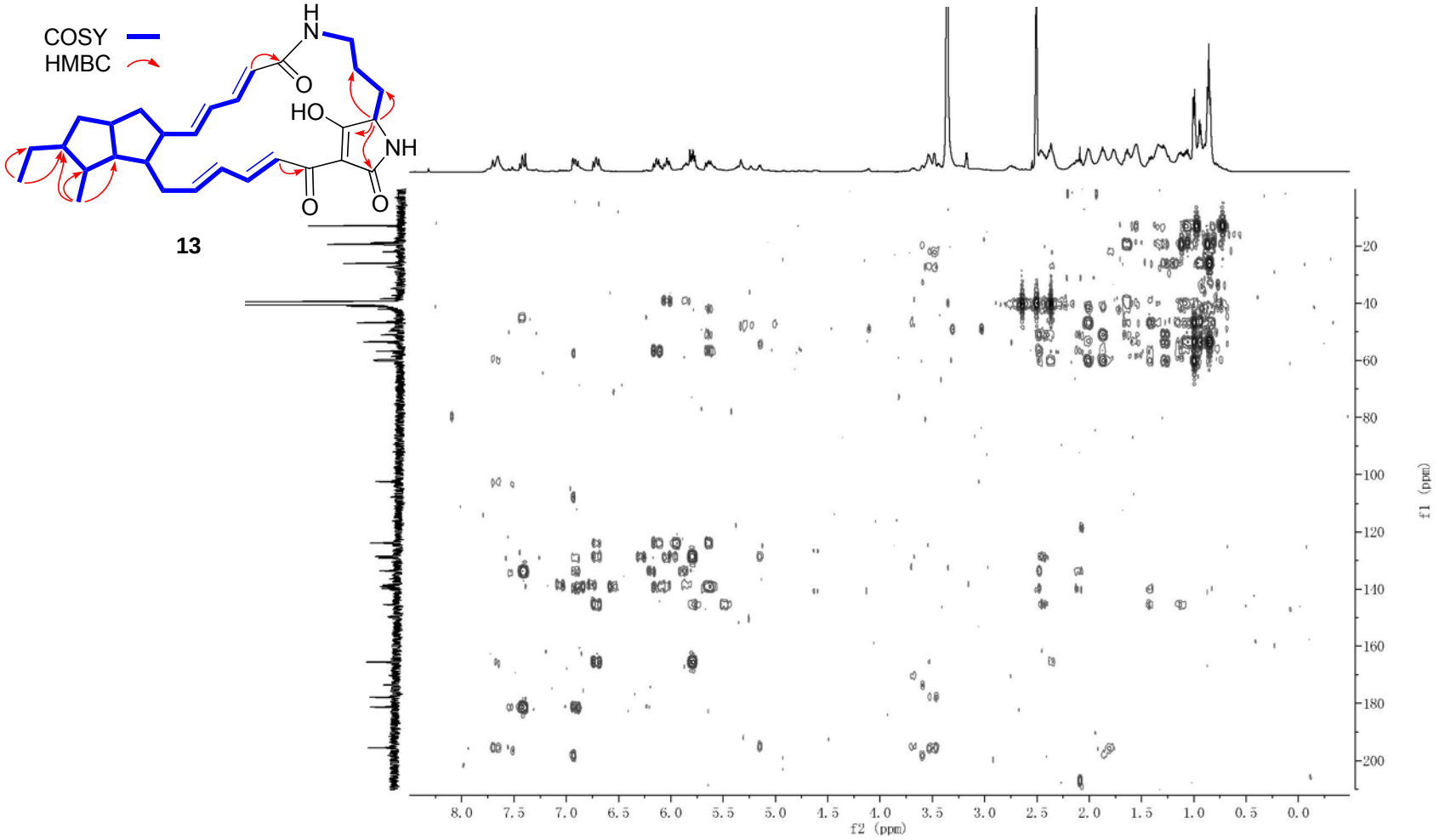

Fig. S10. Spectral data for pactamide C (**13**) (continued).
(**F**) The COSY spectrum of pactamide C (**13**) in DMSO-d_6.

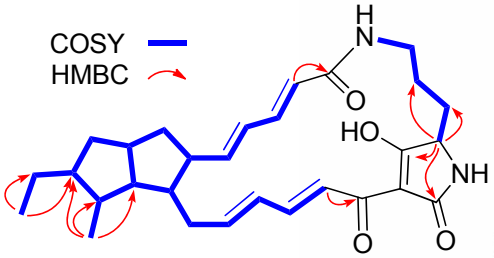

13

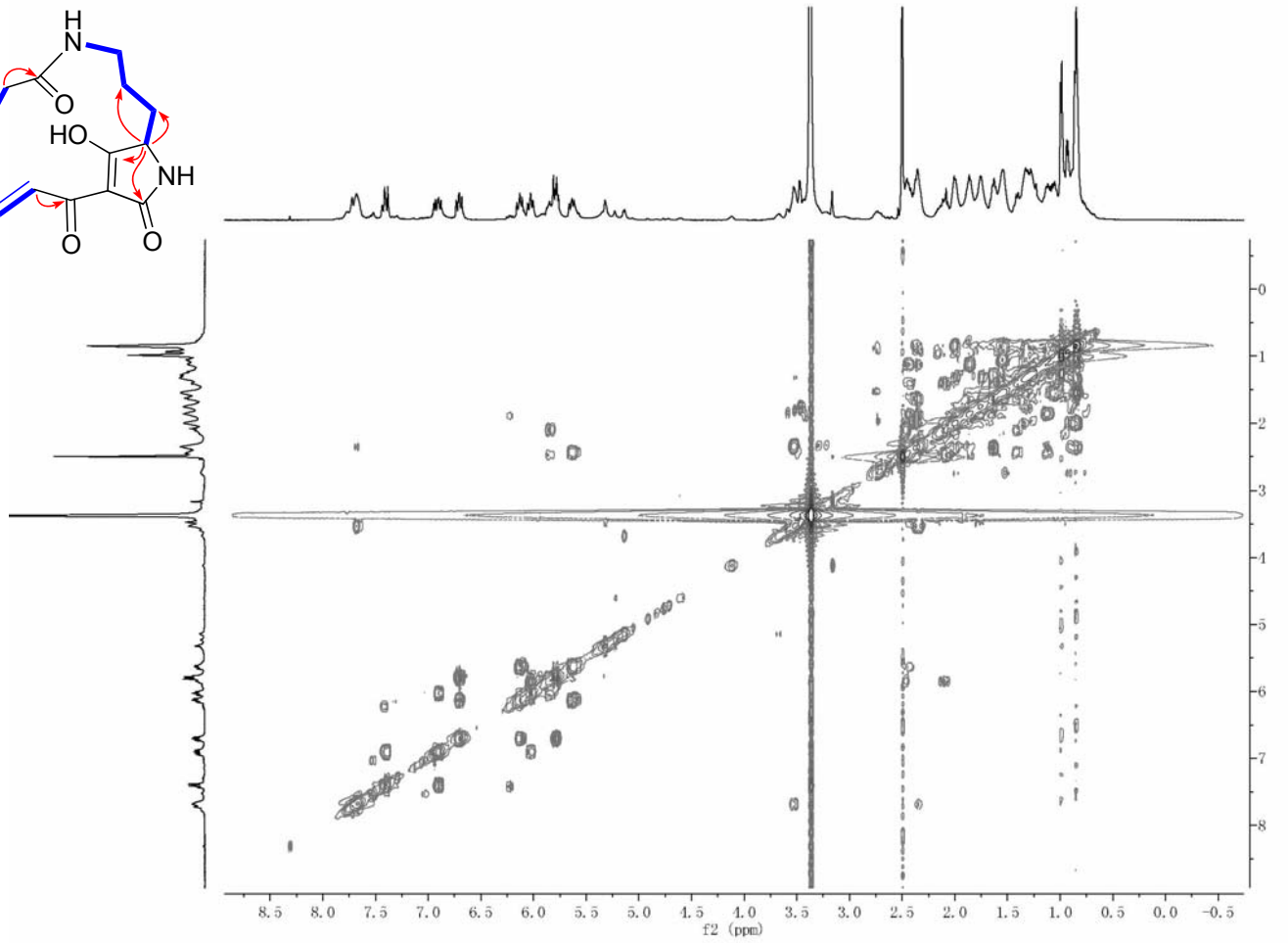

Fig. S10. Spectral data for pactamide C (**13**) (continued).
(**G**) The NOESY spectrum of pactamide C (**13**) in DMSO-d_6.

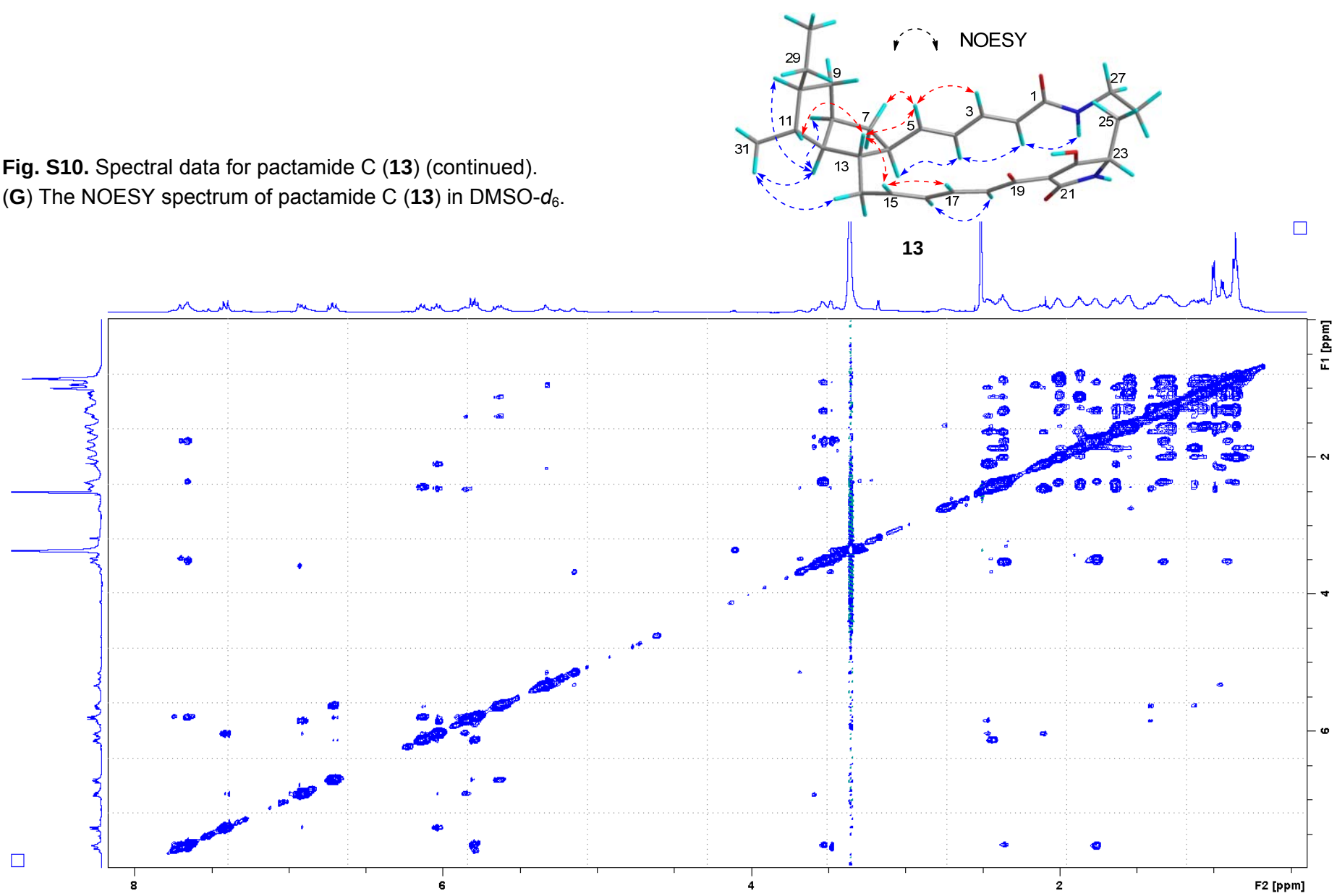

Fig. S10. Spectral data for pactamide C (**13**) (continued).
(**H**) The NOESY spectrum of pactamide C (**13**) in DMSO-d_6.

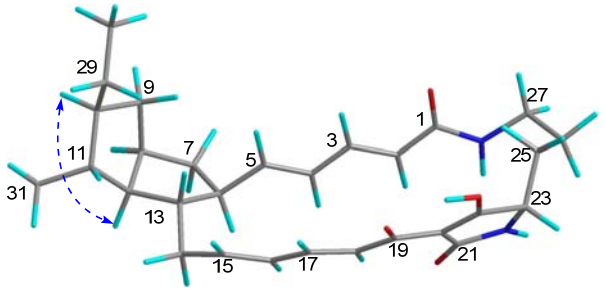

13

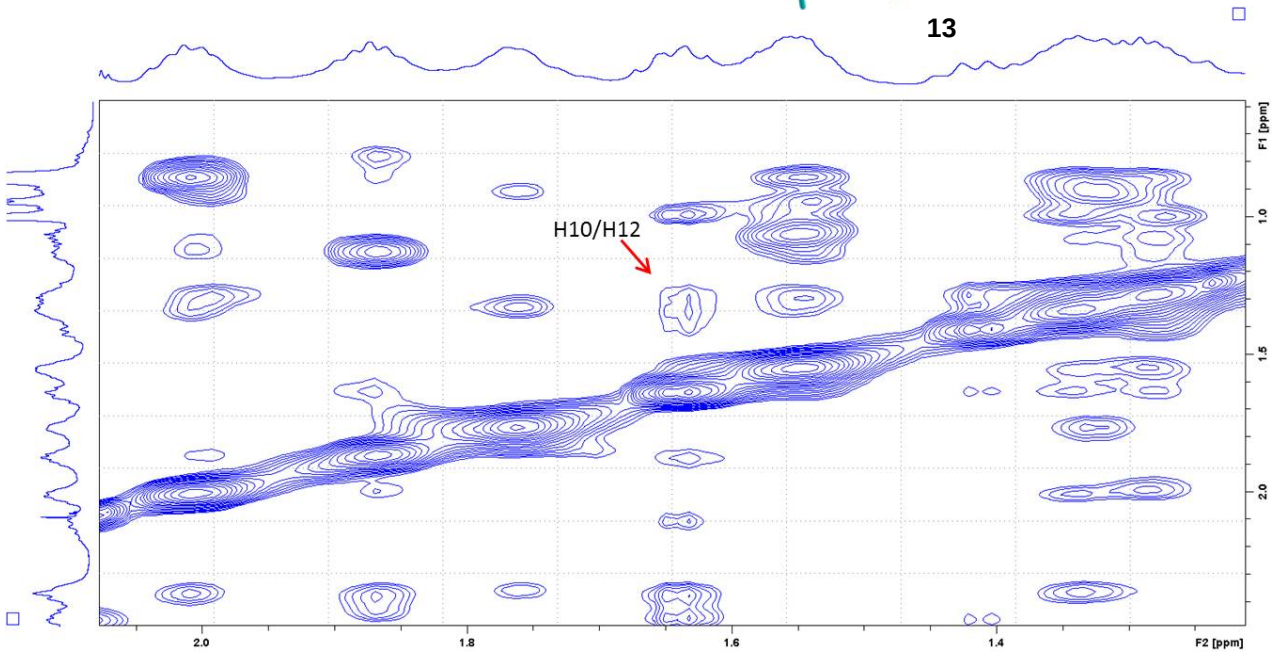

Fig. S11. Spectral data for pactamide D (**14**).
(**A**) HRESIMS.

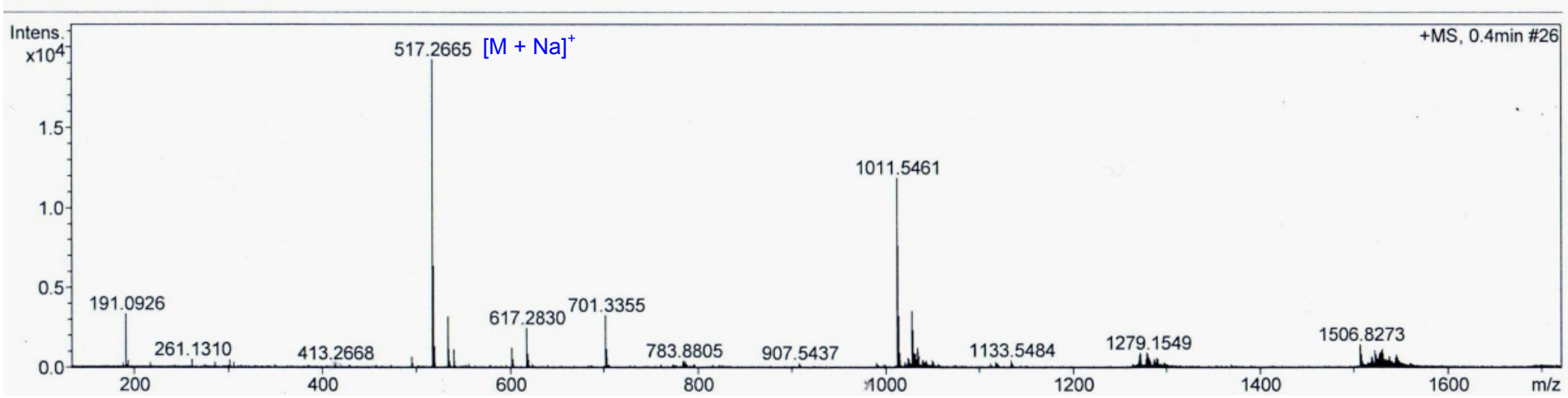

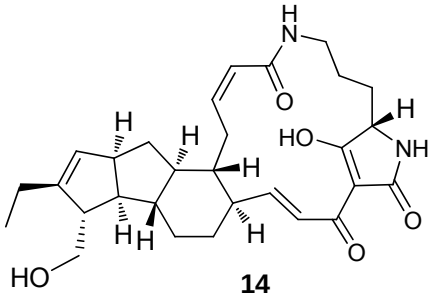

14

Chemical Formula: $C_{29}H_{38}N_2O_5$
calculated for $[M + Na]^+$: 517.2678

Fig. S11. Spectral data for pactamide D (**14**) (continued).
(**B**) The ^{1}H NMR spectrum of pactamide D (**14**) in DMSO-d_6.

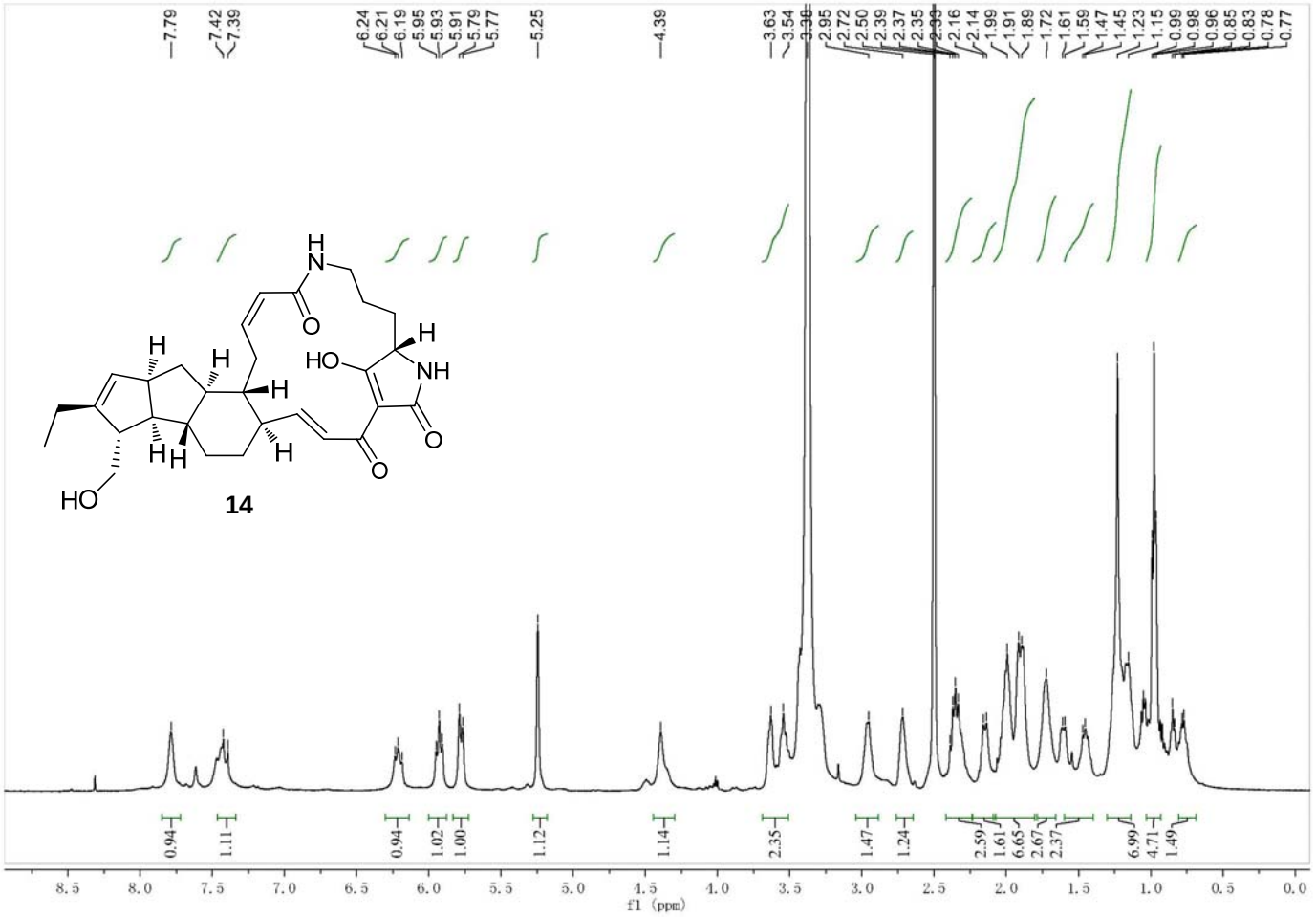

Fig. S11. Spectral data for pactamide D (**14**) (continued).
(**C**)The ^{13}C NMR spectrum of pactamide D (**14**) in DMSO-d_6.

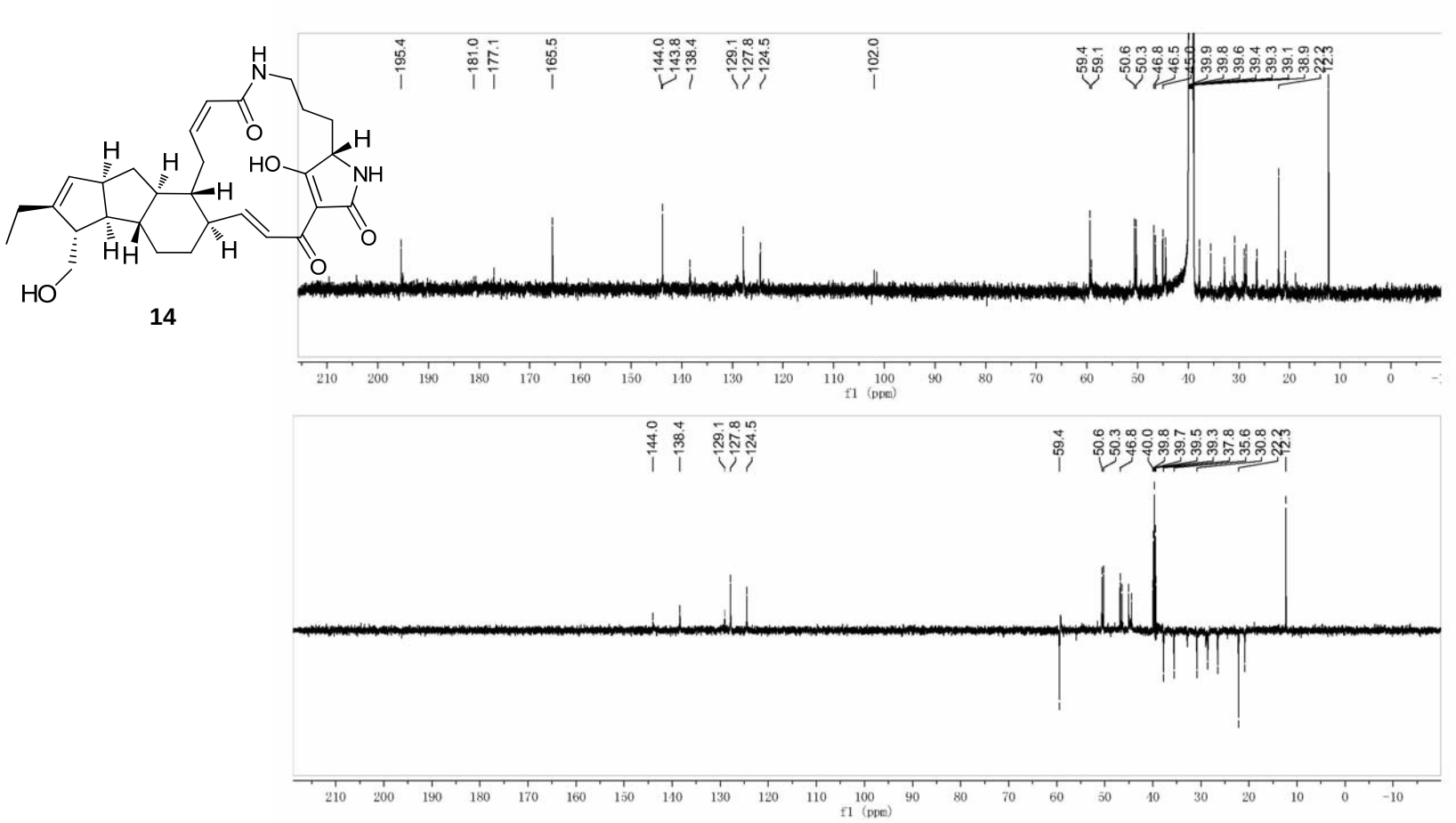

14

Fig. S11. Spectral data for pactamide D (**14**) (continued).
(**D**)The HSQC spectrum of pactamide D (**14**) in DMSO-d_6.

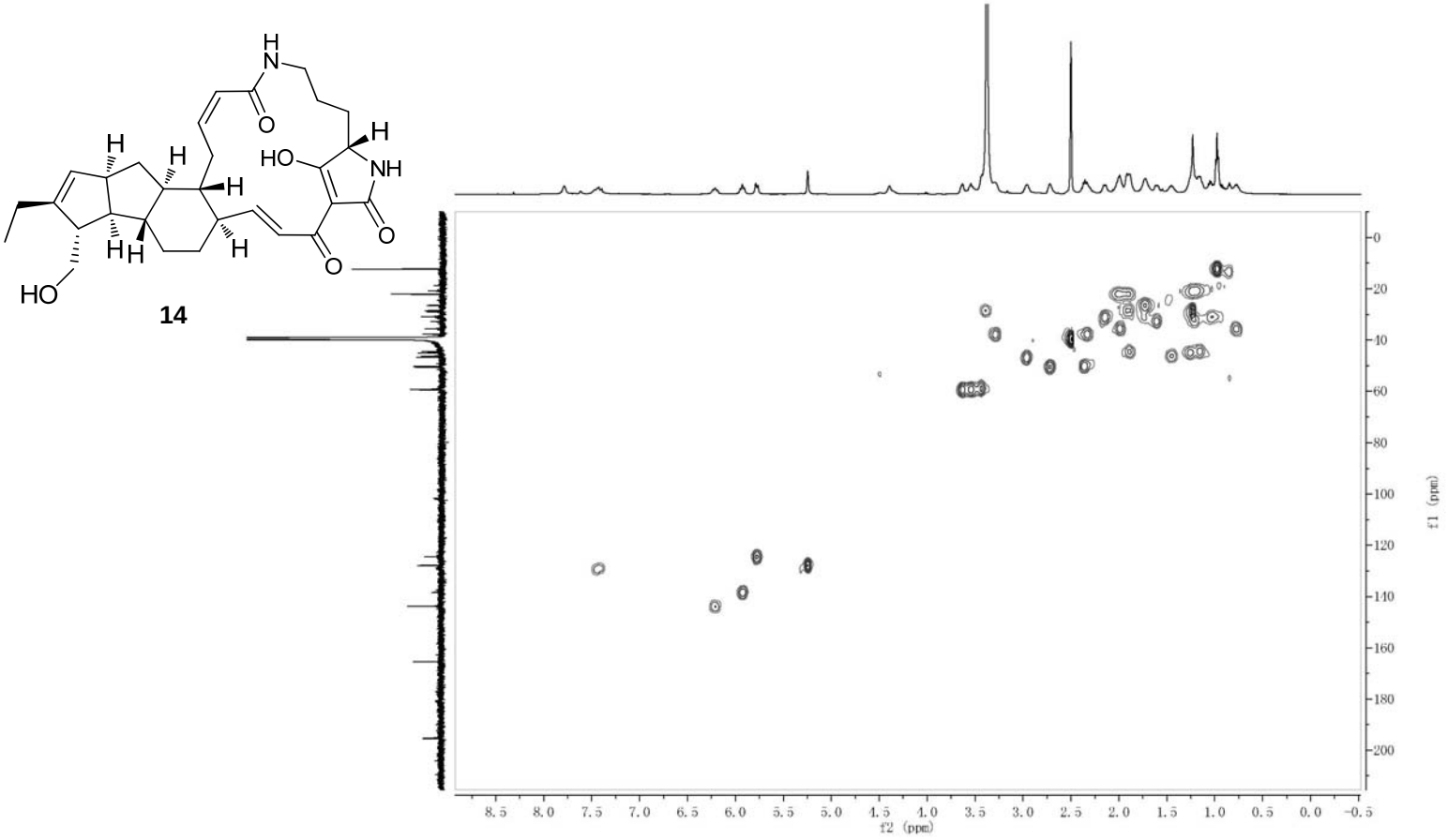

Fig. S11. Spectral data for pactamide D (**14**) (continued).
(**E**)The COSY spectrum of pactamide D (**14**) in DMSO-d_6.

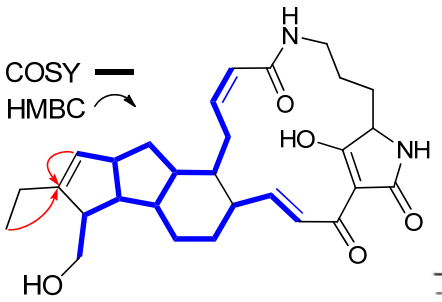

14

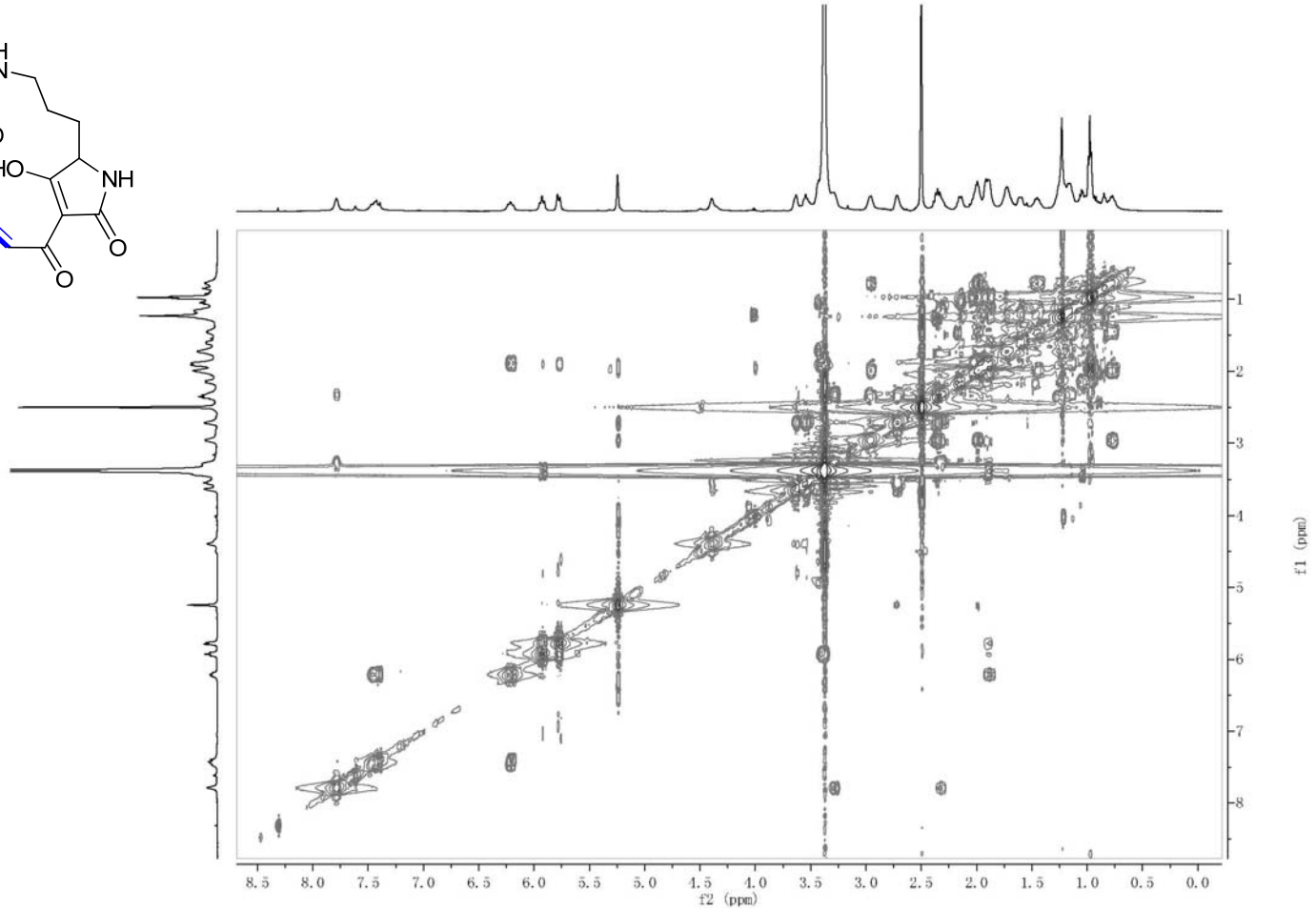

Fig. S11. Spectral data for pactamide D (**14**) (continued).
(**F**)The HMBC spectrum of pactamide D (**14**) in DMSO-d_6.

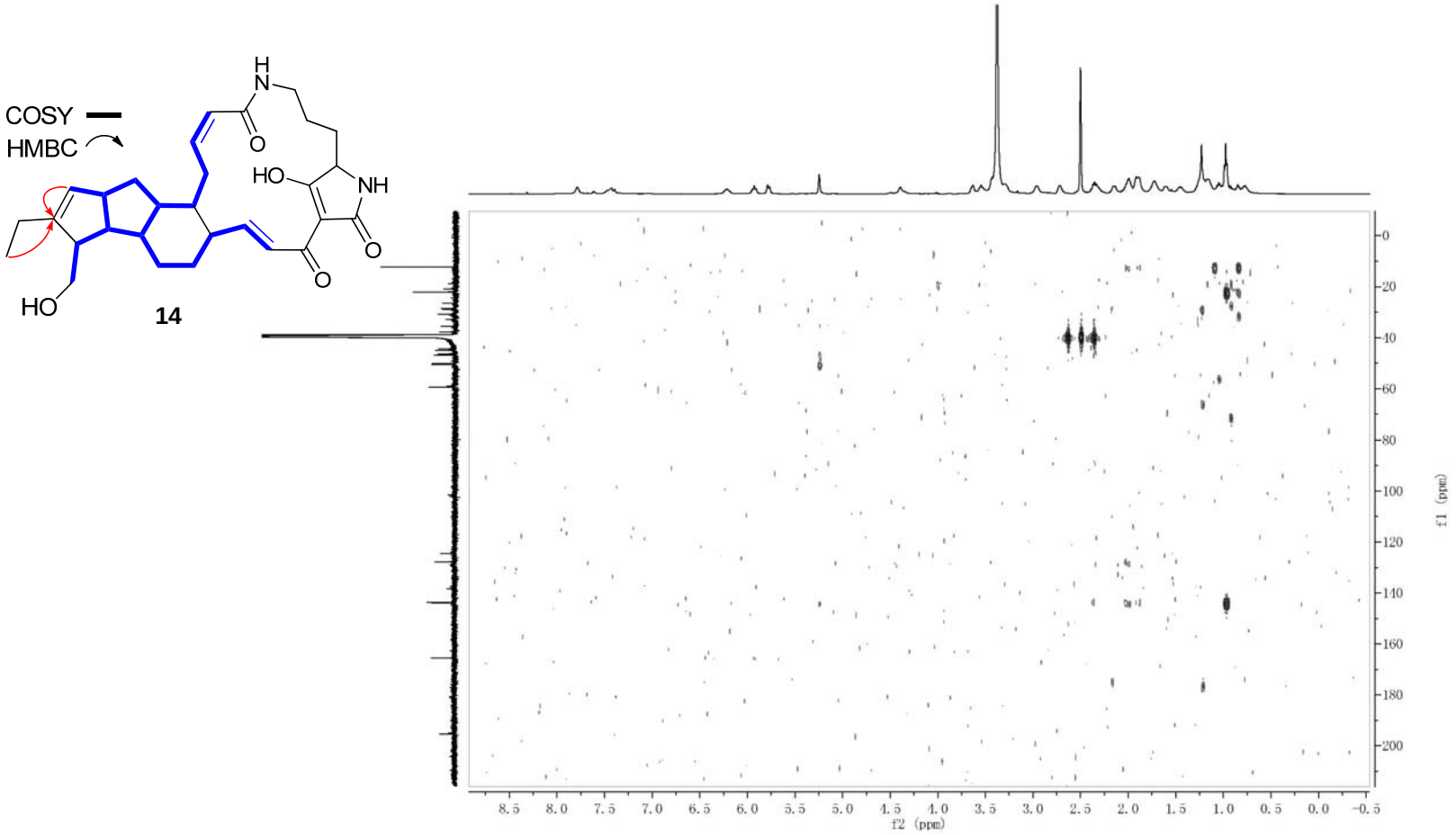

Fig. S11. Spectral data for pactamide D (**14**) (continued).
(**G**)The NOESY spectrum of pactamide D (**14**) in DMSO-d_6.

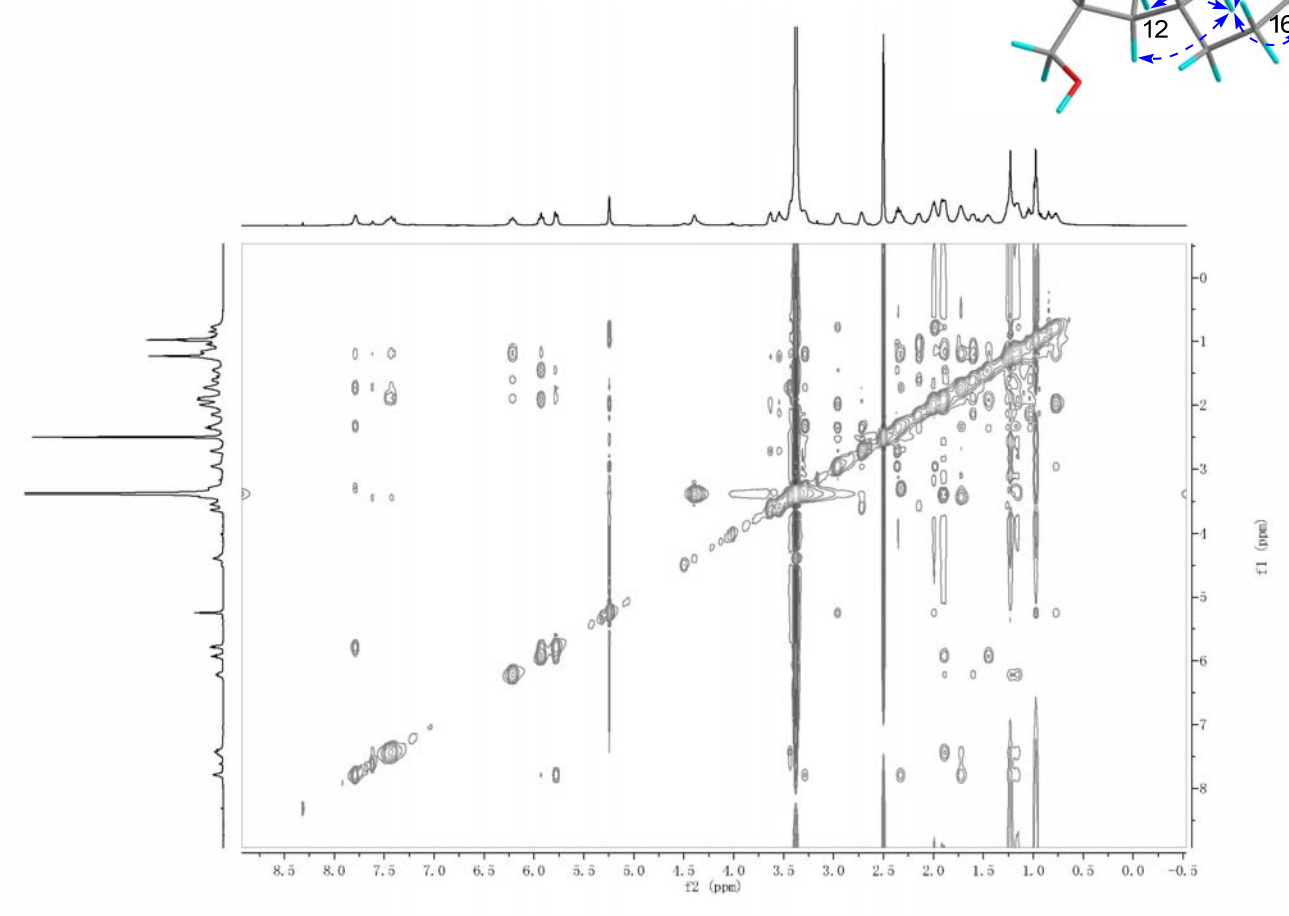

Fig. S12. Spectral data for pactamide E (**15**).

(A) HR-ESI-MS.

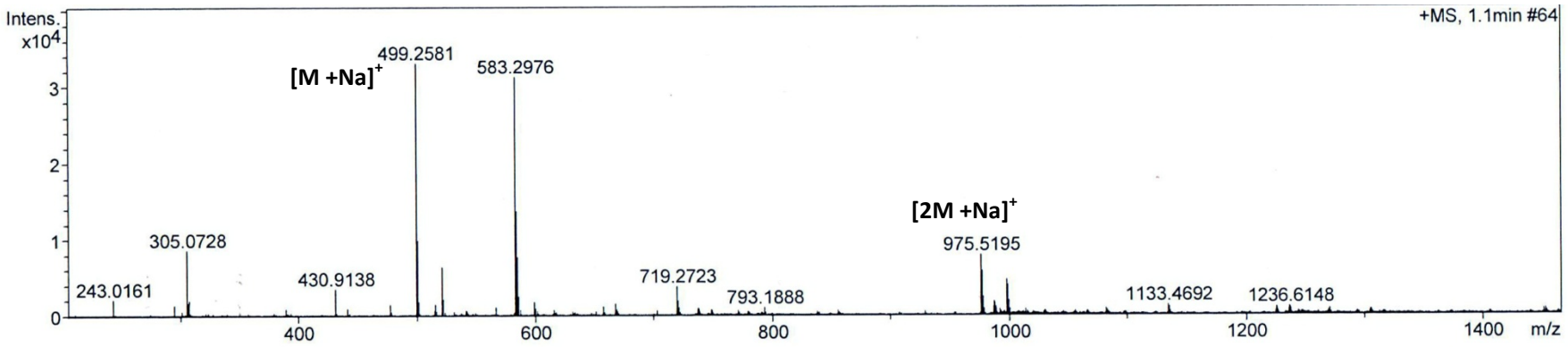

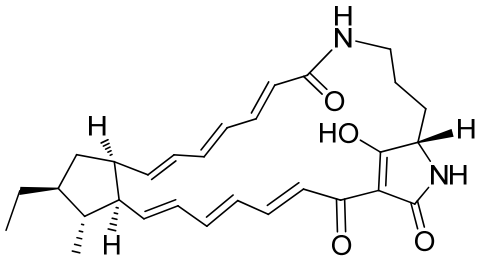

Chemical Formula: $C_{29}H_{36}N_2O_4$

calculated for $[M + Na]^+$ 499.2567

15

Fig. S12. Spectral data for pactamide E (**15**) (continued).
(**B**) The ^{1}H NMR spectrum of pactamide E (**15**) in DMSO-d_6.

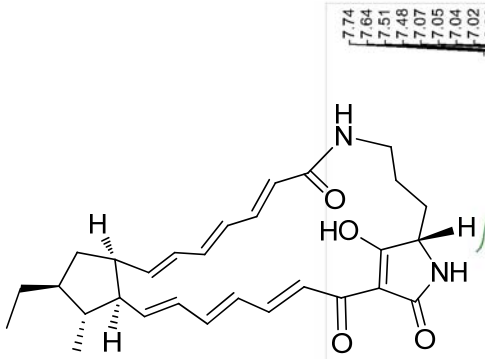

15

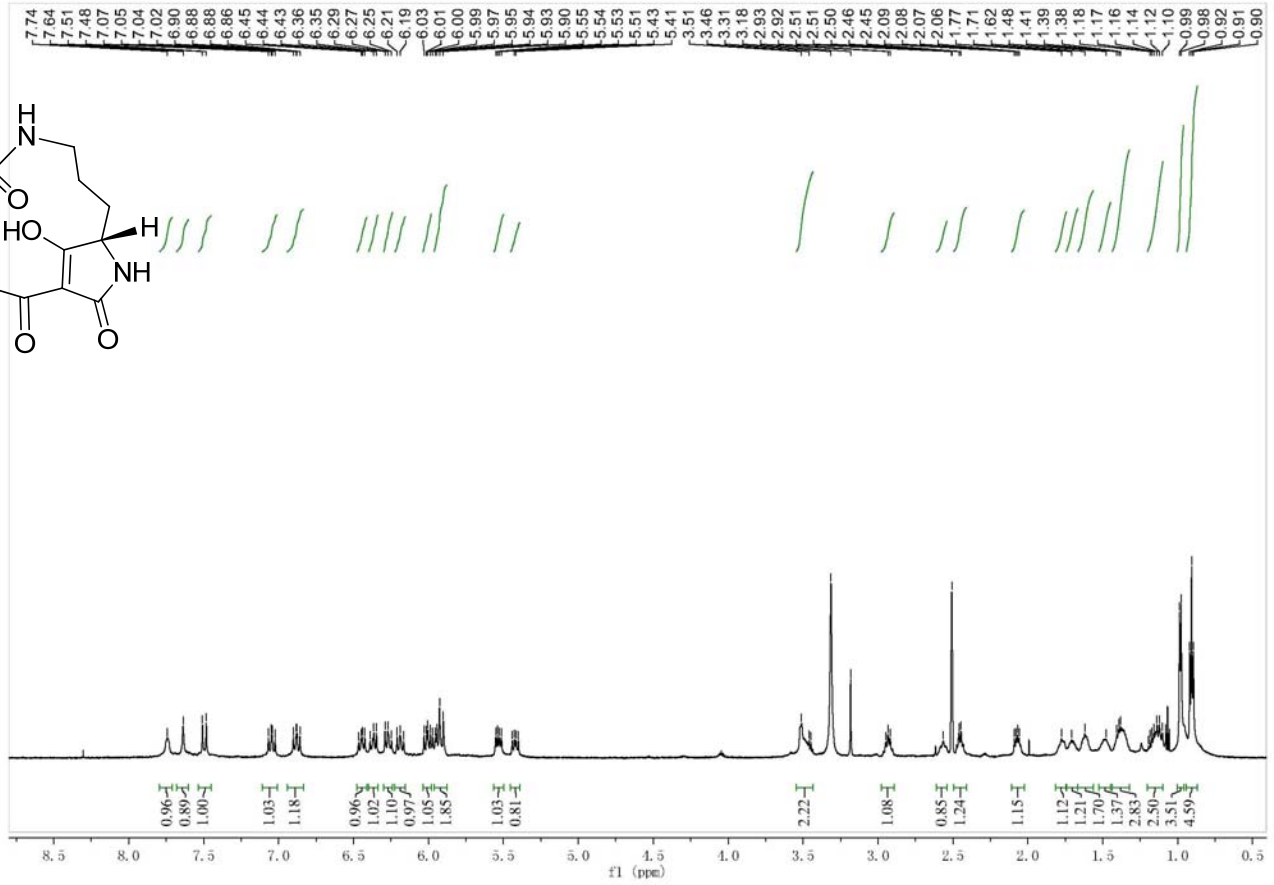

Fig. S12. Spectral data for pactamide E (**15**) (continued).
(**C**) The ^{13}C and DEPT 135 NMR spectrum of pactamide E (**15**) in DMSO-d_6.

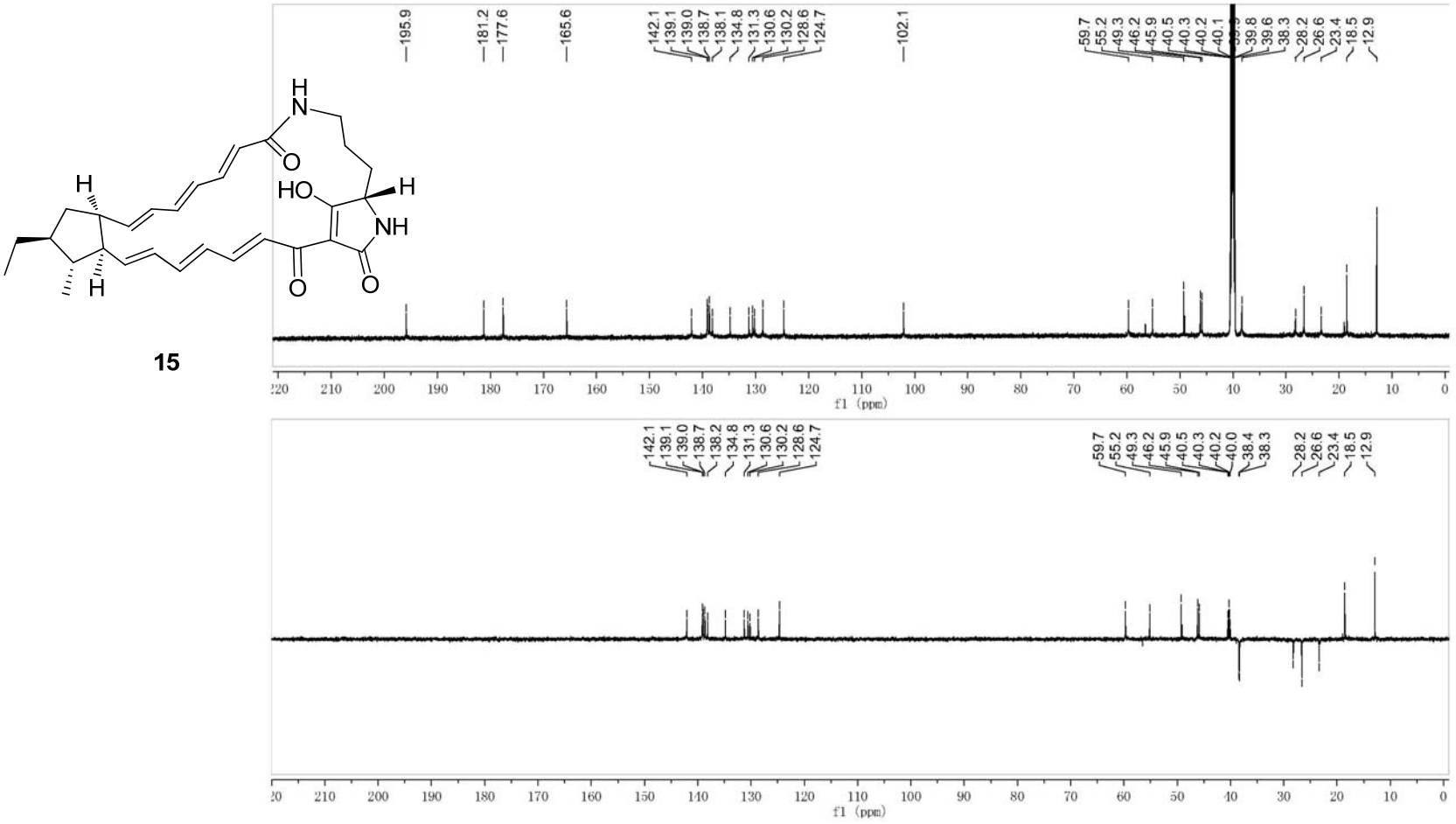

15

Fig. S12. Spectral data for pactamide E (**15**) (continued).
(**D**) The COSY spectrum of pactamide E (**15**) in DMSO-d_6.

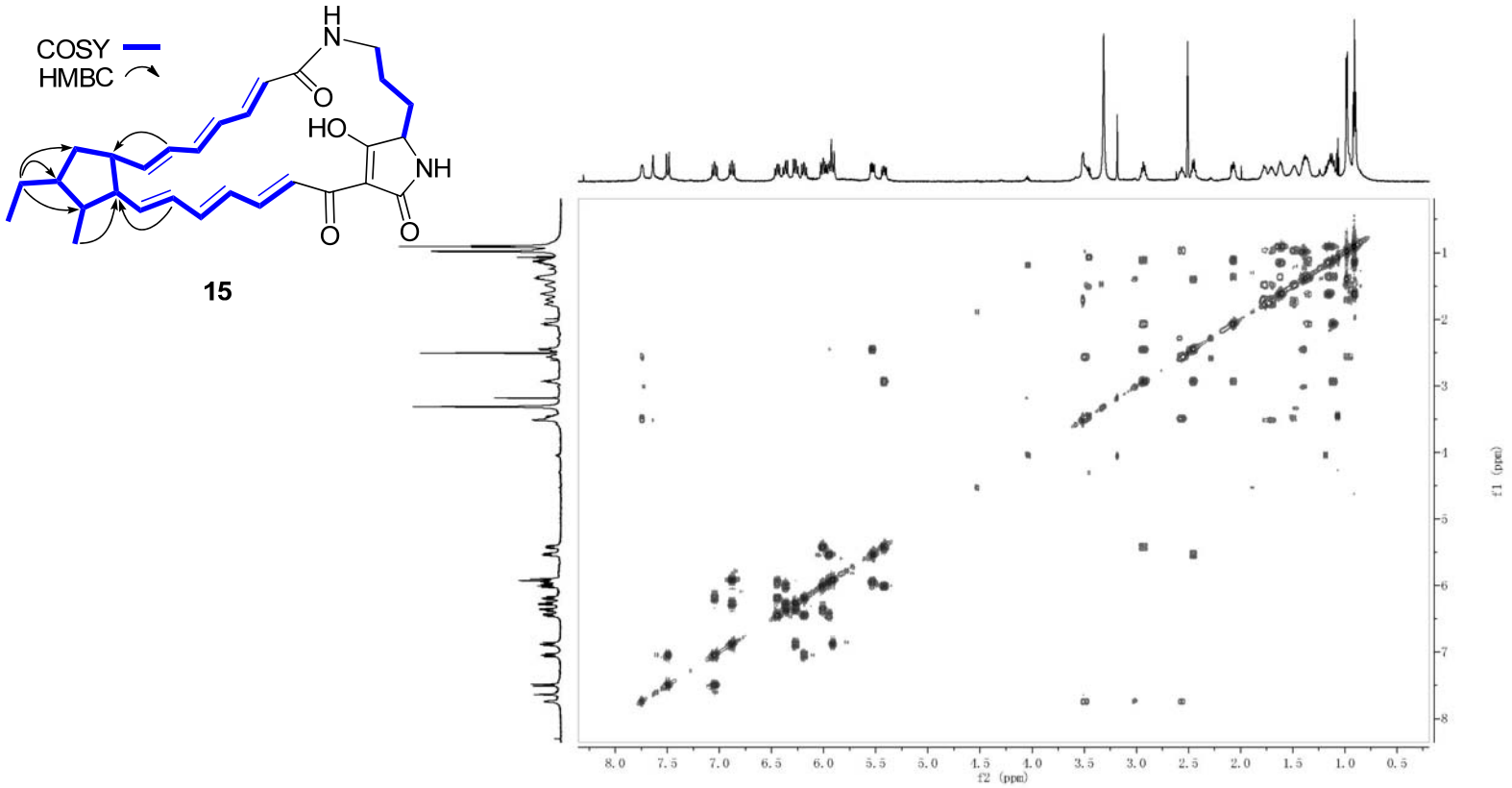

Fig. S12. Spectral data for pactamide E (**15**) (continued).
(**E**) The HSQC spectrum of pactamide E (**15**) in DMSO-d_6.

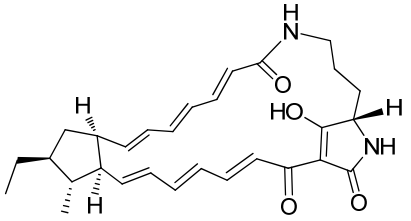

15

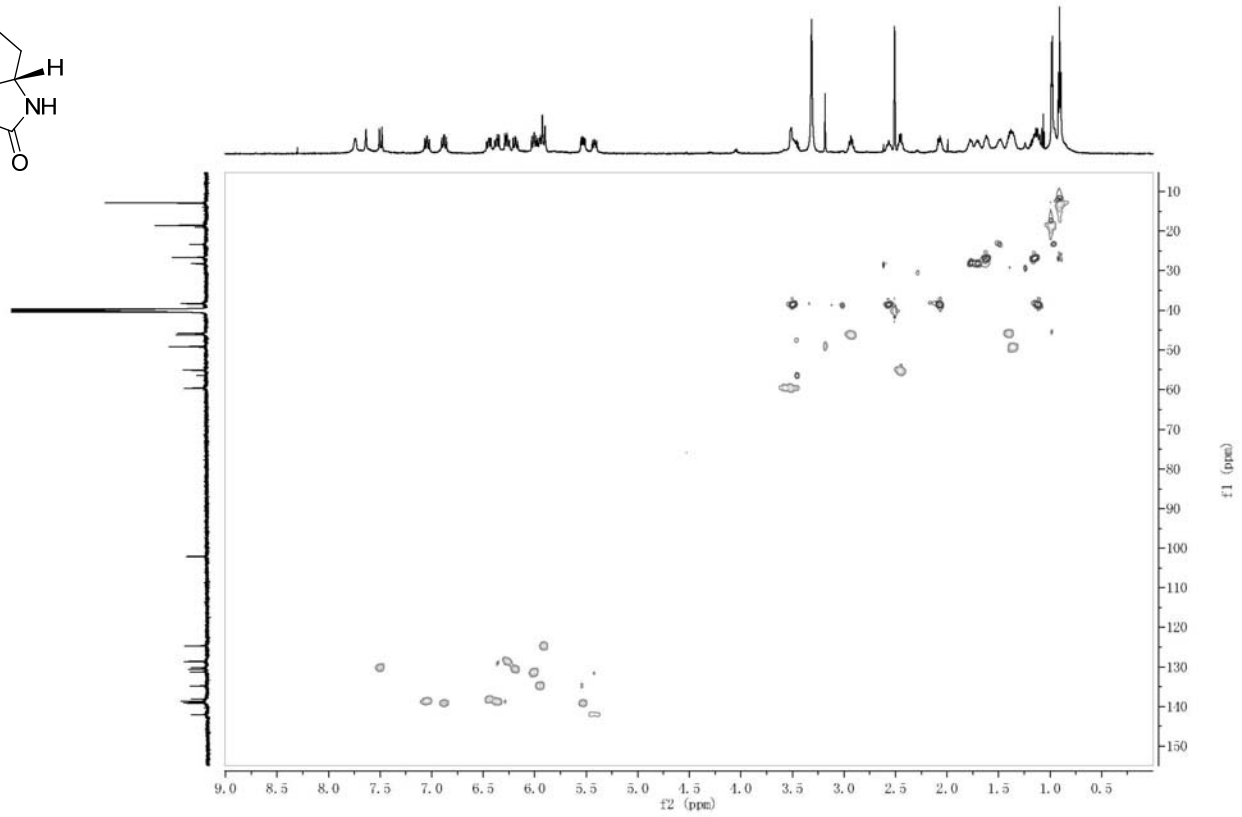

Fig. S12. Spectral data for pactamide E (**15**) (continued).
(**F**) The HMBC spectrum of pactamide E (**15**) in DMSO-d_6.

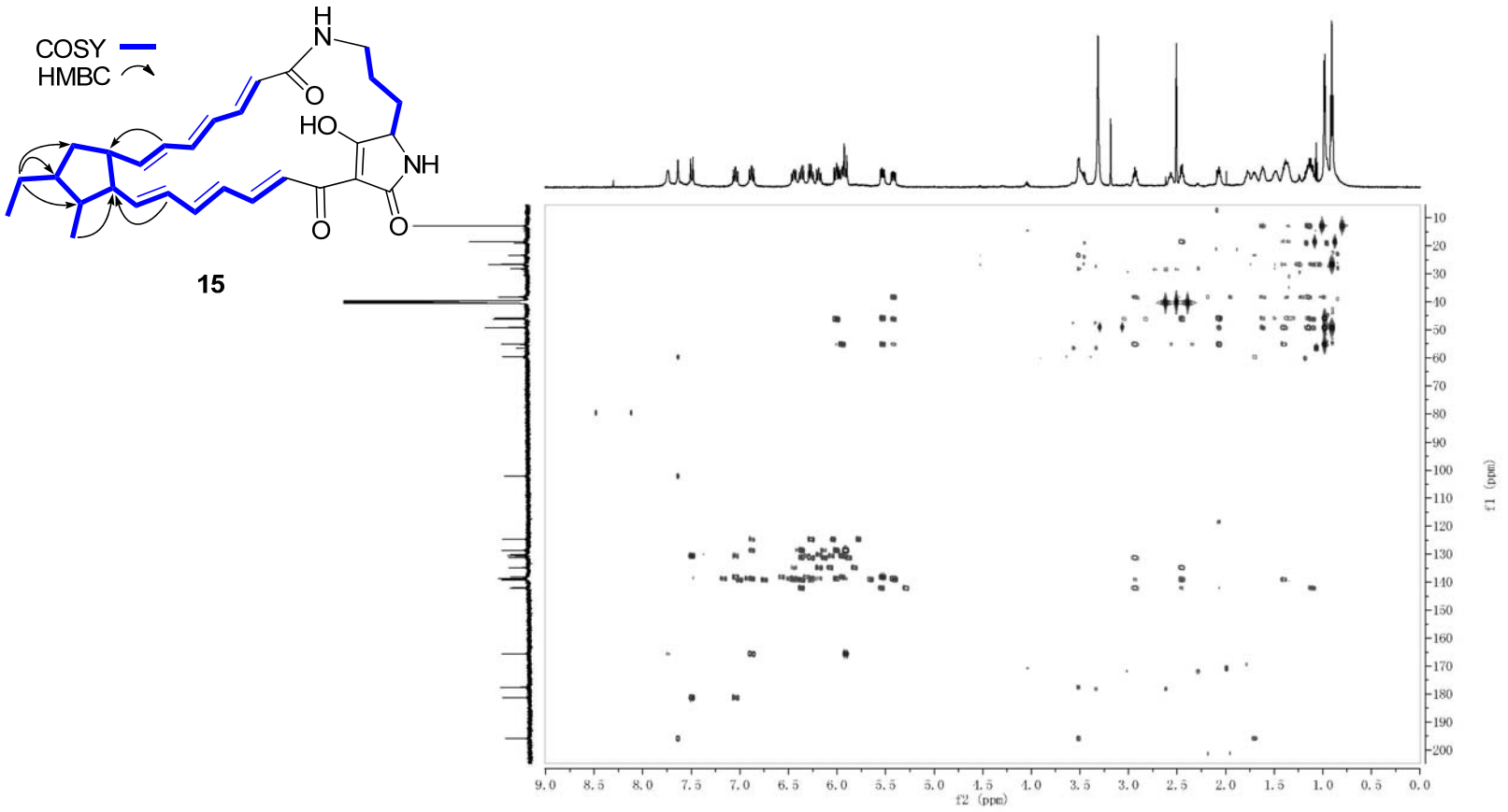

Fig. S12. Spectral data for pactamide E (**15**) (continued).
(**G**) The NOESY spectrum of pactamide E (**15**) in DMSO-d_6.

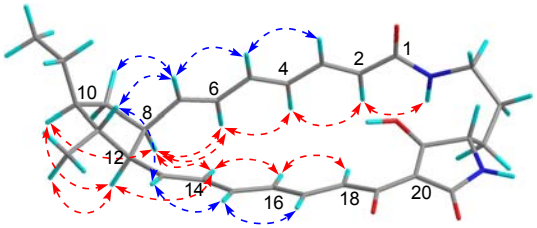

15

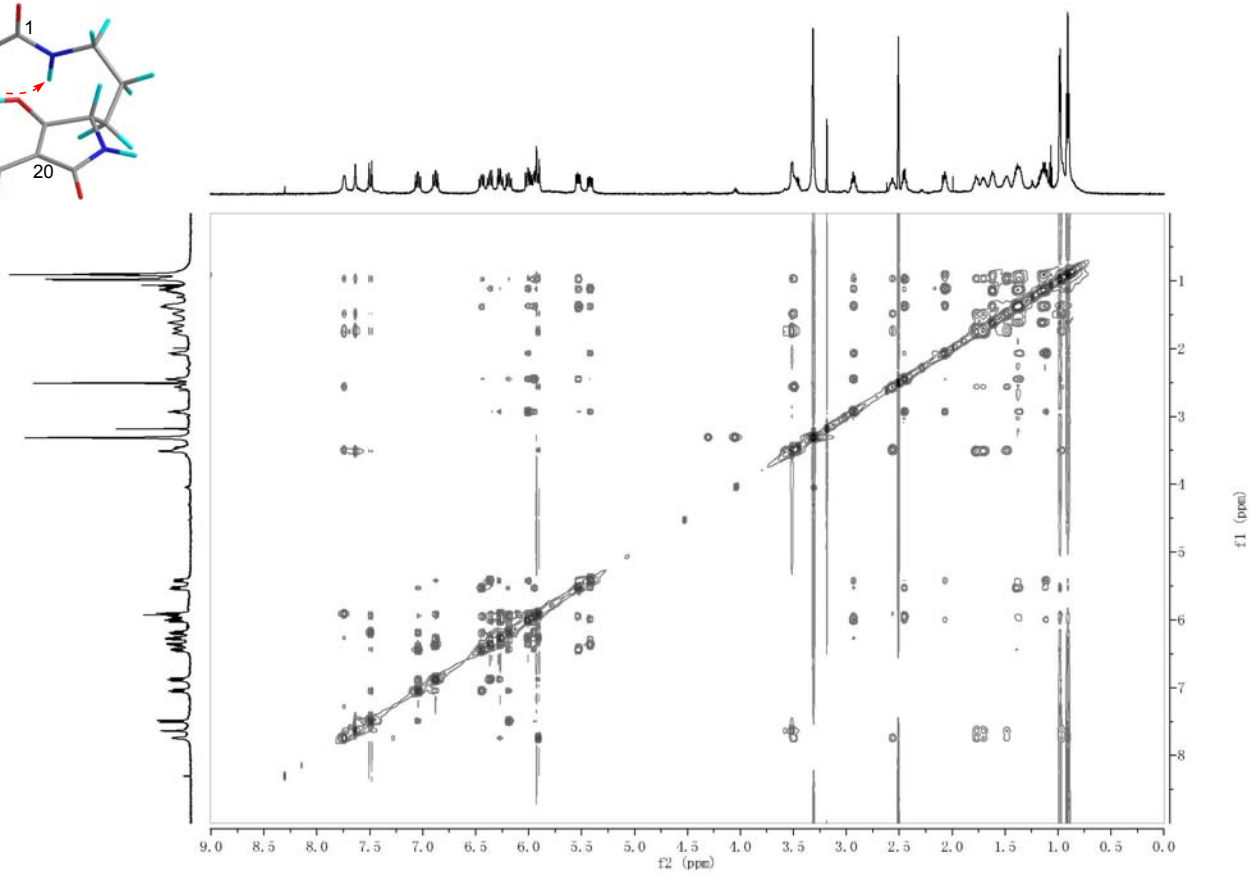

Fig. S13. Spectral data for pactamide F (**16**).

(**A**) HR-ESI-MS.

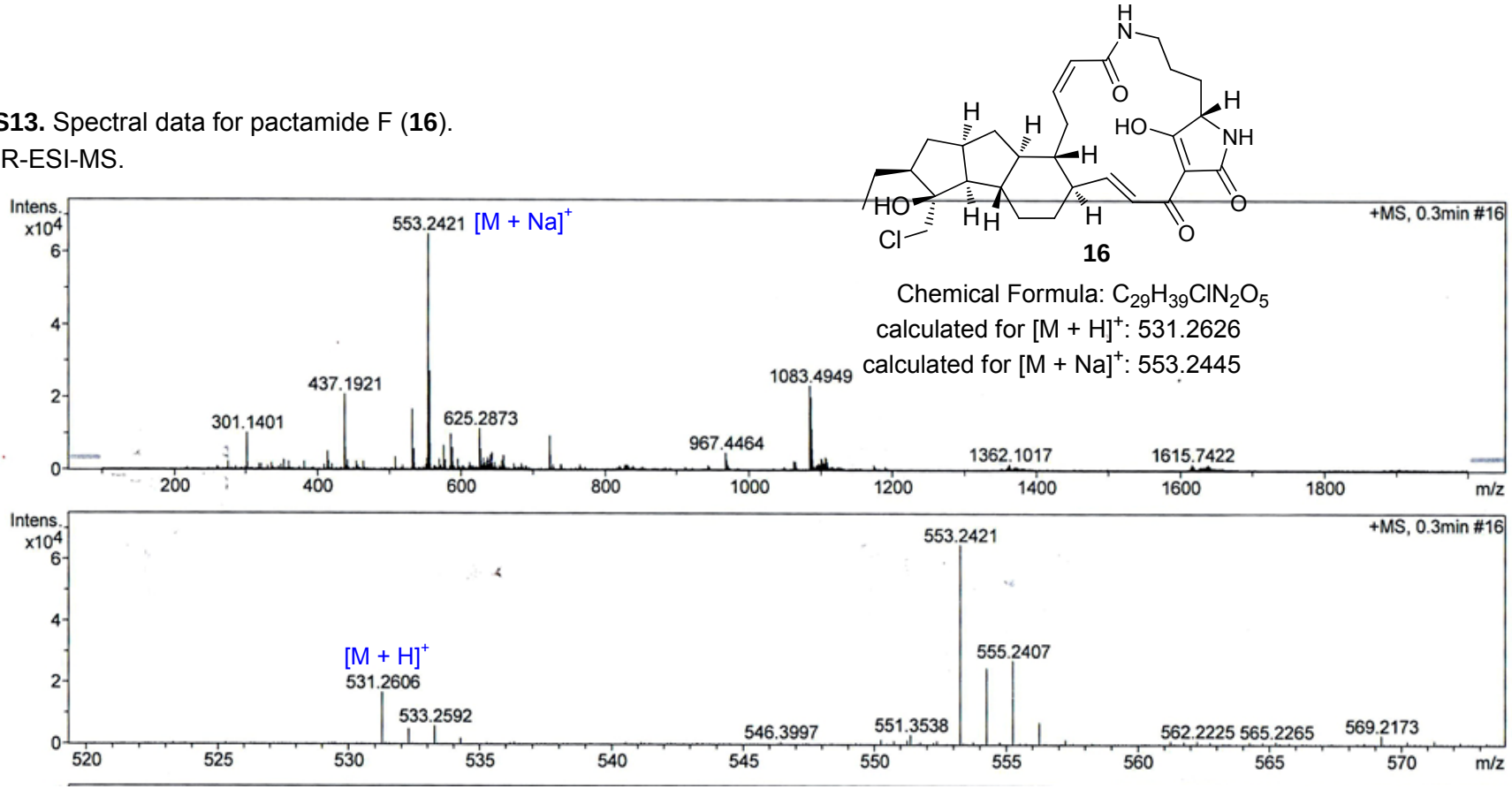

16

Chemical Formula: $C_{29}H_{39}ClN_2O_5$

calculated for $[M + H]^+$: 531.2626

calculated for $[M + Na]^+$: 553.2445

Fig. S13. Spectral data for pactamide F (**16**) (continued).
(**B**) The ^{1}H NMR spectrum of pactamide F (**16**) in DMSO-d_6.

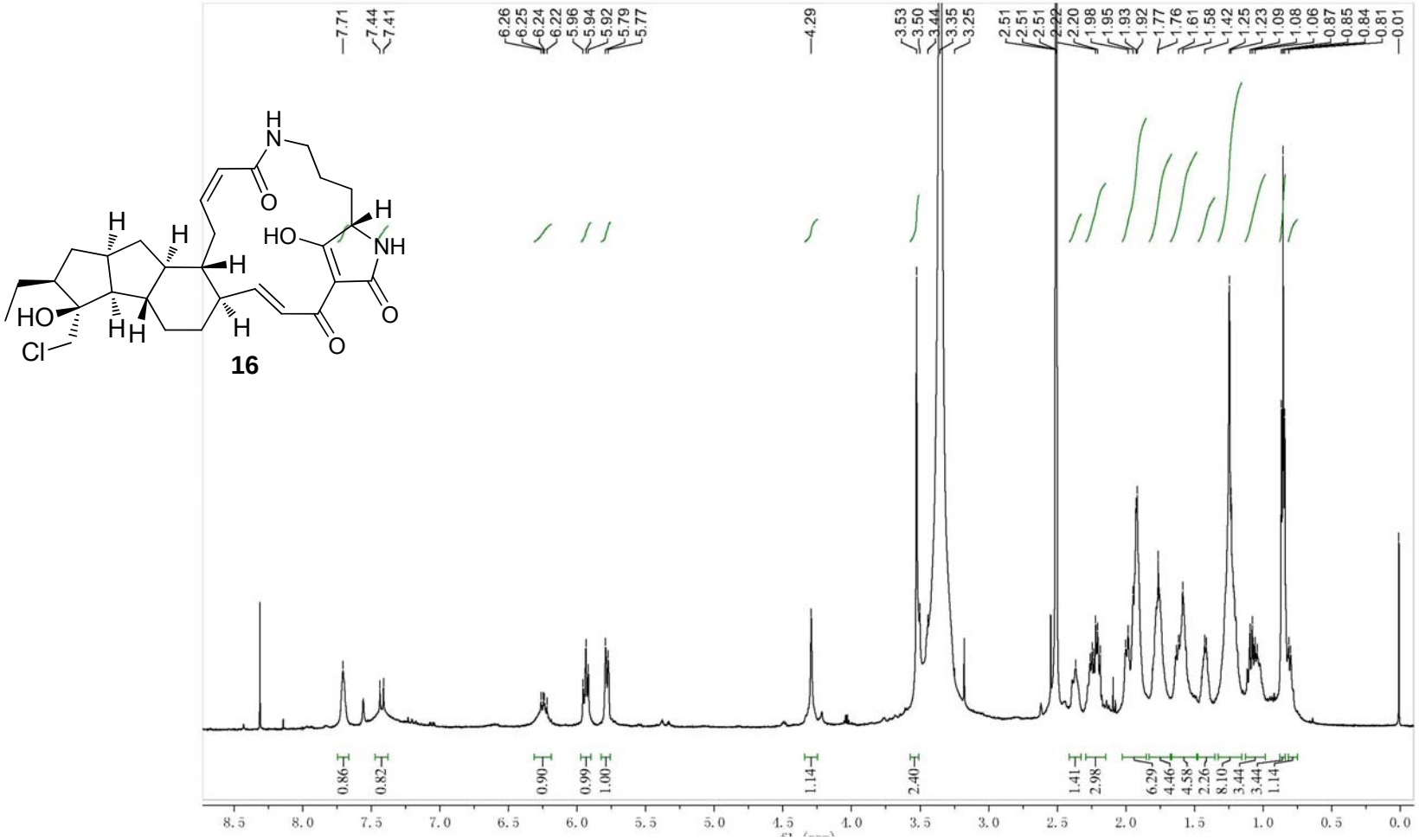

16

Fig. S13. Spectral data for pactamide E (**16**) (continued).
(**C**)The ^{13}C NMR spectrum of pactamide E (**16**) in DMSO-d_6.

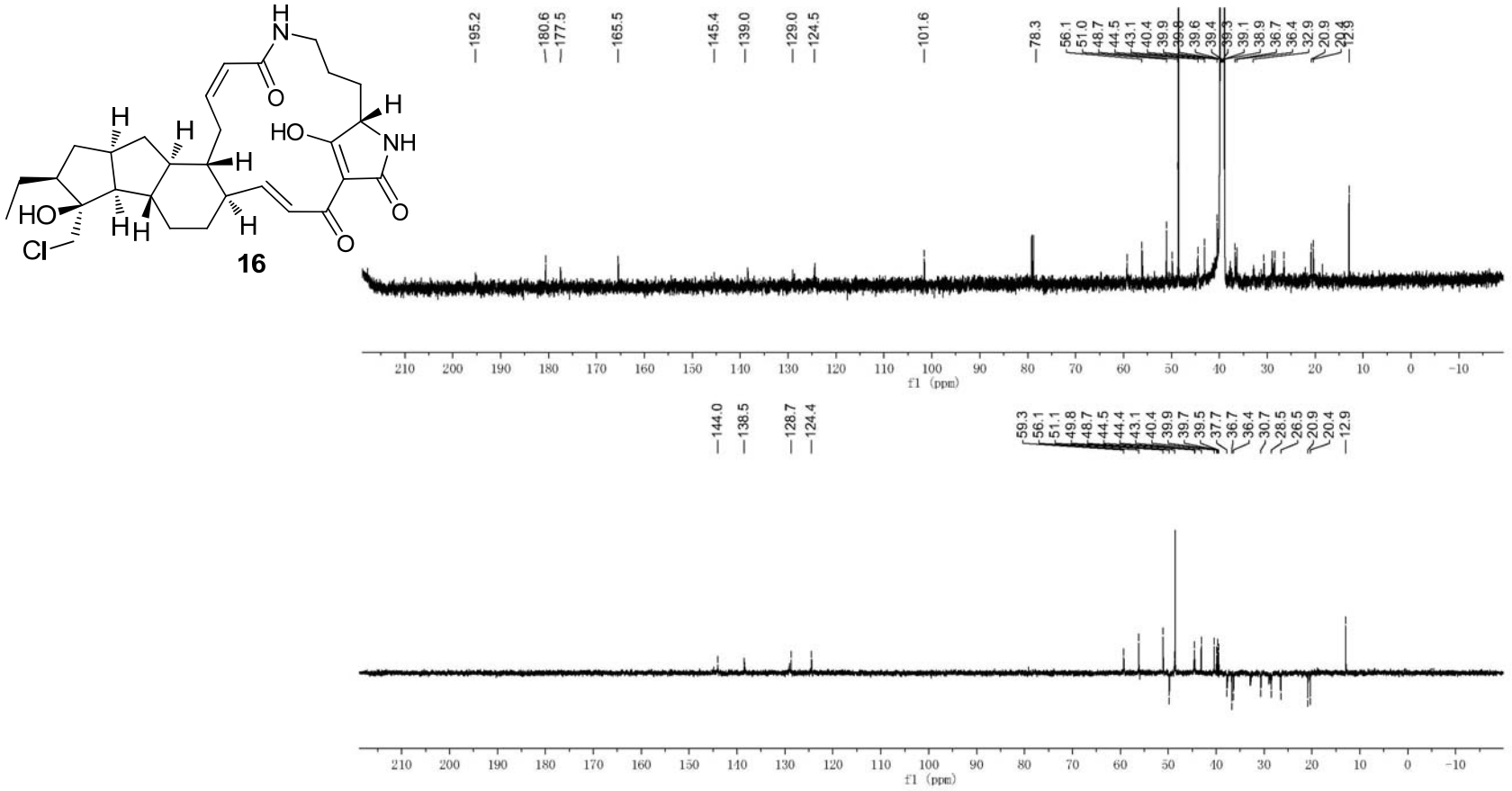

Fig. S13. Spectral data for pactamide E (**16**) (continued).
(**D**) The HSQC spectrum of pactamide E (**16**) in DMSO-d_6.

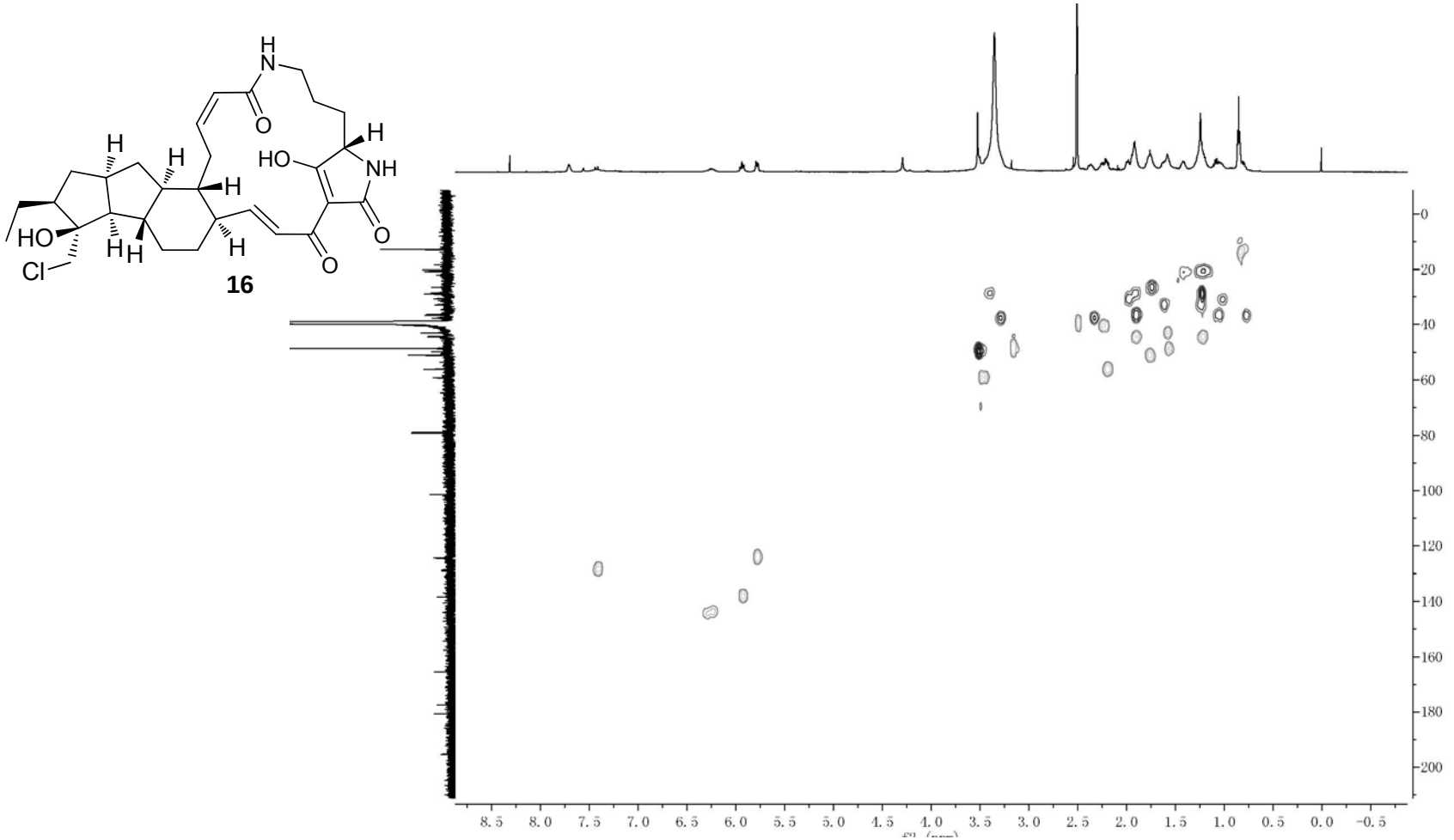

Fig. S13. Spectral data for pactamide E (**16**) (continued).
(**E**) The HMBC spectrum of pactamide E (**16**) in DMSO-d_6.

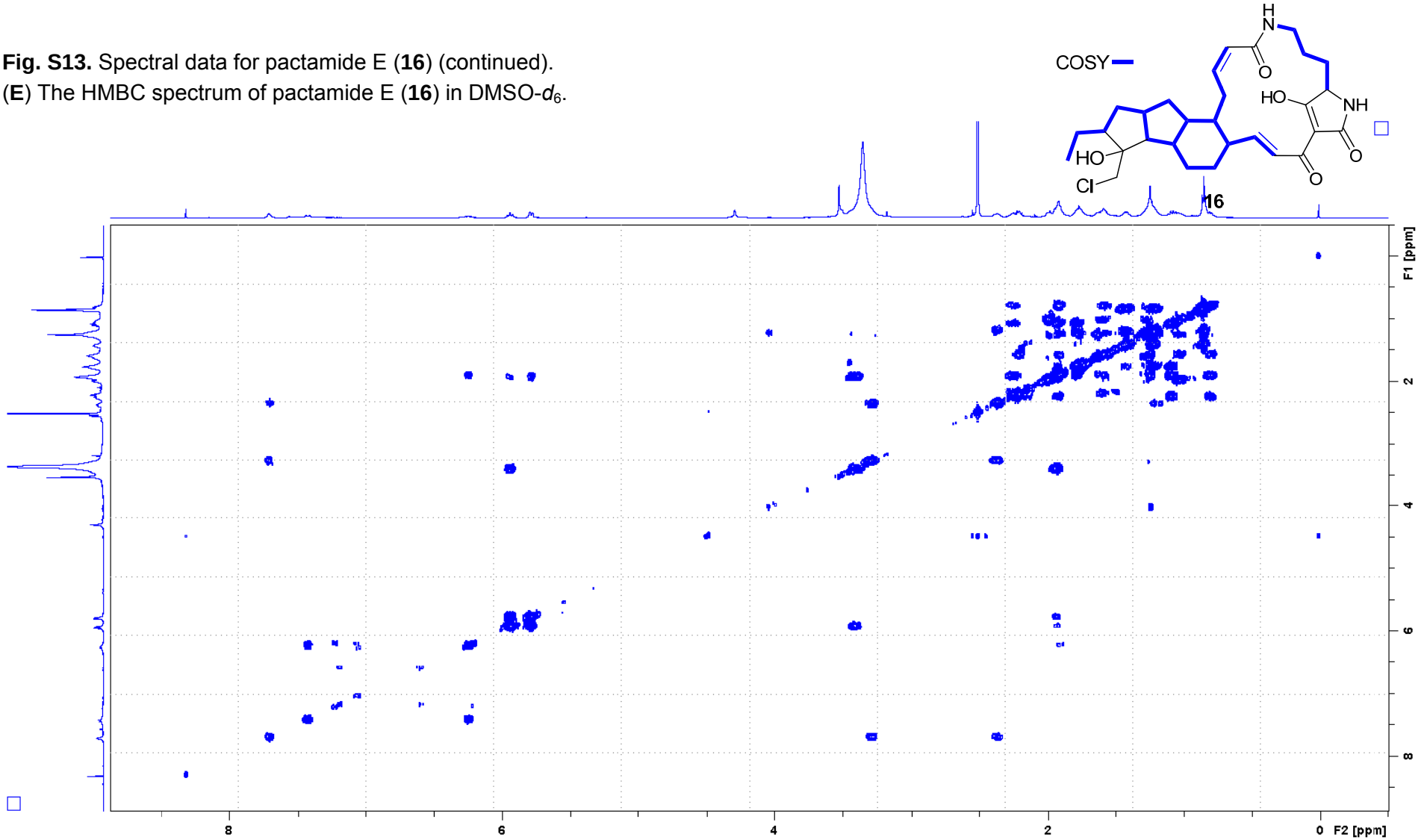

Fig. S13. Spectral data for pactamide E (**16**) (continued).
(**F**) The HMBC spectrum of pactamide E (**16**) in DMSO-d_6.

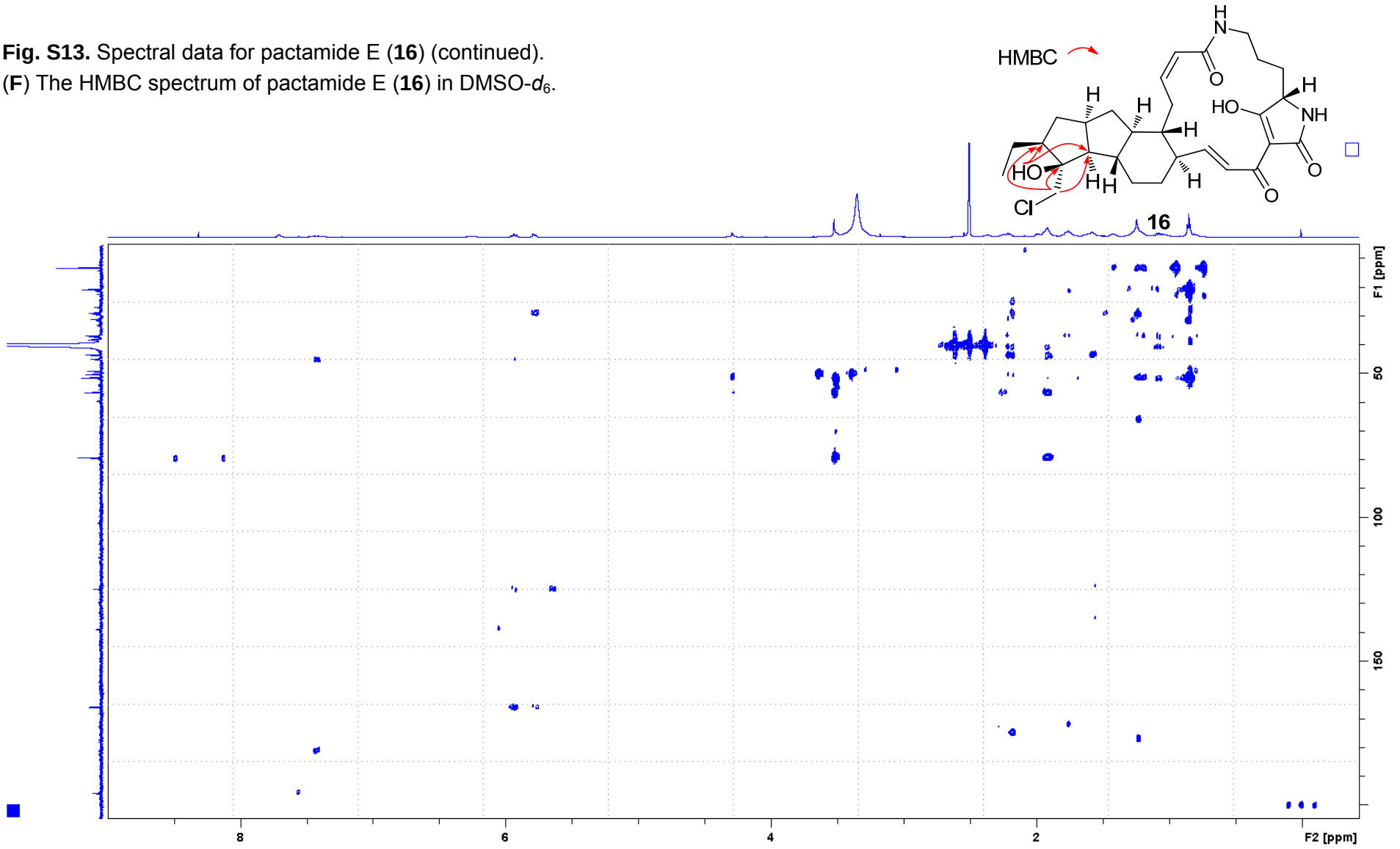

Fig. S13. Spectral data for pactamide E (**16**) (continued).
(**G**) The NOESY spectrum of pactamide E (**16**) in DMSO-d_6.

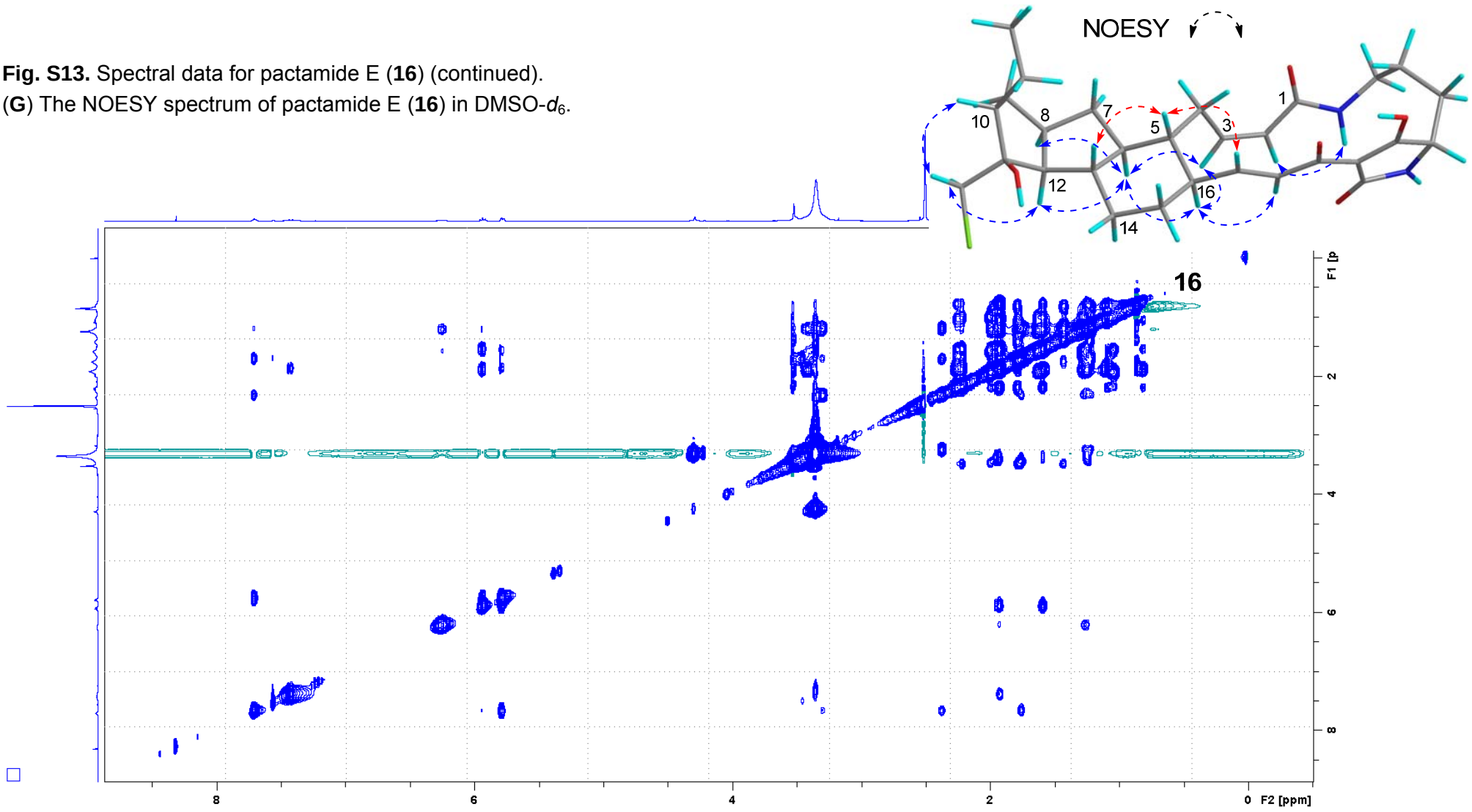

Fig. S14. Chemical structures of some other PTMs.

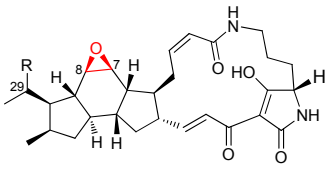

epoxyikarugamycin: R = H
capsimycin: R = OMe

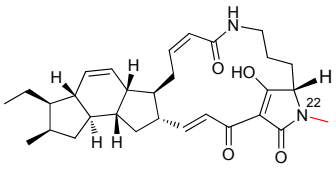

N-methyl-ikarugamycin

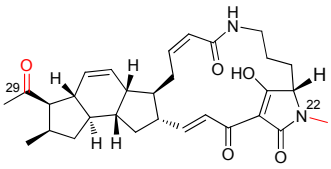

29-oxo-*N*-methyl-ikarugamycin

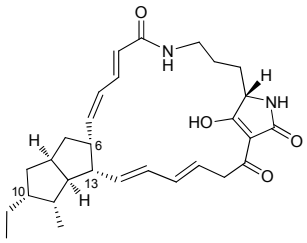

lysobacteramide A

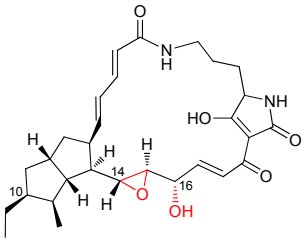

compound b

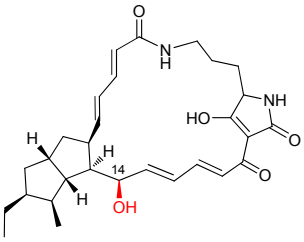

compound c

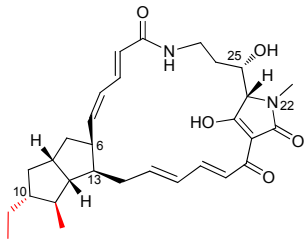

aburatubolactam A

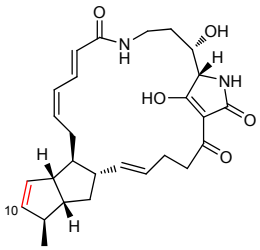

cylindramide

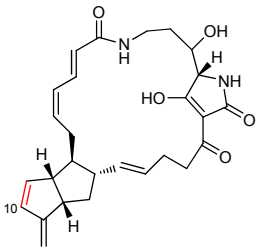

geodin A

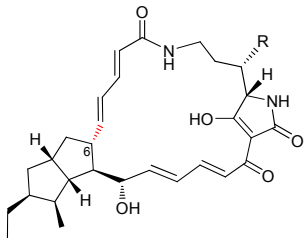

6-*epi*-alteramide A: R = OH
6-*epi*-alteramide B: R = H

Fig. S15. SDS-PAGE analysis of purified proteins.

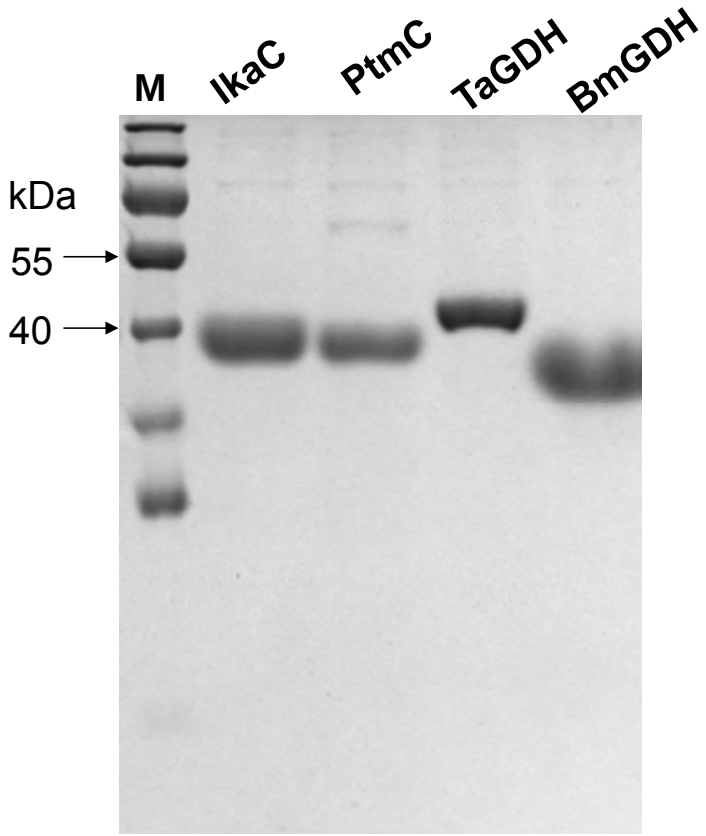

SDS-PAGE analysis of purified proteins of recombinant IkaC, PtmC, TaGDH and BmGDH. Lane M, protein molecular weight marker (Fermentas PageRuler Prestained Protein Ladder).

Fig. S16. LC-MS analysis of PtmC reactions with deuterium labelling.

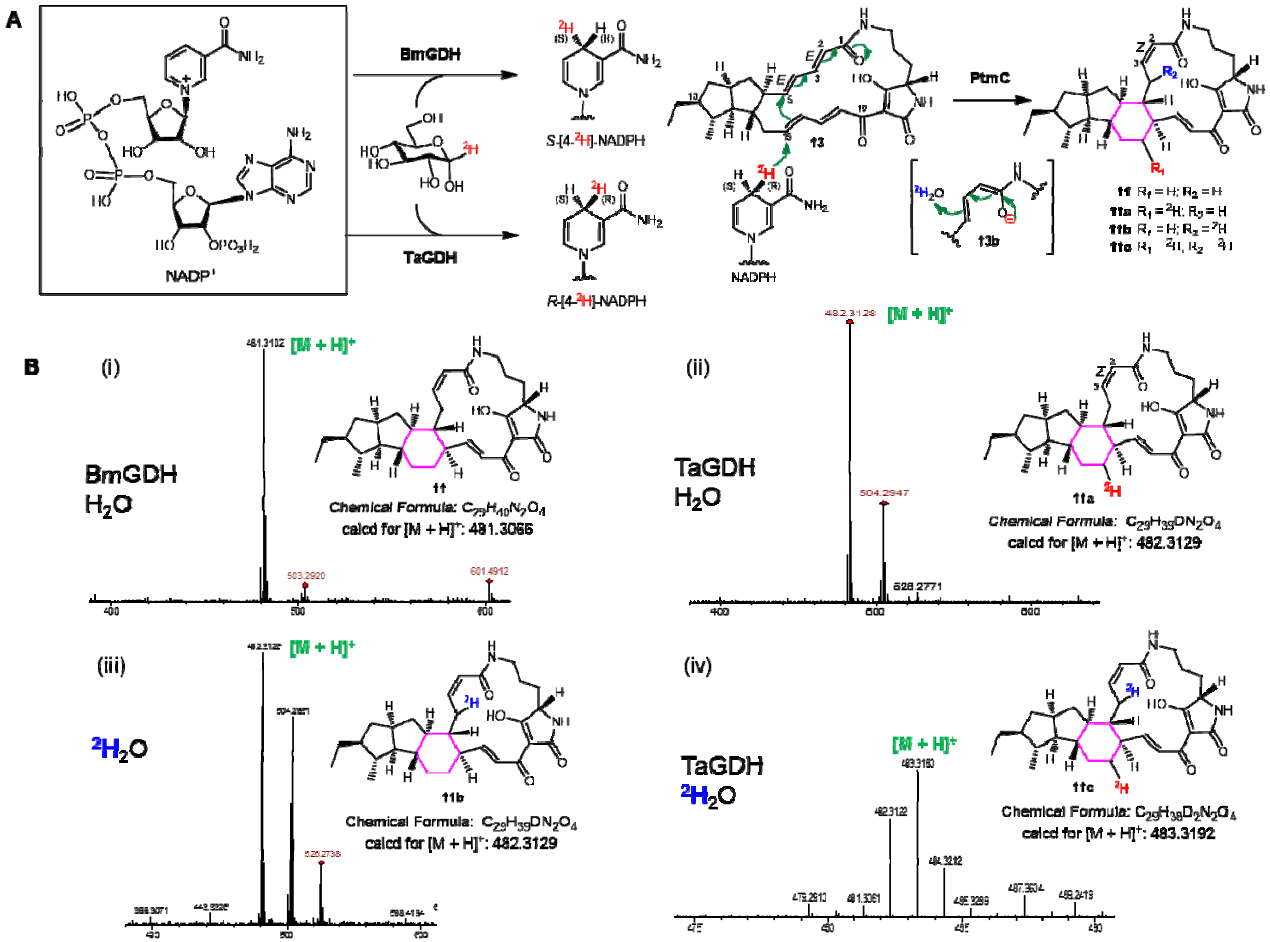

(A) A scheme for coupling PtmC reaction with glucose dehydrogenases BmGDH or TaGDH. (B) LC-HRESIMS data for PtmC assays coupling with (i) BmGDH in H_2O with D-[1-^{2}H]glucose; (ii) TaGDH in H_2O with D-[1-^{2}H]glucose; (iii) ^2H_2O; (iv) TaGDH in ^2H_2O with D-[1-^{2}H]glucose.

Fig. S17. Spectral data for isoikarugamycin (**18**).
(**A**) HRESIMS.

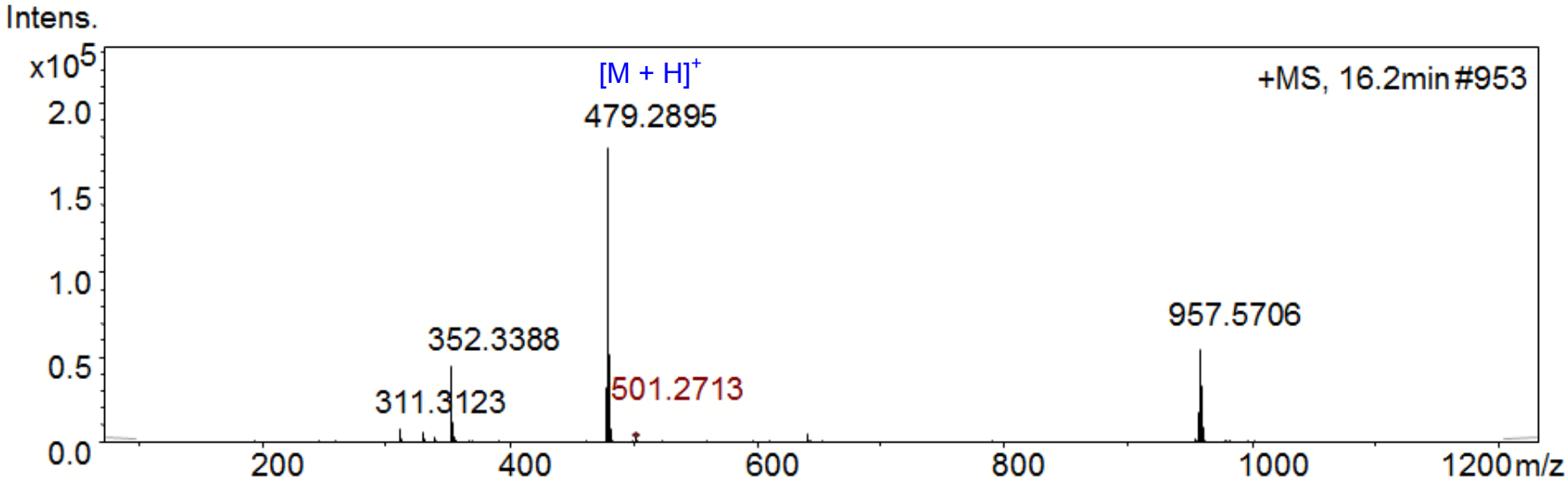

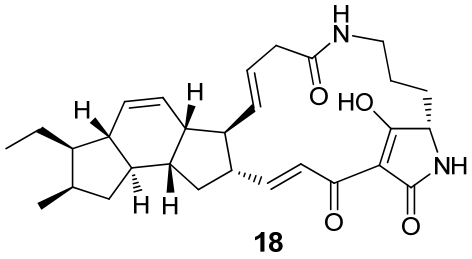

18

Chemical Formula: $C_{29}H_{38}N_2O_4$
calculated for $[M + H]^+$: 479.2910

Fig. S17. Spectral data for isoikarugamycin (**18**) (continued).
(**B**) The ^{1}H NMR spectrum of isoikarugamycin (**18**) in $CDCl_3/CD_3OD$ (9:1).

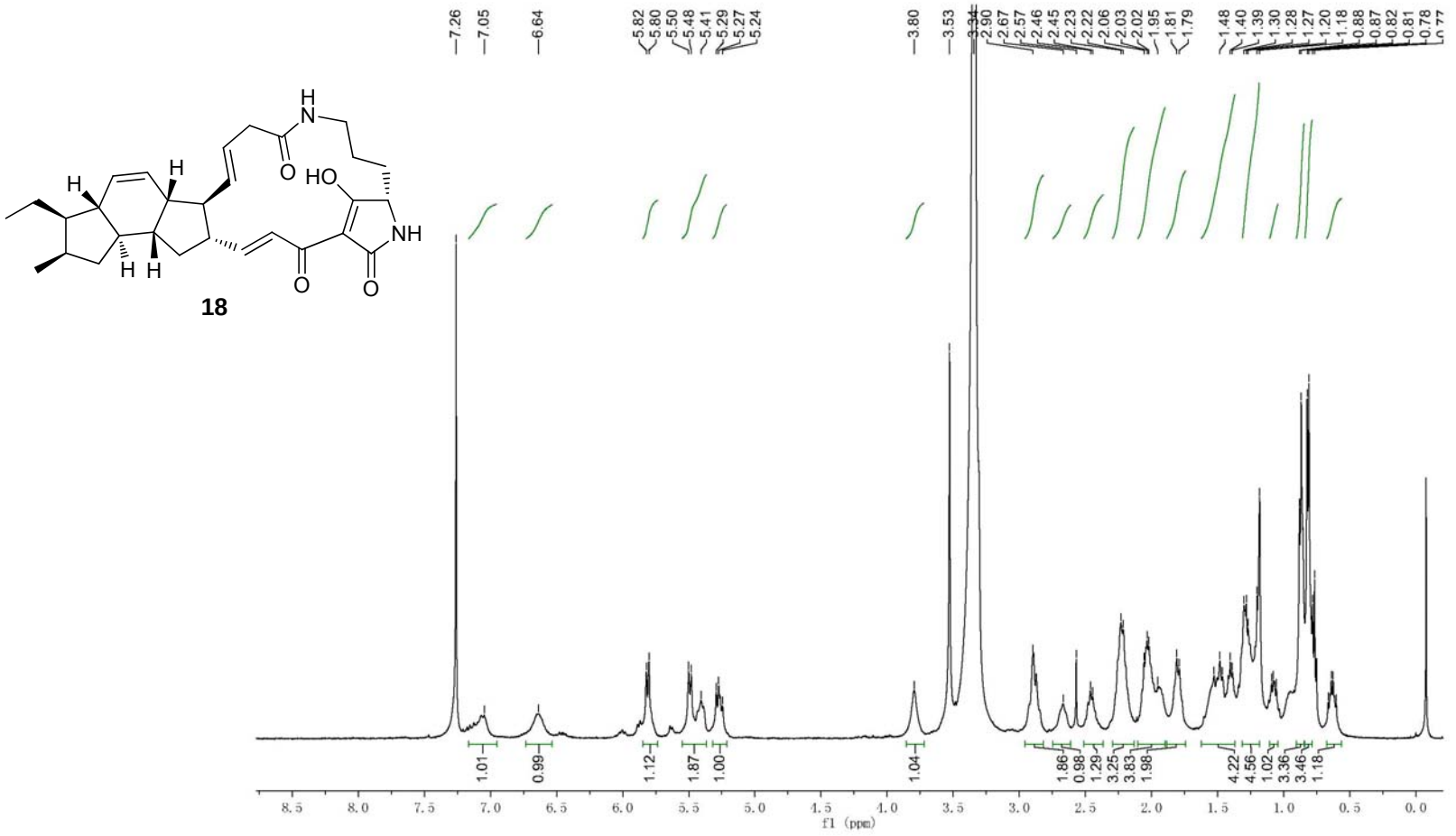

18

Fig. S17. Spectral data for isoikarugamycin (**18**) (continued).
(**C**) The ^{13}C NMR spectrum of isoikarugamycin (**18**) in $CDCl_3/CD_3OD$ (9:1).

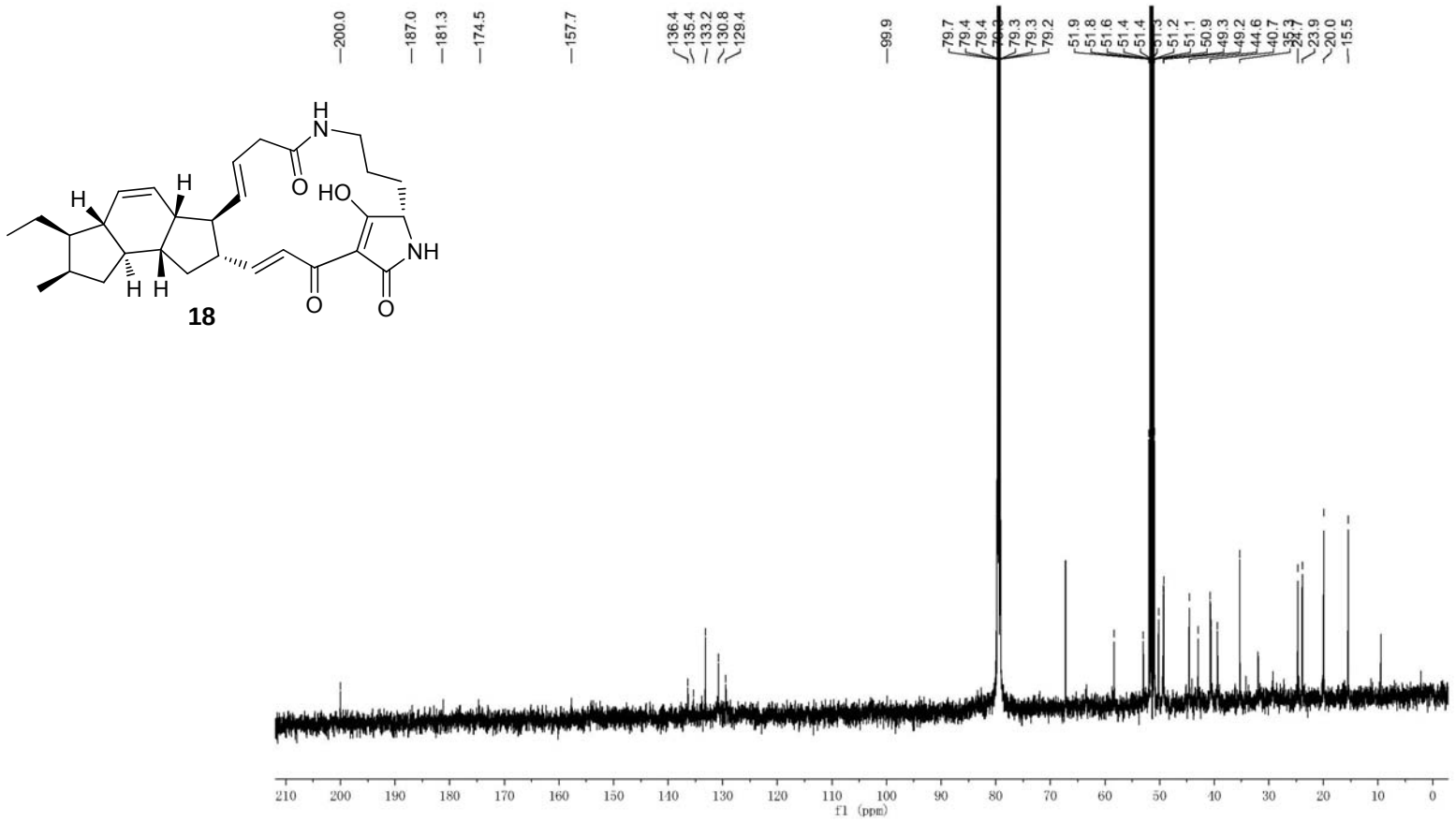

Fig. S18. *Streptomyces*-mediated Biotranformation of compound **15**.

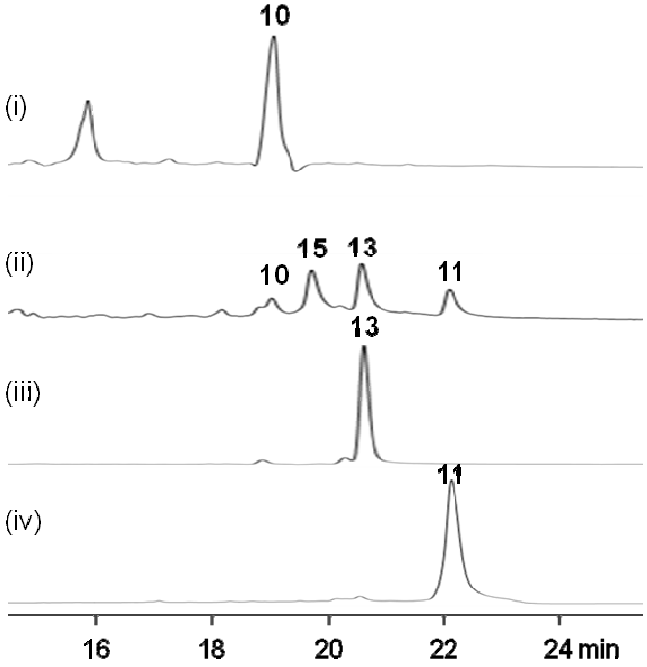

(i) *S. lividans* TK64/pCSG2814 (detection at 360 nm)
(ii) *S. lividans* TK64/pCSG2814 feeding with 50 μM compound **15**;
(iii) Standard compound **13**;
(iv) Standard compound **11**.

The strains *S. lividans* TK64/pCSG2814 were inoculated into 30 mL of AM6 medium containing 50 μg/mL apramycin with or without 50 μM compound **15**, and were grown at 28 °C for 5 days. The mycelia were extracted by butanone and were analyzed by HPLC analysis. HPLC was carried out using a reversed phase column Luna C18, 5 μm, 150 × 4.6 mm (Phenomenex), with UV detection at 360 nm (for trace i) or 310 nm (for traces ii – iv) under the following program: solvent system (solvent A, 10% acetonitrile in water supplementing with 0.1% formic acid; solvent B, 90% acetonitrile in water); 5% B to 100% B (linear gradient, 0−18 min), 100% B (18−23 min), 100% B to 5% B (23−27 min), 5% B (27−32min); flow rate at 1 mL/min.

Fig. S19. Phylogenetic analysis of PtmD and its analogues.

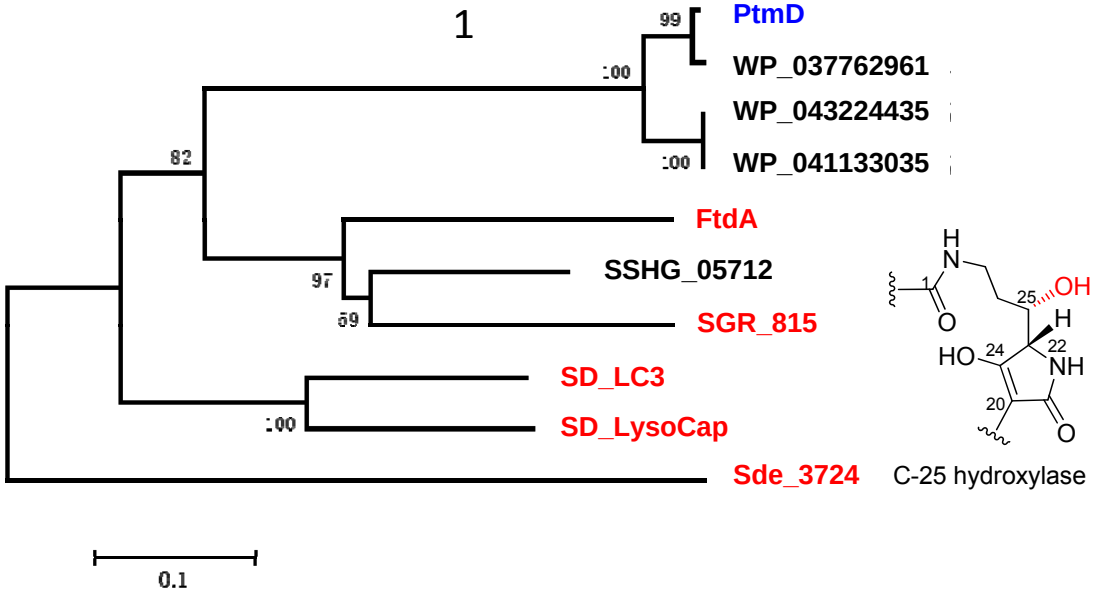

Protein	Source	Identity% to PtmD	Similarity% to PtmD	GenBank accession number	Reference
FtdA	*Streptomyces* sp. SPB78	56	69	EFL02192.1	[15]
SD_LC3	*Lysobacter enzymogenes*	54	67	ABL86392.1	[16]
SD_LysoCap	*Lysobacter capsici*	54	69	ALN85284.1	[17]
SSHG_05712	*Streptomyces albus* J1074	59	69	EFE85270.1	
SGR_815	*Streptomyces griseus* NBRC 13350	54	65	BAG17644.1	[18]
Sde_3724	*Saccharophagus degradans* 2-40	44	61	ABD82979.1	[17]
WP_037762961	*Streptomyces* sp. FXJ7.023	99	99	WP_037762961	
WP_043224435	*Streptomyces* sp. NRRL F-5193	92	94	WP_043224435	
WP_041133035	*Streptomyces vietnamensis*	91	93	WP_041133035	

The function of enzymes in red has been confirmed as C-25 hydroxylases.

Fig. S20. Comparison of highly similar PTM gene clusters and their distinct products.

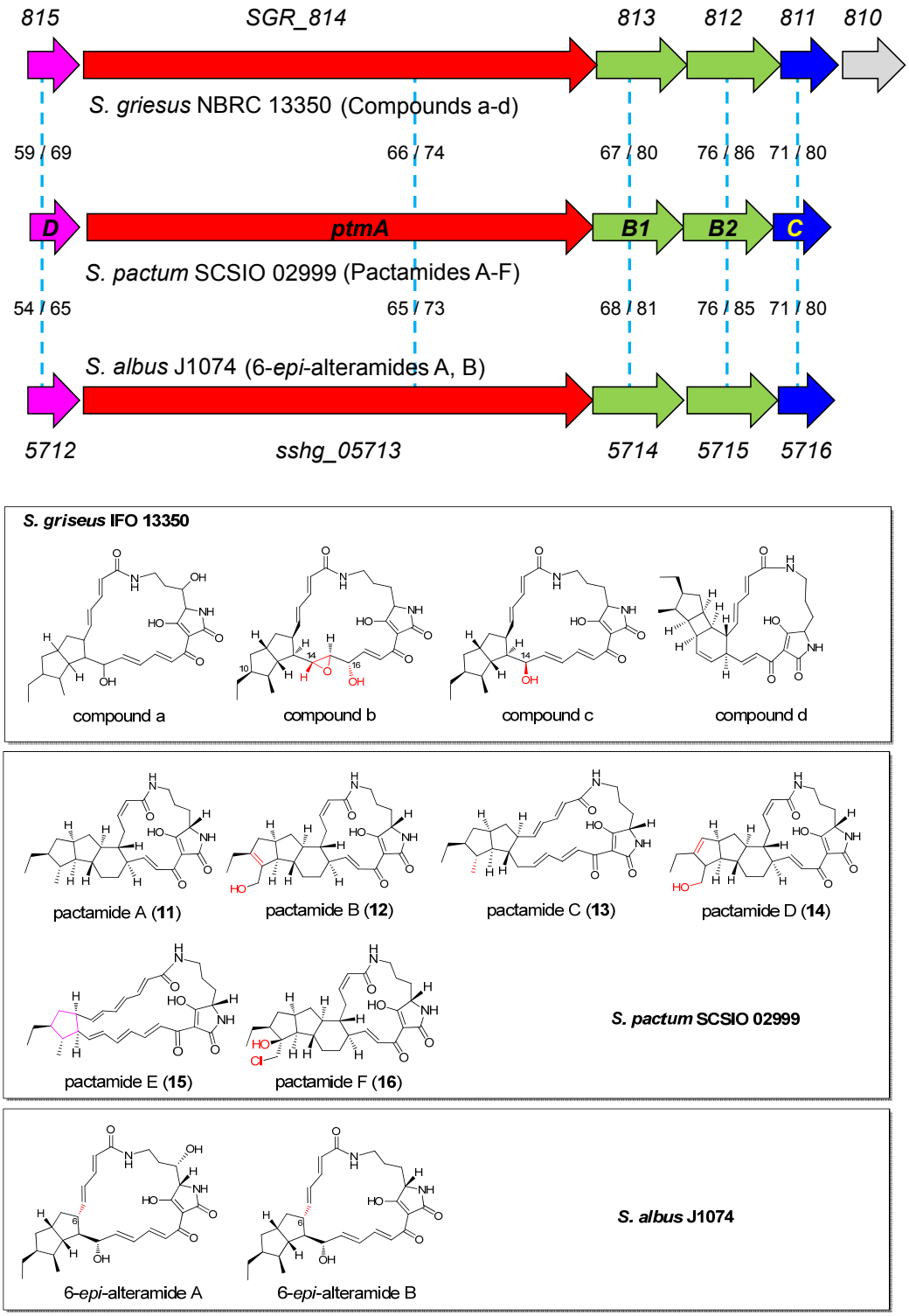

Supplementary References

1. M. Doumith, P. Weingarten, U. F. Wehmeier, K. Salah-Bey, B. Benhamou, C. Capdevila, J. M. Michel, W. Piepersberg and M. C. Raynal, *Mol. Gen. Genet.*, 2000, **264**, 477-485.
2. Y. Zhang, H. Huang, Q. Chen, M. Luo, A. Sun, Y. Song, J. Ma and J. Ju, *Org. Lett.*, 2013, **15**, 3254-3257.
3. H. Li, Q. Zhang, S. Li, Y. Zhu, G. Zhang, H. Zhang, X. Tian, S. Zhang, J. Ju and C. Zhang, *J. Am. Chem. Soc.*, 2012, **134**, 8996-9005.
4. Q. Zhang, A. Mándi, S. Li, Y. Chen, W. Zhang, X. Tian, H. Zhang, H. Li, W. Zhang, S. Zhang, J. Ju, T. Kurtán and C. Zhang, *Eur. J. Org. Chem.*, 2012, **2012**, 5256-5262.
5. T. Kieser, Bibb, M. J., Buttner, M. J., Chater, K. F. & Hopwood, D. A., *Practical Streptomyces Genetics*, Norwich, 2000.
6. L. Xu, P. Wu, S. J. Wright, L. Du and X. Wei, *J. Nat. Prod.*, 2015, **78**, 1841-1847.
7. G. Zhang, W. Zhang, S. Saha and C. Zhang, *Curr. Top. Med. Chem.*, 2016, **16**, 1727-1739.
8. G. T. Zhang, W. J. Zhang, Q. B. Zhang, T. Shi, L. Ma, Y. G. Zhu, S. M. Li, H. B. Zhang, Y. L. Zhao, R. Shi and C. S. Zhang, *Angew. Chem. Int. Ed.*, 2014, **53**, 4840-4844.
9. Z. C. Wu, D. L. Li, Y. C. Chen and W. M. Zhang, *Helv. Chim. Acta*, 2010, **93**, 920-924.
10. K. A. Datsenko and B. L. Wanner, *Proc. Natl. Acad. Sci. USA*, 2000, **97**, 6640-6645.
11. D. J. MacNeil, K. M. Gewain, C. L. Ruby, G. Dezeny, P. H. Gibbons and T. MacNeil, *Gene*, 1992, **111**, 61-68.
12. Y. Zhu, P. Fu, Q. Lin, G. Zhang, H. Zhang, S. Li, J. Ju, W. Zhu and C. Zhang, *Org. Lett.*, 2012, **14**, 2666-2669.
13. B. Gust, G. L. Challis, K. Fowler, T. Kieser and K. F. Chater, *Proc. Natl. Acad. Sci. USA*, 2003, **100**, 1541-1546.
14. R. Lacret, D. Oves-Costales, C. Gomez, C. Diaz, M. de la Cruz, I. Perez-Victoria, F. Vicente, O. Genilloud and F. Reyes, *Mar. Drugs*, 2015, **13**, 128-140.
15. J. A. V. Blodgett, D. C. Oh, S. G. Cao, C. R. Currie, R. Kolter and J. Clardy, *Proc. Natl. Acad. Sci. U S A.*, 2010, **107**, 11692-11697.
16. Y. Y. Li, J. Huffman, Y. Li, L. C. Du and Y. M. Shen, *MedChemComm*, 2012, **3**, 982-986.
17. C. Greunke, J. Antosch and T. A. Gulder, *Chem. Commun.*, 2015, **51**, 5334-5336.
18. Y. Luo, H. Huang, J. Liang, M. Wang, L. Lu, Z. Shao, R. E. Cobb and H. Zhao, *Nat. Commun.*, 2013, **4**, DOI: 10.1038/ncomms3894.